The University Of Sheffield.

Arctic browning: impacts of extreme events on vegetation and carbon balance in high latitude ecosystems

Rachael Treharne

A thesis submitted in partial fulfilment of the requirements for the degree of
Doctor of Philosophy

The University of Sheffield
Faculty of Science
Department of Animal and Plant Sciences

September 2018

Three Minute Thesis

What pops into your head if I ask you to think about the Arctic? Probably polar bears, maybe shrinking sea ice? Whatever it is, it probably isn't carbon.

But actually the Arctic is the world's carbon capital: Arctic soils contain more carbon than all the world's vegetation, and the entire atmosphere, combined. This carbon accumulates in deep soils because it's too cold for much decomposition. By locking carbon away from the atmosphere, the Arctic is therefore playing a pivotal role in regulating global climate.

However, the Arctic is warming, and it's warming fast – twice as fast as the rest of the world. This rapid climate change is threatening the Arctic carbon store, by speeding up decomposition, but also by causing huge changes in plant communities – and it is these plant communities that determine rates of carbon gain and loss.

You might expect a warmer Arctic to mean more vibrant, productive plant communities taking up more carbon, and in some cases you would be right. However, recently this picture has been complicated by extreme winter events. These events are associated with climate change, so they're happening more and more often in the Arctic. They can also cause large scale vegetation damage and death. We call this Arctic browning - and we know almost nothing about its implications for carbon, or for global climate.

In my PhD, I'm making the first full assessments of the impacts of Arctic browning on the uptake and release of carbon. I want to know: what actually are those impacts, how do they differ when caused by different types of extreme event, and can we predict them just from the severity of the browning that we see?

Luckily for me this has meant spending a lot of time in the Arctic. I've taken nearly 3000 measurements of carbon uptake and release, covering 7 heathland field sites affected by extreme events. In all cases I have found that browning massively reduces the ability of

heathland to take up carbon. In fact, net carbon uptake across each site was reduced by as much as 80% - meaning more carbon staying in the atmosphere, instead of being locked away in that Arctic carbon store.

The silver lining is that browning impacts are surprisingly similar even when caused by very different extreme events. So much so that we can estimate the reduction in carbon uptake, just by knowing how severe browning is.

This is crucial, because we can see browning severity from satellite data - suggesting we could upscale its impacts across entire Arctic landscapes quickly, easily and remotely.

So will the Arctic continue to buffer us against climate change, or will it accelerate warming? We don’t know yet, but my PhD is helping to develop the tools we need to find out.

Scientific summary

Climate change is happening faster in the Arctic than almost anywhere else in the world, and Arctic winters are warming especially rapidly. Among the consequences of this is an increase in the frequency of winter extreme events. These include climatic events, such as periods of extreme warmth, and biological events, such as outbreaks of defoliating insects.

Such events are already having major impacts on Arctic landscapes, driving vegetation damage and decline across thousands of square kilometres. This loss of biomass and vegetation greenness is termed 'Arctic browning'. Extreme events which drive Arctic browning are already occurring more frequently and with greater severity: a trend predicted to continue as climate change progresses.

However the effects of these events on high latitude ecosystems are not well understood. In particular, their impacts on ecosystem CO_2 balance are almost unknown. Furthermore, methods to upscale impacts across Arctic regions, or to assess the regional importance of extreme event-driven browning, do not yet exist. As the Arctic plays an important role in regulating global climate, there is an urgent need to address these uncertainties and to understand the role of extreme events in determining vegetation change and carbon balance at high latitudes.

Therefore this thesis assesses the consequences of extreme events and subsequent browning for key ecosystem CO_2 fluxes. How impacts vary with event type, across the growing season, and when associated with different browning responses is quantified. In all cases, major reductions in ecosystem CO_2 uptake are found. Mechanistic insight into these changes is provided through additional field and remotely sensed data. Finally, the interacting climatic drivers underlying extreme event driven browning are analysed and upscaled. This represents the most comprehensive assessment to date of the causes and consequences of extreme winter events which drive Arctic browning.

Acknowledgements

First and foremost, I would like to thank my primary supervisor Professor Gareth Phoenix for his encouragement, for his excellent scientific advice throughout my PhD and for his unwavering enthusiasm for this project. I could not have had a better PhD supervisor and am deeply grateful to have simultaneously been given so much support and so much flexibility and control over the direction of my PhD.

My second supervisors, Dr Hans Tømmervik, Professor Lisa Emberson, and in particular Dr Jarle Bjerke, have always found time for discussion and have provided invaluable ideas and advice. I am especially grateful to Jarle and Hans for giving me the chance to collect data on Svalbard, and to their colleagues Geraldine Mabille and Sidsel Grønvik, who were excellent company while I was there.

Many thanks must go to those who helped me in the field. In particular to Laura Stendardi for cheerfully enduring leaky tents and leaky huts to support both of my field seasons, and to Karen Hei-Laan Leung and Jade Rodgers for help with measurements. Thanks are also due to everyone at NINA in Tromsø, especially Britt Solli, who provided me with advice and logistical support during my time in Norway.

I would also like to thank Dr James Fisher, whose training and encouragement taught me to take a pragmatic and independent approach to field work and gave me the confidence to apply for a PhD in the first place.

There are too many people to mention who have made the University of Sheffield a wonderful place to work. Members of C57 lab group, in particular Kassandra and Scott, have always been happy to talk through ideas, and PhD colleagues across the department have provided a huge amount of support through the highs and lows of the last four years. Special mention must go to Alun, who has been exceptionally patient in convincing me that R does, in fact, work.

Table of contents

List of Figures

List of Tables

Chapter 1

General Introduction

1.1 Climate change and the Arctic

Climate change is arguably the greatest challenge of our time. Globally, air temperatures have increased by 0.65 to 1.06˚C since 1880, and warming is likely to exceed 2˚C by the end of this century (IPCC, 2013; UNEP, 2017). In the Arctic, temperatures have been increasing more than twice as fast as the global average for the past 50 years, with the most rapid warming seen in winter months (Christensen et. al., 2007; AMAP, 2017). In January 2016, the Arctic was a full 5˚C warmer than the 1981-2000 average, and by 2040 average autumn and winter temperatures are expected to have increased by 4˚C. The significance of these changes is such that the Arctic is widely considered to be shifting to a new climate state (Arctic Council, 2016; AMAP, 2017; Bintanja & Andry, 2017).

The consequences of rapid climate change in Arctic regions, however, go beyond gradual temperature increases. The nature and timing of Arctic precipitation is changing; later snow fall and earlier spring snow melt mean that the duration of winter snow cover is falling by 3-5 days per decade across the Arctic (Callaghan et al., 2011; Bokhorst et al., 2016). Total precipitation is predicted to increase across the Arctic (IPCC, 2013), but a much larger proportion of this precipitation is expected to fall as rain rather than snow, resulting in an overall reduction in snow fall and therefore in the depth and areal extent of winter snow cover (Bokhorst et al., 2016; Bintanja & Andry, 2017). Furthermore, as rain increasingly dominates Arctic precipitation, a higher proportion of this will fall during heavy, intense rainfall events (Hansen et al., 2014), while an increase in temperature variability alongside rising mean temperatures is leading to more and longer periods of extreme warmth (IPCC, 2013).

The ecological implications of these changes are varied and complex. A longer snow free period in combination with summer warming is extending the growing season, promoting

enhanced growth, cover and productivity of plant communities (termed "Arctic greening"), and in particular the expansion of deciduous shrubs (Bhatt et. al. 2013, Jia et. al. 2009, Myers-Smith et al., 2015). A warmer, longer growing season may also promote belowground biogeochemical cycling, including nitrogen mineralisation and heterotrophic respiration (Rustad et al., 2001). However, evidence increasingly suggests that the effects of climate change during Arctic winters have impacts on plant communities which are in direct opposition to those of summer warming. In particular, an increase in the frequency and severity of a range of extreme events linked to aspects of winter climate change (including extreme warmth, heavy rainfall and reduced snow cover) is driving extensive mortality and severe stress at landscape or greater scales in widespread Arctic heathland communities (Bjerke et al., 2017). This extreme event-driven plant damage is thought to be an important contributor to declines in biomass and productivity (termed "Arctic browning") observed across Arctic regions in recent years (Bjerke et al., 2014; Epstein et al., 2015, 2016).

The scale and severity of the browning following extreme events, and its direct contrast with the more well-understood impacts of gradual summer warming, create considerable uncertainty around the responses of Arctic ecosystems to climate change. Initial assessments of extreme event-driven Arctic browning have demonstrated that such events can drive severe vegetation damage over thousands of square kilometres, or even (when events combine) across entire Arctic regions (Bokhorst et al., 2011; Bjerke et al., 2014). Such studies have also developed a qualitative understanding of the mechanisms underlying browning (*section 1.3*) (Bokhorst et al., 2009; Bjerke et al., 2017). However, the impacts of Arctic browning on ecosystem function, including on ecosystem carbon balance, remain largely unknown, while we have almost no understanding of how these impacts may differ with event type or across the growing season. Beyond an ecological understanding of impacts, our ability to define browning events

quantitatively, as opposed to relying on qualitative descriptions, is also currently severely limited. This hinders our ability to project their future frequency and severity.

Resolving these questions is of global importance. The Arctic is a vast carbon store, with more than twice as much carbon stored in its soils as in the atmosphere (Schuur et al., 2009). Loss of carbon from this store could produce a substantial positive feedback to climate change, accelerating warming, while any increase in carbon uptake in the Arctic could help to mitigate future climate change. As rates of carbon gain and loss in Arctic soils are in part determined by the biomass and productivity of Arctic plant communities, their responses to climate change, including extreme winter events, are not just of critical ecological importance, but have implications for the current and future role of the Arctic in global climate.

1.2 Arctic heathlands

Heathland communities are widespread across high latitude ecosystems, from boreal to High Arctic regions (Walker et al., 2005; Bokhorst et al., 2010). These communities are dominated by ericaceous dwarf shrubs such as *Calluna vulgaris* and *Empetrum nigrum* (which are most common across boreal and sub-Arctic regions) or *Cassiope tetragona* (which is distributed widely across Arctic regions, including some areas of the High Arctic) (Bliss, 1971; Callaghan et al., 1989). Mosses, particularly those of the *Hypnaceae* family such as *Hylocomium splendens* and *Pleurozium schreberi*, are also a key component of high latitude heathland ecosystems, often providing continuous or near continuous ground cover. Other common genera include *Vaccinium* (dwarf shrubs), *Salix*, *Betula* (shrubs and trees) and *Carex* (sedges).

Arctic plant communities, including heathlands, are adapted to harsh winter conditions, and to spending 8 or more months under snow cover (Callaghan et al., 2011). At the onset of winter, these plants acclimate to cold temperatures, increasing their frost tolerance through processes such as altering membrane structure and accumulating cryoprotective sugars (Kreyling, 2010; Crawford, 2013). Following this, Arctic heathland plants may tolerate air temperatures as low as -60˚C (Sakai & Larcher 1987). Many Arctic heathland species sustain considerable metabolic activity while cold acclimated and, typically, snow covered (Brooks et al., 2011). This means that substantial carbon losses occur due to respiration in winter, but also that plants are able to respond rapidly to changing conditions, and therefore make the most of favourable spring conditions. Dehardening, for example, may occur in just a few days, and evergreen species may become photosynthetically active in response to light penetration through snow even before spring snow melt (Strimbeck et al., 1995; Starr & Oberbauer, 2003; Kreyling, 2010). Following dehardening, frost damage in evergreen shrubs has been recorded following temperatures just a few degrees below 0˚C (Bjerke et al., 2014).

These characteristics of the ericaceous dwarf shrubs which dominate Arctic heathland ecosystems - particularly evergreen leaves, sustained metabolic activity throughout winter, and rapid responses to changing environmental conditions - leave them particularly susceptible to damage following the extreme winter climatic events described in the following section.

1.3 Mechanisms of extreme event-driven Arctic browning

Extreme winter events that result in Arctic browning are most often climatic or biological. Among the most damaging of these are frost drought, extreme winter warming, and ice encapsulation (climatic events) and outbreaks of defoliating insects (a biological event).

Current understanding of the mechanisms underlying these events has been developed through *a posteriori* field studies of extreme event impacts and field simulations of extreme winter warming (Bokhorst et al., 2008, 2009, 2010, Bjerke et al., 2014, 2017).

1.3.1 Frost drought

Frost drought occurs when low snow conditions during winter leave vegetation exposed to cold temperatures, wind and irradiance. The absence of snow cover, and therefore of a protected, insulated sub-nivean environment, causes transpiration in exposed vegetation to increase (Sakai & Larcher, 1987). At the same time, frozen or near-frozen soils prevent water being replaced through uptake. The resulting desiccation may happen as a short, acute event or gradually over a relatively long period of exposure (Tranquillini, 1982). Acute frost drought typically results from an increase in temperature, sufficient to stimulate stomatal opening in vegetation exposed to ambient air temperatures, but not sufficient to cause soil thaw; resulting in rapid desiccation (Larcher & Siegwolf, 1987). Conversely, prolonged exposure may accelerate water loss from the cuticle and/or periderm even where temperatures remain low and stomata closed. While in many environments high irradiance may have the strongest potential impact on this process, in high latitude ecosystems specifically, wind abrasion of the cuticle surface is likely to contribute more significantly (Hadley & Smith, 1986, 1989).

1.3.2 Extreme winter warming

Extreme winter warming events are characterised by periods of unseasonable warmth combined with loss or absence of snow cover. Temperatures may increase abruptly by as much as 25°C in 24 hours during winter, and remain above 0°C for several days, resulting in substantial snowmelt and warming of exposed plant communities (Phoenix & Lee, 2004;

Bokhorst et. al. 2008). This warmth can trigger a spring-like response in the exposed vegetation, which may prematurely lose its cold tolerance and become increasingly metabolically active, even bursting bud in the middle of the Arctic winter (Bokhorst et. al. 2010). These winter warm periods are typically transient and can be followed by a rapid return to sub-zero temperatures. Cold temperatures and freeze-thaw cycles subsequently cause frost damage in exposed, de-hardened vegetation, a situation exacerbated due to the initial loss of the insulating snow layer (Callaghan et. al. 2013, Phoenix & Lee, 2004).

1.3.3 Ice encapsulation

Ice encapsulation of vegetation follows rain on snow (ROS) and/or snow thaw-freeze events. These are often associated with periods of winter warmth, and result from partial melt of snow (due to warmth and/or winter rain) followed by refreezing of that meltwater and, in the case of ROS, freezing of rainwater. This leads to the formation of thick, persistent ice lenses within the snow pack or at ground level (termed 'ground icing'). Following one severe ROS event across Svalbard in the High Arctic, during which temperatures reached almost 20˚C above daily normal values and 25% of mean annual precipitation fell in 24 hours, ground ice 10-20cm thick persisted at almost all sites sampled across the Svalbard archipelago from February to mid-June (Hansen et al., 2014). Encapsulation within ice lenses is thought to damage vegetation through exposure to cold temperatures, due to the loss of insulating snow cover and the high conductivity of ice, (Callaghan et al., 2004) and through hypoxia and CO_2 accumulation due to the low permeability of ice to gases - though experimental evidence suggests the latter reasons are less important than initially believed (Preece et al., 2012; Preece & Phoenix, 2013; Preece & Phoenix, 2014).

1.3.4 Insect defoliation

Increases in mean annual and minimum winter temperatures elevate survival of insect herbivores of sub-Arctic birch forest and dwarf birch shrubland, in particular geometrid moths whose eggs, laid on birch, over-winter before the caterpillars hatch in synchrony with birch leaf out (Jepsen et al., 2008). Since eggs are killed at low temperatures (often around -35°C) warming winters drive lower egg mortality and greater frequency, intensity and range of outbreaks (Wolf et. al., 2008; Jepsen et al., 2013). Outbreaks of these species in Arctic regions initially results in defoliation of the tree canopy, often leading to substantial shoot mortality (Tenow & Bylund, 2000; Callaghan et. al., 2013). However, caterpillars also frequently defoliate the understory, especially when their birch tree leaf food source is exhausted, resulting in wilting and browning (Tenow, 1996; Callaghan et. al. 2013). The degree of understory defoliation varies between plant species (Olofsson et. al., 2013). *Betula nana* and *Vaccinium* spp. are often heavily defoliated, while the evergreen dwarf-shrub *Empetrum nigrum* is less intensively browsed. Despite this, *E. nigrum* typically displays extensive browning after defoliation events (Heliasz et. al., 2011; Jepsen et. al., 2013). This response is not fully understood, but is likely related to caterpillars puncturing the cuticle of *E. nigrum* leaves in their attempts to feed on this unpalatable species, exacerbating water stress (Heliasz et. al., 2011) and/or enhancing susceptibility to fungal pathogens (Olofsson et. al., 2013).

1.4 Impacts of extreme event-driven Arctic browning

1.4.1 Plant physiology

The distinguishing consequence of browning following any of the above event types is shoot mortality in the dwarf shrubs which dominate Arctic heathland communities. This response is

particularly strong in evergreen compared to deciduous dwarf shrubs due to the former having leaves which are exposed over winter (Bokhorst et al., 2011). Shoot mortality is visible initially as brown discoloration which then becomes grey (due to the elimination of all pigmentation) following more than one growing season (Bjerke et al., 2017). This damage can be severe and extensive; mortality of more than 60% of all shoots and increases in shoot mortality of up to 10 times have been recorded following conditions associated with frost drought and extreme winter warming (Bokhorst et al., 2011; Blume-Werry et al., 2016). Furthermore, signs of severe stress visible as deep red colouration - but without shoot mortality - have been increasingly reported following extreme climatic events. This reflects unusually high, persistent anthocyanin pigmentation in leaves and shoots, and may affect as much as 70% of shoots (Bjerke et al., 2017). Mortality and stress combined drive major loss of greenness across affected landscapes, with reductions in NDVI (Normalised Difference Vegetation Index; a measure of vegetation greenness) of 50% or more reported following these events (Bjerke et al., 2014). Defoliating insect outbreaks cause mortality and an associated loss of greenness at similar scales to climatic events; understory NDVI reductions of up to a third have been recorded following defoliating insect outbreaks. Severe damage to the understory following insect outbreaks can even result in a shift in vegetation state from evergreen dwarf shrub dominated heathland to grassland (Jepsen et al., 2013; Karlsen et al., 2013).

In surviving vegetation, extreme events can have major impacts on phenology, growth and reproduction. A single simulated extreme winter warming event with a duration of one week was shown to delay bud-burst by up to 3 weeks and reduce reproductive output by more than 80% in key vascular understory species (Bokhorst et. al., 2008). Repeating this simulated event the following year almost halved summer growth of *Empetrum nigrum*, the most abundant species, in addition to causing marked shoot mortality. Similar growth reductions (including

an 87% reduction in growth of *Empetrum nigrum*) followed a natural event in 2007 that impacted vegetation across more than 1400 km^2 (Bokhorst et. al., 2009). Reduced flowering and berry production (by up to 83% in Empetrum nigrum) were also observed following simulated ice encapsulation, although growth was not affected in this case (Preece et al., 2012; Preece & Phoenix, 2014). However, there are interspecific differences in responses to extreme winter events, with not all species responding negatively; shoot growth in *Vaccinium myrtillus* almost doubled following two simulated extreme winter warming events (Bokhorst et al., 2011). This is interpreted as a compensatory growth response, utilising resources stored belowground to increase photosynthetic leaf area and compensate for lost CO_2 uptake earlier in the growing season. Similarly, compensatory growth responses in the birch canopy, including a second flush of leaves, are typically observed following outbreaks of defoliating insects (Callaghan et al., 2013). Nonetheless, very severe outbreaks can overcome this resilience and cause large-scale total tree mortality, while compensatory growth in understory species has not been reported following these outbreaks (Callaghan *et. al.* 2013, Post & Pederson, 2008).

Cryptogams, including bryophytes and lichens, are a key component of Arctic ecosystems (Street et al., 2013). They account for significant proportions of plant biomass and have major roles in carbon and nutrient cycling, soil structure and permafrost protection (Chapin & Bledsoe, 1992; Tenhunen et. al. 1992). The sensitivity of bryophytes to some extreme winter climatic events may be similar to that of vascular plants, as the moss *Hylocomium splendens* experienced reductions in photosynthesis and growth of 52% and 48% respectively in response to simulated extreme winter warming (Bjerke et. al., 2011). Extreme winter warming is thought to cause these negative impacts by initiating growth of frost-sensitive shoot apices which are then damaged by the return of cold temperatures (Bjerke et al., 2011) – a similar mechanism

to that thought to drive damage in vascular vegetation. However, the impacts, and their mechanisms, of other extreme climatic events on bryophytes, particularly frost drought, are not known.

In contrast to bryophytes, existing work on the responses of lichens to extreme winter climatic events suggests they are rather tolerant. The most regionally abundant lichen species in northern Scandinavia, *Peltigera aphthosa*, was not affected by simulated extreme winter warming, and no negative effect of ice encapsulation was found for Arctic or alpine lichens (Bjerke et. al., 2009, 2011). This is likely to be because lichens do not undergo winter hardening and instead are well adapted to regulate their metabolism in response to acute temperature fluctuations (Benedict, 1990; Bjerke et al., 2011).

1.4.2 Ecosystem CO_2 balance

Until now, the impacts of extreme events on Arctic ecosystem CO_2 fluxes have received little attention. In the case of extreme climatic events, there has been only one previous full season assessment of CO_2 flux impacts following an event, which found a substantial 12% reduction in Gross Primary Productivity (GPP) (Parmentier et al., 2018). However, this eddy-covariance study was confounded by inter-annual variability in summer warmth, which made attributing and quantifying CO_2 flux changes to browning difficult. Similarly, a single time-point assessment of CO_2 fluxes following a field simulation of an extreme winter warming event found reductions in GPP of up to 93%, and variable impacts on ecosystem respiration. These results demonstrate potential for extreme climatic events to have a substantial impact on ecosystem CO_2 balance by altering soil and vegetation fluxes during the growing season. However the resolution of measurements currently available is insufficient to determine the magnitude of this impact, or how it may vary across the growing season or with event type.

Furthermore, the impacts of extreme climatic events specifically on bryophytes, a key component of high latitude ecosystems, are almost entirely unknown.

The impacts of insect defoliation events on ecosystem CO_2 balance are better understood than those of climatic extreme events. A range of examples from outside of the Arctic clearly demonstrate that defoliation can have major impacts on carbon balance (Kurz et. al., 2008; Clark et al., 2009; Shafer et al., 2010), while in the sub-Arctic an outbreak of the defoliating larvae of a geometrid moth reduced the CO_2 sink strength of mountain birch forest by 89% across the growing season (Heliasz et. al., 2011), illustrating that these substantial effects can also be felt in Arctic regions. However, given differences in the ecological process associated with browning driven by insect outbreak when compared with other extreme event drivers (in particular high nutrient inputs of insect frass and carcases during insect outbreaks), it is unclear whether effects on belowground processes, and therefore on ecosystem CO_2 fluxes, will differ between insect defoliation and climatic events. In addition, previous assessments of insect outbreak impacts on CO_2 fluxes have typically focussed on the tree canopy, despite major damage to the understory often also occurring (Karlsen et. al., 2013; Bjerke et. al., 2014).

1.5 Approaches to studying extreme event-driven Arctic browning

Approaches to studying winter extreme events which drive Arctic browning include (i) field observation studies, (ii) field manipulation experiments and (iii) remote sensing.

Of these approaches, field observation studies are the most commonly used, and for the widest range of event types. These allow for relatively easy and opportunistic assessment of the impacts of extreme events. Such studies have reported severity of browning, provided important insights into impacts on biomass, growth and phenology and shown initial evidence

of large-scale impacts on ecosystem CO_2 fluxes for both climatic winter extreme events (Bokhorst et al., 2009, 2011; Bjerke et al., 2014, 2017; Parmentier et al., 2018) and insect defoliation events (Heliasz et al., 2011; Jepsen et al., 2013; Parker et al., 2017) in Arctic regions. However, as field studies typically assess the consequences of a single, or a few events *a posteriori*, their ability to compare the impacts of different event types, or impacts in different vegetation types, is limited. In the case of climatic extreme events this approach is also unable to definitively assess the drivers of browning, or consider how variation in climatic conditions may drive variation in browning severity. Further, studying single events *a posteriori* relies on chance identification of browning in the field. This not only limits our understanding of extreme event driven browning to relatively accessible, populated Arctic regions, but also results in a reliance on peak season measurements, as identifying browned areas shortly after snowmelt is especially challenging. This is particularly problematic in Arctic regions, where the growing season is short and shoulder season are ecologically important (Ernakovich et al., 2014; Blume-Werry et al., 2016b).

In some cases, inferences from field studies have been built on and extended through field manipulations, notably of extreme winter warming in the Scandinavian sub-Arctic, simulated using infrared heat lamps and soil heating cables (Bokhorst et al., 2008). These extreme winter warming simulations, which produced impacts consistent with browning observed following natural events (Bokhorst et al., 2009), have demonstrated the mechanisms underlying the damaging effects of extreme winter warming events (see *1.3.2.*), suggested reasons for interspecific differences in sensitivity, and provided a detailed assessment of impacts on physiology throughout the growing season and over several years/successive events (Bokhorst et al., 2010; 2011; 2012). Similarly, field simulations of ice encapsulation in the Swedish sub-Arctic found major reductions in flowering and shoot mortality in some *Vaccinium* species

(Preece et al., 2012), possibly related to CO_2 accumulation (Preece & Phoenix, 2013), while other heathland species were generally tolerant (see also *1.3.3.*). However, the impacts of ice encapsulation were not as severe as expected, and these simulations did not reproduce the severe levels of mortality and stress observed following ice encapsulation at High Arctic regions (Hansen et al., 2014; Bjerke et al., 2017). It is not clear whether this is due to interspecific differences in sensitivity, or to differences in natural event severity, duration or other conditions compared to field simulations.

Field manipulations such as these provide critical process-based and mechanistic insight into extreme events drivers of browning, helping to improve our understanding of how the frequency and severity of browning may change as climate change progresses. There is scope to expand the use of this approach, possibly using laboratory as well as field experiments, to identify the physiological thresholds involved in identified responses involved in event-driven browning (e.g. premature dehardening during extreme winter warming events), thereby improving our ability to predict when browning may occur, and how its severity may scale with changing climatic conditions.

Another means of studying extreme event-driven browning which has potential both to enhance understanding of the relationship between browning severity and climatic drivers, and to assess and upscale impacts of browning across Arctic regions, is remote sensing. In particular the vegetation index NDVI (Normalised Difference Vegetation Index), a measure of vegetation greenness, has been used extensively to assess the scale and extent of browning trends across Arctic regions (Bhatt et al., 2013; Xu et al., 2013; Bieniek et al., 2015; Epstein et al 2015; 2016). NDVI has also been used to investigate the extent of known extreme event-driven browning events, providing an important indication of their consequences for greenness at

landscape or greater scales, and study the rate of ecosystem recovery (Bokhorst et al., 2009, 2012; Bjerke et al., 2014). However, using such assessments to upscale the impacts of browning events currently faces substantial challenges. This is not only because some impacts of browning, in particular impacts on CO_2 balance, remain relatively unknown, but also because it is not known whether relationships between NDVI and CO_2 uptake established in healthy vegetation (Street et al., 2007; Shaver et al., 2007, 2013) are maintained following extreme event-driven browning, or, if so, whether such relationships are broadly applicable or event type specific. Furthermore, the use of remote sensing to study extreme event-driven browning is challenged by the nature of the underlying drivers. Extreme events which drive browning are typically compound events; they are driven by multiple conditions and the interactions between them, rather than by the crossing of any single climatological threshold (Bjerke et al., 2017). They have therefore so far been defined by the initiation of an extreme ecological response, most obviously extensive mortality or a clear visible stress response (e.g. high, persistent anthocyanin pigmentation) in plant communities. The reduction in greenness associated with this extreme response at the scale of the satellite pixel will vary depending on not only the damage severity, but the density of the heathland vegetation which is most commonly affected by browning and a range of other ecological and physical factors (such as the presence of a tree canopy, the nature and abundance of moss and/or lichen ground cover, presence of bare ground/rock and moisture status). Therefore using NDVI to specifically detect extreme event driven browning is currently problematic.

An alternative approach would be to quantify the interacting climatological drivers which drive browning. This approach, when combined with mechanistic insights into browning from field studies and manipulation experiments, could facilitate assessment of when these drivers trigger ecologically extreme response, deepening our understanding of how variation in different

climatic conditions influences the severity and likelihood of browning, and allowing comparison between different event types. Process-based and mechanistic knowledge has previously been used in a similar way to develop metrics which improve detection of where simple (i.e. linked to a single climatic variable – such as droughts), climatologically defined extreme events are likely have an ecological impact (Sarojini et al., 2016).

1.6 Aim and scope of the project

Given the severity of browning following extreme events, predicted increases in the frequency of these events, and the direct contrast between their impacts and those of the more well understood Arctic greening trend, it is essential that we fully understand the consequences of extreme event-driven browning. Impacts on ecosystem carbon balance are especially important to this understanding in light of the crucial role of Arctic ecosystems in regulating global climate.

So far, most assessments of the consequences of extreme event-driven Arctic browning for ecosystem carbon balance have provided snapshots of impacts at peak season; impacts of browning across the growing season remain little understood. In addition, while it is increasingly recognised that browning responses to extreme events can include stress responses (visible as high anthocyanin pigmentation) as well as mortality, whether or how these stress responses influence CO_2 fluxes is not known. In addition to a full assessment of these impacts, accounting for the full growing season and the full range of browning responses, a process-based understanding of the underlying mechanisms is needed, showing how changes in above and below-ground processes contribute to net impacts on CO_2 exchange. Similarly, to definitively link specific climatic variables to extreme event-driven browning, or to determine

the contribution of extreme events to browning at regional or greater scales, a process-based understanding of how climatic drivers associated with winter extreme events interact to result in browning is needed.

Therefore, in this thesis, three core aspects of extreme-event driven Arctic browning are addressed:

i) The impacts of extreme events on net ecosystem CO_2 exchange, incorporating different types of event, the seasonality of impacts, and both mortality and visible stress responses.

ii) How changes in key CO_2 fluxes (i.e. productivity and respiration of vegetation and respiration from soils), and in related processes such as growth and decomposition rates, can provide mechanistic insight into the overall impacts on net ecosystem CO_2 exchange.

iii) The potential to upscale or assess the extent of browning impacts, either by establishing emergent relationships between browning impacts and remotely sensed vegetation indices, or using remotely sensed or modelled climatic data to quantify extreme event drivers and relate these to browning severity.

1.6.1 Impacts on net CO_2 balance

Impacts on net ecosystem CO_2 exchange (NEE) are central to determining the consequences of extreme event driven browning for ecosystem carbon balance, and, ultimately, the role of the Arctic in global climate. Studies of browning following insect outbreaks report major reductions in carbon sink capacity (Kurz et. al. 2008; Clark et al., 2009; Heliasz et al., 2011). However, although initial assessments of NEE following climatic extreme events indicate the

potential for large scale impacts, these are based on a single 'snapshot' of peak season CO_2 fluxes (Bokhorst et al., 2011), or are confounded by inter-annual variability in summer climate (Parmentier et al., 2018). The impacts of different extreme events which cause browning on NEE therefore remain little understood.

To address this, a study of the impacts of browning caused by a range of extreme event types on NEE was conducted at 5 sites along a latitudinal gradient spanning more than 1500km and 15˚ of latitude (Chapter 2). The use of multiple sites situated in different regions (boreal, sub-Arctic and High Arctic Norway), where browning is typically driven by different extreme event types, facilitated a comparison of the impacts of a range of event types on NEE. Building on this study of peak season impacts, a more detailed assessment of the impacts of climatic extreme events on NEE was completed at a single site in the Norwegian sub-Arctic (Chapter 3). This study measured NEE at control plots, plots dominated by shoot mortality, and plots dominated by a visible stress response, during early, peak and late season. It was therefore possible to assess differences in the impacts of extreme events which primarily cause stress or mortality, and to show how these impacts vary across the growing season.

1.6.2 Mechanisms of impacts on net CO_2 balance

An understanding of the processes underlying overall changes in NEE is central to considering how impacts on ecosystem carbon balance may differ between vegetation communities or with the severity of browning. Previous work has considered physiological impacts of browning, including on phenology, growth and reproduction (Bokhorst et al., 2008, 2010; Bjerke et al., 2014; 2017), and initial assessments of browning impacts on ecosystem CO_2 exchange have included measurements of ecosystem respiration and gross primary productivity (GPP; Bokhorst et al., 2011; Parmentier et al., 2018). However, there has been no attempt to link

productivity and respiration in different ecosystem components (vascular vegetation, moss layer and soil) to overall NEE impacts, or to relate CO_2 flux impacts to ecosystem processes such as growth and decomposition.

Therefore, GPP and ecosystem respiration were calculated alongside measurements of NEE in areas browned by a range of extreme event types from boreal to High Arctic regions (Chapter 2), and alongside a detailed assessment of the impacts of browning associated with both mortality and stress at a single sub-Arctic site across the growing season (Chapter 3). In the latter assessment, additional measurements of soil respiration and decomposition rates, as well as a small dataset of shoot-level CO_2 fluxes, were used to develop a process-based understanding of the causes of variation in NEE in browned vegetation across the growing season, and between browned plots dominated by mortality and by stress. This understanding was developed through both conventional analysis and Structural Equation Modelling (SEM). Measurements of shoot condition (indicated by colouration) and growth facilitated a link between assessments of productivity and consequences for physiology.

The moss layer is an important component of Arctic ecosystems, both in terms of biomass and productivity (Turetsky *et al.* 2010, 2012). A stand-alone assessment of the impacts of vascular understory browning on net CO_2 exchange, GPP and respiration in the moss layer was therefore used to investigate how moss activity contributed to overall browning impacts on NEE (Chapter 4). With field work completed alongside Chapter 3, this assessment indicated where there were similarities, and where there were differences, in the responses of bryophytes to extreme events compared to vascular vegetation, and related these responses to physiology using measurements of bryophyte segment growth rates.

1.6.3 Upscaling extreme event-driven browning

Although, as discussed in "Approaches to studying extreme event-driven browning", vegetation indices such as NDVI have been used to assess the areal extent of known browning events, further work is needed to extend this to upscaling and estimating the impacts of these browning events. Similarly, quantitative frameworks are needed to identify and upscale the impacts of browning events which are not identified through opportunistic field studies (for example to identify browning events in remote or under-studied areas), and to investigate the contribution of extreme events to browning at regional or greater scales.

Two approaches to these upscaling needs are taken in this work. Firstly, emergent linear relationships which can consistently and predictably link the observed severity of browning (measured both by visual assessment and plot-level NDVI measurements) with its impacts on CO_2 fluxes are investigated (Chapter 2). Limitations to these relationships, where browning impacts may not be clearly linked to visible browning (Chapter 3), or where browning may have contrasting impacts on difference vegetation components (Chapter 4), are also considered. Secondly, climate data, combined with measurements of browning severity and NDVI at a range of sites affected by extreme event-driven browning, is used to develop new metrics to quantify the climatic drivers of browning, and to identify correlations between these metrics and NDVI across the Norwegian Arctic region (Chapter 5). This demonstrates the potential to use simple climatic metrics to investigate the regional scale importance and impacts of extreme event driven Arctic browning.

Chapter 2

Extreme event impacts on CO_2 fluxes across a range of high latitude, shrub-dominated ecosystems.

2.1 Summary

1. Arctic ecosystems are warming at twice the global average rate. This rapid climate change is leading to more frequent extreme events, many of which can cause landscape-scale vegetation damage.

2. Extreme event-driven damage is strongly implicated as a driver of declines in vegetation productivity and biomass observed in many Arctic regions. This 'browning' has become an increasingly important trend in pan-Arctic vegetation change in recent years

3. However, despite the scale of extreme event-driven damage observed so far, assessments of the impacts on ecosystem CO_2 fluxes are rare. Given predicted increases in extreme event frequency and recent evidence of increasing browning, this creates considerable uncertainty around future Arctic landscape CO_2 balance.

4. To address this, impacts of damage driven by different extreme events (frost-drought, extreme winter warming, ground icing and insect outbreak) on the key growing season CO_2 fluxes Net Ecosystem Exchange, Gross Primary Productivity and ecosystem respiration were assessed at a range of sites from boreal to High Arctic regions (64˚N-79˚N) of the maritime European Arctic.

5. Despite the contrasting sites and browning drivers, damage had consistent, major impacts on all fluxes, causing site-level reductions of up to 81% of Net Ecosystem Exchange, 51% of Gross Primary Productivity and 37% of ecosystem respiration.

6. Furthermore, at sites where plot-level NDVI (greenness) data was obtained, linear relationships between NDVI and Gross Primary Productivity (explaining up to 91% of variation in the latter) were identified, indicating potential to estimate the regional impact of browning on CO_2 balance using remotely sensed vegetation indices.

7. This represents the first attempt to fully quantify the consequences of Arctic browning driven by different types of extreme events for the ecosystem CO_2 fluxes Net Ecosystem Exchange, Gross Primary Productivity and ecosystem respiration.

8. Understanding these impacts provides an important step towards incorporating extreme events into an understanding of how ecosystem CO_2 balance in high latitude ecosystems will respond to continuing climate change.

2.2 Introduction

Temperatures in the Arctic are increasing at twice the global average rate, with the most pronounced warming taking place in the winter months (Christensen *et. al.,* 2007; Peterson & Rocha, 2016, AMAP, 2017). Among the key consequences of this rapid increase in winter temperatures is an increase in the frequency of extreme events. These can cause vegetation damage and mortality at landscape or even regional scales (> 1000km^2, Jentsch et. al., 2007; Bokhorst et al., 2009; Vikhamar-Schuler et al., 2016), as has been observed through plot-level, regional and remote sensing studies (Beniston et. al., 2011; Bhatt et. al., 2013; Bjerke et. al., 2014, 2017). Extreme events, particularly those associated with winter conditions, have therefore been implicated as one of the key drivers of high latitude declines in biomass and productivity, or "Arctic browning", which has become an increasingly important process at regional to pan-Arctic scales in recent years (Epstein et al., 2015, 2016; Phoenix & Bjerke, 2016). Despite this, and despite predictions that the frequency and severity of a range of extreme event types will continue to increase as climate change progresses (Beniston et al., 2011; Graham et al., 2017), the impact of extreme event-driven vegetation damage on ecosystem CO_2 balance at high latitudes is largely unknown.

Extreme event drivers of Arctic browning may be climatic, biological (e.g. defoliating insect outbreak) or physical (e.g. fire) (Bokhorst et al., 2008; Mack et al., 2011; Jepsen et al., 2013; Phoenix & Bjerke, 2016; Bjerke et al., 2017). Among the most damaging climatic events are extreme winter warming, frost drought and ice encapsulation. Extreme winter warming events involve abrupt temperature increases of as much as 25°C in 24 hours, causing rapid snowmelt and premature dehardening and initiation of spring-like bud burst in exposed vegetation. A return to sub-zero winter temperatures then results in freezing damage (Bokhorst et. al., 2008, 2009, 2010). Frost drought occurs when vegetation adapted to a stable, insulating snow cover

becomes exposed during winter due to snow melt or removal (e.g. due to high winds). Enhanced transpiration in exposed vegetation, in combination with frozen soils, then results in desiccation and mortality, often at landscape scales (Tranquillini, 1982, Bjerke et al., 2017). This process is accelerated by high winds and irradiation (Hadley & Smith, 1986, 1989). Ice encapsulation through snow thaw-freeze and rain on snow events can cause severe damage to vegetation through a combination of hypoxia, CO_2 accumulation and exposure to greater temperature variability (Hansen et al., 2014; Milner et al., 2016), though some species may be generally tolerant (Preece *et. al.*, 2012; Preece & Phoenix, 201, 2014). Changes in winter conditions are also altering the frequency and severity of some biological events, for instance by increasing population outbreaks of defoliating insects, such as the caterpillars of the geometrid moths *Epirrita autumnata* and *Operophtera brumata* (Jepson et. al., 2008; Callaghan et al., 2010). Higher winter temperatures improve egg survival and facilitate range expansion in some defoliating species, increasing the incidence, intensity and duration of outbreaks (Jepson et. al., 2008; Wolf et. al., 2008; Johansson et. al., 2011).

The damage following such events can be considerable. In 2007 for instance, extreme winter warming in the Nordic Arctic Region (NAR) reduced Normalised Difference Vegetation Index (NDVI, a measure of greenness) by 26% over 1424km^2 the following growing season (Bokhorst et. al., 2009). In 2012, a combination of anomalous conditions caused NDVI across the NAR as a whole to decline to the lowest values ever recorded (Bjerke et. al., 2014). Such examples, while best documented in maritime, relatively southern regions of the Arctic, have been reported from sub-Arctic to High Arctic latitudes, and are expected to become increasingly significant at the pan-Arctic scale (Callaghan et. al., 2010; Hansen et. al., 2014; Graham et al., 2017).

However, while insect outbreak studies show event-driven browning can be decisive in determining ecosystem source-sink behaviour (Kurz et. al., 2008; Heliasz et. al., 2011; Parker et al., 2017), the consequences of other browning events for landscape CO_2 balance are largely unknown. Only one previous study has made an assessment of CO_2 fluxes following browning driven by an extreme climatic event in a northern peatland (Parmentier et al., 2018). While this work indicated a 12% reduction in GPP, full assessment of this event's effect on eddy covariance CO_2 fluxes was confounded by large inter-annual variability in summer climate. Similarly, a single time-point assessment taken during the growing season after an extreme winter warming field simulation found a reduction of more than 50% of GPP (Bokhorst et al., 2011). While that finding reflects just a snap-shot of the GPP response, it highlights that browning has the potential to substantially impact CO_2 balance through shoot mortality and loss of photosynthetic area; thus potentially altering soil and vegetation fluxes throughout the growing season.

This is of particular concern given that Arctic browning is in sharp contrast to a well-established consequence of summer warming at high latitudes; increased vegetation stature and productivity, termed 'Arctic greening' (Myneni et. al., 1997; Sturm et. al., 2001; Myers-Smith et. al., 2011). Greening reflects a considerable expansion of deciduous shrubs, as demonstrated by remote sensing, dendrochronology and plot-level studies (Sturm et. al., 2005; Tape et. al., 2006; Elmendorf et. al., 2012; Macias-Fauria et. al., 2012), and has been reported at global and regional scales (e.g. Jia et. al., 2009; Bhatt et. al., 2010; Xu et. al., 2013). However, while many climate models continue to assume arbitrary levels of greening across the Arctic (Pearson et al., 2013), evidence of browning has increased at local, regional and even pan-Arctic scales over the past decade (Bieniek et. al., 2015; Epstein et. al., 2015; Miles & Esau, 2016; Phoenix

& Bjerke, 2016), placing considerable uncertainty on the future of Arctic vegetation and productivity change, and therefore on the role of the Arctic in global climate.

There is therefore an urgent need to quantify the impacts of browning on the major ecosystem CO_2 fluxes (GPP, NEE and ecosystem respiration; R_{eco}), while also considering the different drivers of browning and the main affected vegetation types. Furthermore, as detailed CO_2 flux assessments in remote Arctic regions are problematic, determining the regional importance of Arctic browning would benefit from methods that allow prediction of carbon flux impacts remotely. Linear relationships have been reported between Leaf Area Index (LAI), as predicted from NDVI, and GPP and NEE across multiple vegetation types in high latitude ecosystems, allowing considerable simplification in quantifying ecosystem productivity across the Arctic (Street et. al., 2007; Shaver et. al., 2007). However, there is evidence that vegetation which survives extreme events can experience negative physiological effects, including reduced growth and berry production and delayed phenology (Bokhorst et al., 2008). It is therefore plausible that extreme event exposure may also reduce the photosynthetic capacity of surviving, green vegetation. This would weaken the relationship between NDVI and GPP in vegetation affected by extreme events. In addition, Emmerton et. al., (2015) found GPP correlated poorly with NDVI in polar semi-desert, attributing this to weak plant growth. It is thus unclear whether NDVI-CO_2 flux relationships will be maintained in vegetation damaged following extreme events.

To address these issues we assessed the impacts of extreme event-driven browning on growing season CO_2 fluxes in widespread, yet contrasting, heathland vegetation types affected by different browning drivers. Five sites along a 1600km latitudinal gradient, spanning 15˚ of latitude, allowed us to capture emergent variation and commonalities in response in boreal,

sub-Arctic and High Arctic regions, covering extreme winter warming, frost-drought, ground icing and insect outbreak as the drivers of damage. Plot-level measurements of NEE, GPP and R_{eco} were completed at each site at peak biomass across a range of undamaged to maximally damaged (heavily browned) plots, while transects were used to survey site-level damage severity and scale up plot-level CO_2 fluxes across each site. In addition, plot-level NDVI was recorded at a sub-set of sites to assess whether clear relationships between NDVI and ecosystem CO_2 fluxes exist in browned vegetation.

It was hypothesised that (i) browning would cause significant reductions in GPP and NEE (CO_2 uptake) across sites; (ii) R_{eco} (CO_2 release) would decrease due to less carbon available from lower GPP (though increased leaf and root litter inputs might, in contrast, stimulate microbial activity); (iii) Site-level reduction in GPP and NEE would decrease with increasing latitude due to lower leaf area and productivity of healthy vegetation; (iv) Where measured, clear relationships between CO_2 uptake (GPP and NEE) and NDVI would be identifiable across all latitudes and event types.

2.3 Methods

2.3.1 Site descriptions

Sites were located in the Norwegian boreal, sub-Arctic and High Arctic regions (covering latitudes from 64˚N to 79˚N) in areas known to have experienced extreme events during winter in the preceding three years (Table 2.1). Initials following site names denote region and primary driver of damage (e.g. "B_WW" = boreal, extreme winter warming).

Table 2.1: Summary of site characteristics

Name of site	Latitude (˚N)	Ecosystem type	Dominant heathland species	Browning driver	Years of damage
Flatanger_B_WW	64.4	Boreal	*Calluna vulgaris*	Primary: extreme winter warming. Secondary: frost drought	Winter 2013-2014
Storfjord_S_FD	69.3	Sub-Arctic	*Empetrum nigrum*	Frost drought	Winter 2011-2012
Håkøya_S_IO	69.7	Sub-Arctic	*Empetrum nigrum*	Insect outbreak	Summer 2014, 2015
Longyearbyen_H_IE	78.2	High Arctic	*Cassiope tetragona*	Ice encapsulation	Winter 2012, 2015
Ny-Ålesund_H_IE	78.9	High Arctic	*Cassiope tetragona*	Ice encapsulation	Winter 2012, 2015

Details of each study site in latitudinal order are as follows:

Flatanger-B-WW (boreal, Calluna vulgaris *heathland, 64.4˚N): Extreme winter warming and frost drought.*

Damage resulted from a combination of extreme winter warming and frost-drought in the winter of 2013-2014. Extreme winter warming in mid-December saw temperatures reach nearly 10˚C and remain elevated for around three weeks, causing complete snowmelt. Temperatures then rapidly fell back below 0˚C, dropping by 11.9˚C in 24 hours in early January, resulting in winter warming damage. High winds and exposure to some light are likely to have also caused desiccation over this period of exposure. The site was located on a shallow SE - facing slope and dominated by the dwarf shrub *Calluna vulgaris* (mean cover of 67%)

with ground cover of *Hylocomium splendens* and *Racomitrium* mosses (30%). *Vaccinium* species and *Erica tetralix* (all dwarf shrubs) were also common. Soils were thin (mean depth to underlying rock = 14.6cm) and patches of bare rock were common. The tree canopy was absent or sparse in this coastal area.

Storfjord-S-FD (sub-Arctic, Empetrum nigrum *heathland, 69.3˚N): Frost drought an extreme winter warming.*

Winter damage was identified in *Empetrum nigrum* heathland in this area in 2012 (see Bjerke et al. 2014 for further detail). The 2011-2012 winter was extremely dry, with total precipitation in December and January reaching 40% and 18% of the respective monthly means. The snowpack was therefore shallow (< 5cm) or absent for much of this period, which was also characterised by high temperature variability, leading to winter warming damage. Vegetation consists of almost continuous cover of *Empetrum nigrum* (79%) with thin, sparse ground cover of *Cladonia* lichens, and *Polytrichum* and *Hylocomium splendens* mosses (45%). Soils were thin (mean = 10.3cm).

Håkøya-S-IO (sub-Arctic, Empetrum nigrum *heathland, 69.7˚N):* Epirrita autumnata *caterpillar outbreak.*

Håkøya was damaged by two successive, severe outbreaks of *Epirrita autumnata* (autumn moth) caterpillars in 2014 and 2015. This led to not only defoliation of the tree birch canopy (the caterpillar's primary food source) but also defoliation of the deciduous understory and subsequent shoot mortality in ericaceous dwarf shrubs, particularly *Empetrum nigrum*. While not defoliated, damage in the evergreen *Empetrum nigrum* is thought to result from desiccation following the caterpillars puncturing the leaf cuticle while attempting to feed (Heliasz et. al., 2011). Vegetation is *Empetrum nigrum* (67%) dominated heath with ground cover of

Hylocomium splendens and *Pleurozium schreberi* mosses (54%). *Vaccinium* species and other small woody shrubs are also common. The site was located on a shallow N - facing slope with variable tree canopy density. There was, however, little entirely unaffected vegetation becasue caterpillars typically drop down from defoliated trees to feed on the understory below. Therefore a sub-site 580m downslope, where the lack of any tree canopy meant that vegetation was not damaged, was used to provide healthy vegetation plots. Soils were thin and comparable between sub-sites (mean = 13.62cm).

Svalbard sites: Longyearbyen-H-IE & Ny-Ålesund-H-IE (high Arctic, Cassiope tetragona *and* Dryas octopetala *heathland at both sites, 78.2˚N & 78.9˚N respectively): Ice encapsulation.*
All sites on Svalbard experienced winter warmth in combination with exceptionally heavy rain (up to 25% of mean total annual precipitation in one day), resulting in the formation of a thick layer of ground ice with the return (after the unusual winter warmth) of cold temperatures in January – February 2012 (Hansen et. al., 2014). Similar conditions and subsequent damage were observed in February 2015. Vegetation at both Longyearbyen and Ny-Ålesund was dominated by *Cassiope tetragona* (40%) and *Dryas octopetala* (10%). *Salix polaris* and *Saxifraga* species were also common. All sites were located on shallow slopes with no tree cover or field layer vegetation with a higher stature than that of *Cassiope tetragona*. Soil to bedrock or thaw depths were shallow (Longyearbyen mean = 14.60, Ny-Ålesund mean = 13.45).

2.3.2 Ecosystem CO_2 flux measurements (NEE, GPP and R_{eco})

At each site flux measurements were taken on 12-22 plots. Measurements were completed between 3 June and 17 June at Flatanger (17 plots), 21 June and 5 July on Svalbard (12 and 15 plots) and between 8 July and 30 July at Storfjord_S_FD and Håkøya_S_IO (21 and 22 plots).

NEE was measured using a LiCor LI6400 portable photosynthesis system (LiCor, Germany) and a custom 50 x 50 x 25cm transparent acrylic vegetation chamber (following Williams et al., 2006; Street et al., 2007). At sites on Svalbard, a 20 x 20 x 20cm chamber was used due to smaller vegetation stature and transport limitations. The chamber was placed on a rigid frame supported by aluminium poles driven into the ground. A seal was provided between the chamber and frame by a rubber gasket, and between the frame and ground surface by a flexible, transparent plastic skirt weighted down with steel chains. PAR was recorded using a LiCor Quantum sensor mounted inside the vegetation chamber. Enclosed volume was determined by using measurements of the height of the frame from the ground across a grid of nine points to calculate volume as four hexahedrons in addition to the chamber volume (which sat on top of this frame volume). Within the chamber, CO_2 concentration was measured every 2 seconds for 50 seconds. Where PAR varied by >15 %, measurements were discarded at the analysis stage. Measurements were carried out at 5 light levels (full light, 3 successive levels of shading and dark) in a randomised order using optically neutral shade cloths and tarpaulin to cover the chamber.

Light response curves of NEE and GPP were calculated following Street *et al.,* (2007). In brief, CO_2 concentration over time was converted to CO_2 flux, allowing the light response of net ecosystem exchange to be modelled as a rectangular hyperbola with a term for ecosystem respiration (R_{eco}). This modelled term was used for R_{eco}. Subtraction of R_{eco} from CO_2 flux measurements enabled a light response curve of GPP to be fitted, and thus GPP to be standardised at a PAR of 600 µmols PPFD m^{-2} s^{-1} (GPP_{600}). GPP_{600} represents flux at a medium light level and has been used previously to compare GPP between vegetation plots in the field (Shaver et al., 2007; Street et al., 2007). NEE was also standardised at this light level (NEE_{600}).

Surface temperature was recorded concurrently with CO_2 concentration data using a temperature probe inserted into the enclosed ground layer vegetation (bryophyte/lichen) or leaf litter. Air temperature was recorded by the LI-6400. Moss layer and soil surface moisture were recorded after each measurement set using a Delta-T HH2 moisture meter with a Theta probe (Delta-T, Cambridge, UK) inserted first at the surface of the moss layer and secondly at the soil surface at the same point, following removal of the moss layer.

2.3.3 Visual estimates of browning and NDVI

Percentage cover of dominant species, and of browned vegetation, was visually estimated at each plot using a quadrat matched to the size of the plot.

Simple transect surveys of percentage cover of dominant species and of browned vegetation were also recorded along 1 or 2 transects at each site. Transects were either > 20m with 3m intervals or > 30m with 5m intervals. The number and length of transects depended on the spatial extent of the dominant vegetation type at each site, or on the presence of site boundaries, specifically rock outcrops, roads and a fjord. At each interval within transects percentage cover was visually estimated in a 1m x 1m plot using four 50 x 50cm quadrats. Surveying damage in this way facilitated estimating mean percentage cover of damage, as well as mean damage intensity (the percentage of cover showing damage of the dominant species only) across each site.

Reflectance data was recorded at each plot in two sites: Flatanger_B_WW and Håkøya_S_IO. This was done using a standard DSLR camera (Canon 450D) in which the usual light sensor was replaced with an infrared sensor by optics company Llewellyn Data Processing

(MaxMax.com, New Jersey), enabling the camera to record visible light in the blue channel and near infrared in the red channel (Llewellyn Data Processing, New Jersey). This camera was calibrated by using a white square to manually set white balance prior to taking measurements at each site. NDVI was calculated from reflectance data photos using ENVI 5.2.

2.3.4 Statistical analysis

Linear regression was used to identify relationships between CO_2 fluxes and vegetation damage at each site. Linear regression parameters were then used to estimate the site level reductions in CO_2 fluxes at the mean level of damage across each site compared to undamaged vegetation. At Ny-Ålesund, non-linear regressions were also fitted using self-starting asymptotic models, due to visually apparent non-linearity in the plotted data. The goodness of fit provided by linear and non-linear models at Ny-Ålesund was assessed by using an F-test (analysis of variance) to compare residual sum of squares, and by comparing AIC values. All statistical analyses were carried out in R (R Core Team, 2017).

2.4 Results

2.4.1 Site differences in baseline CO_2 fluxes and severity of vegetation damage

Substantial and relatively consistent levels of damage were recorded at all sites (Figure 2.1).

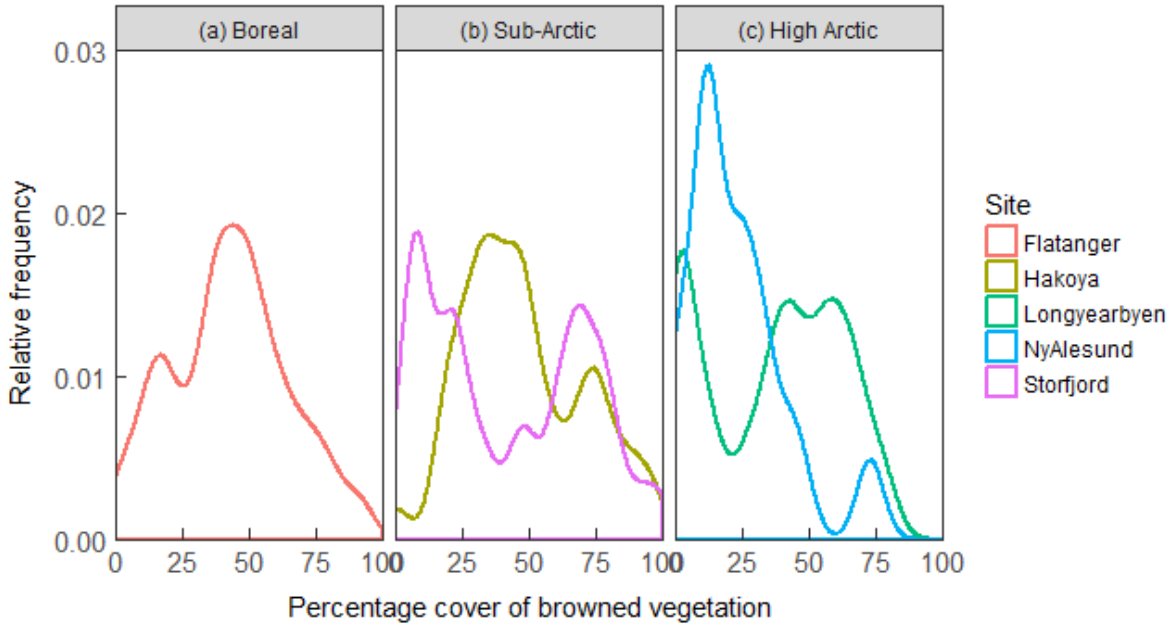

Figure 2.1: Polygons of the relative frequency (on a scale of 0 to 1) of total vegetation damage (percentage cover of browned vegetation) as recorded by transect surveys at (a) boreal, (b) sub-Arctic and (c) High Arctic sites.

Mean percentage cover of damaged vegetation (percent browned) was lowest at the High Arctic sites and similar between sub-Arctic and boreal latitudes (Table 2.2). Percent cover browned ranged from 23% at the High Arctic site Ny-Ålesund-H-IE to almost 50% at the sub-Arctic site Håkøya_S_IO. However, damage intensity (i.e. the proportion of the dominant species showing damage) was more variable, and was highest at Longyearbyen_H_IE (80%). This reflected heavily damaged, but fairly sparse heathland vegetation at this site. Damage intensity was relatively low at Storfjord_S_FD (51%), particularly when compared to the second subArctic site Håkøya_S_IO (76%), or to the boreal site Flatanger_B_WW (66%), where the

mechanism of damage was similar to that at Storfjord_S_FD. The lower damage severity observed at Storfjord_S_FD may be related to differences in recovery time since the extreme event that caused damage (3 full growing seasons at Storfjord_S_FD, compared to 1 at Flatanger_B_WW and less than 1 at Håkøya_S_IO).

Table 2.2: Mean degree of damage assessed visually across transects at each site, presented as both overall mean percentage cover of damage and mean percentage of the cover of the dominant species showing damage.

	Site				
	Flatanger_B_WW	Storfjord_S_FD	Håkøya_S_IO	Longyearbyen_H_IE	Ny-Ålesund_H_IE
Mean percentage cover of damaged vegetation	43	42	48	37	23
Mean damage intensity (percentage of dominant species showing damage)	66	51	76	80	56

2.4.2 Impacts of browning on NEE, GPP and R_{eco}

2.4.2.1 Site-level correlations

CO_2 uptake in undamaged vegetation was highest at boreal latitudes with both GPP_{600} and NEE_{600} declining by around 75% from boreal to High Arctic latitude sites (where CO_2 uptake was lowest). R_{eco} in undamaged vegetation was highest at sub-Arctic latitudes and around 30% and 50% lower at boreal and High Arctic latitudes respectively, compared to sub-Arctic sites.

Significant linear declines in both GPP_{600} and NEE_{600} with increasing percentage browned were identified at all sites (Figure 2.2, Table 2.3 for statistics). These relationships explained up to 82% and 61% of variation in GPP_{600} and NEE_{600} respectively (at Håkøya_S_IO).

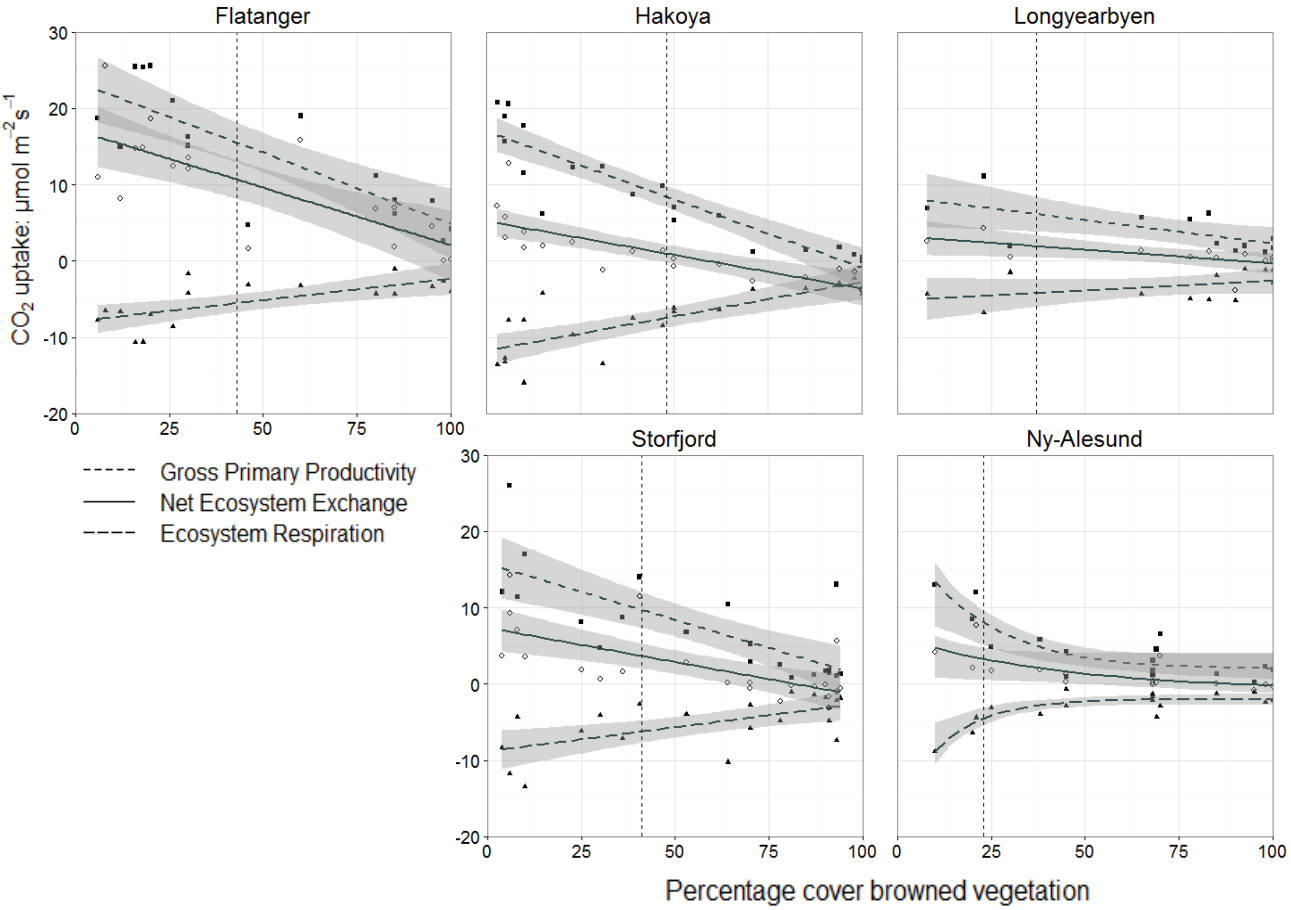

Figure 2.2: Impacts of browning on CO_2 uptake (GPP_{600} and NEE_{600}) and CO_2 release (R_{eco}) at boreal (left), sub-Arctic (centre) and High Arctic (right) latitudes. Vertical dashed lines indicate mean percentage cover of damaged vegetation at each site.

Table 2.3: Coefficients and summary statistics for linear regressions of percentage cover of damaged vegetation against GPP_{600}, NEE_{600} and ecosystem respiration at each site.

Site	Flux											
	Gross Primary Productivity				Net Ecosystem Exchange				Ecosystem Respiration			
	Slope	Intercept	R^2	*p* value	Slope	Intercept	R^2	*p* value	Slope	Intercept	R^2	*p* value
Flatanger_B_WW	-0.207	25.1	0.65	<0.001	-0.151	17.2	0.53	<0.001	0.056	-7.94	0.42	<0.01
Storfjord_S_FD	-0.179	18.2	0.55	<0.001	-0.090	7.38	0.43	<0.001	0.089	-10.8	0.37	<0.01
Håkøya_S_IO	-0.179	17.0	0.82	<0.001	-0.089	5.24	0.61	<0.001	0.090	-11.8	0.59	<0.001
Longyearbyen_H_IE	-0.061	8.4	0.37	0.021	-0.036	3.25	0.32	0.031	0.025	-5.16	0.09	0.18
Ny-Ålesund_H_IE	-0.102	10.4	0.57	<0.001	-0.051	4.38	0.44	<0.01	0.051	-6.00	0.45	<0.01

The negative correlations between percent browned and GPP_{600} and NEE_{600} were steepest at Flatanger_B_WW, the most productive site, where percent browned explained 65% and 53% of variation in each flux respectively. Correspondingly, the slopes of these relationships were shallowest at Longyearbyen_H_IE, the least productive site, while nonetheless explaining 37% and 32% of variation in GPP_{600} and NEE_{600} respectively.

At sub-Arctic and High Arctic sites, the most heavily damaged vegetation was a net CO_2 source, compared to healthy and less heavily damaged vegetation which was a net CO_2 sink. At High Arctic sites this was the case only for extreme levels of damage (> 91% at Longyearbyen_H_IE and > 86% at Ny-Ålesund_H_IE) which were rare in the sparse heathland vegetation at these sites. However, vegetation more than 59% and 83% browned was a CO_2 source at Håkøya_S_IO and Storfjord_S_FD respectively.

R_{eco} also decreased with percent browned; significant declines were seen at all sites except Longyearbyen_H_IE. The negative relationships between R_{eco} and percent browned explained between 37% and 59% of variation in this flux (at Storfjord_S_FD and H Håkøya_S_IO respectively), and were steepest at these sub-Arctic sites, where R_{eco} in undamaged vegetation was higher than at boreal or High Arctic sites. While the decline in R_{eco} with increasing percent browned at Longyearbyen_H_IE was not statistically significant, a significant relationship was established at Ny-Ålesund_H_IE ($R^2 = 0.67$, $p < 0.001$).

At the High Arctic site Ny-Ålesund_H_IE, linear regressions of all three CO_2 fluxes and percent browned were significant. However, visual assessment suggested reductions in CO_2 fluxes with increasing percent browned may be nonlinear. An asymptotic regression model provided a better fit for GPP_{600} (Reduction in RSS = 33.9, $F = 7.86$, $p = 0.015$) and for R_{eco}

(Reduction in RSS = 19.67, $F = 16.37$, $p = 0.001$), but was not significantly different to a linear regression in the case of NEE_{600}. Nonetheless, linear regressions were used to estimate site-level impacts (see below) at Ny-Ålesund_H_IE. This was partly to maximise comparability of estimates between sites, and partly due to concern that the accuracy of the nonlinear regressions fitted may be limited, particularly at low values of percent browned, by a relative lack of plots with very little damage assessed at Ny-Ålesund_H_IE, compared to other sites.

At all sites except Longyearbyen_H_IE, significant linear increases in CO_2 fluxes with increasing total percent cover of green leaf area (percent green) were also found (Appendix 1), with explanatory power similar to or greater than the CO_2 flux- percent browned relationships. When data from all sites was combined, linear declines in all measured fluxes with increasing percent browned remain significant (Appendix 2; GPP_{600}: $R^2 = 0.55$, $p < 0.001$, NEE_{600}: $R^2 = 0.332$, $p < 0.001$, R_{eco}: $R^2 = 0.413$, $p < 0.001$). Multiple regressions of GPP_{600}, NEE_{600} and R_{eco} against percent browned and dominant heathland species (*Calluna vulgaris*, *Empetrum nigrum* or *Cassiope tetragona*) explain 69% of overall variation in GPP_{600}, 63% in NEE_{600} and 50% in R_{eco} ($p < 0.001$).

2.4.2.2 Site level reductions

At the boreal extreme winter warming site Flatanger_B_WW, GPP_{600} at mean percent browned was reduced by 35% compared with that of undamaged vegetation (Figure 2.3a), while NEE_{600} was reduced by 38% (Figure 2.3b) and R_{eco} by 30%. In absolute terms, the reductions at this most productive site were the largest.

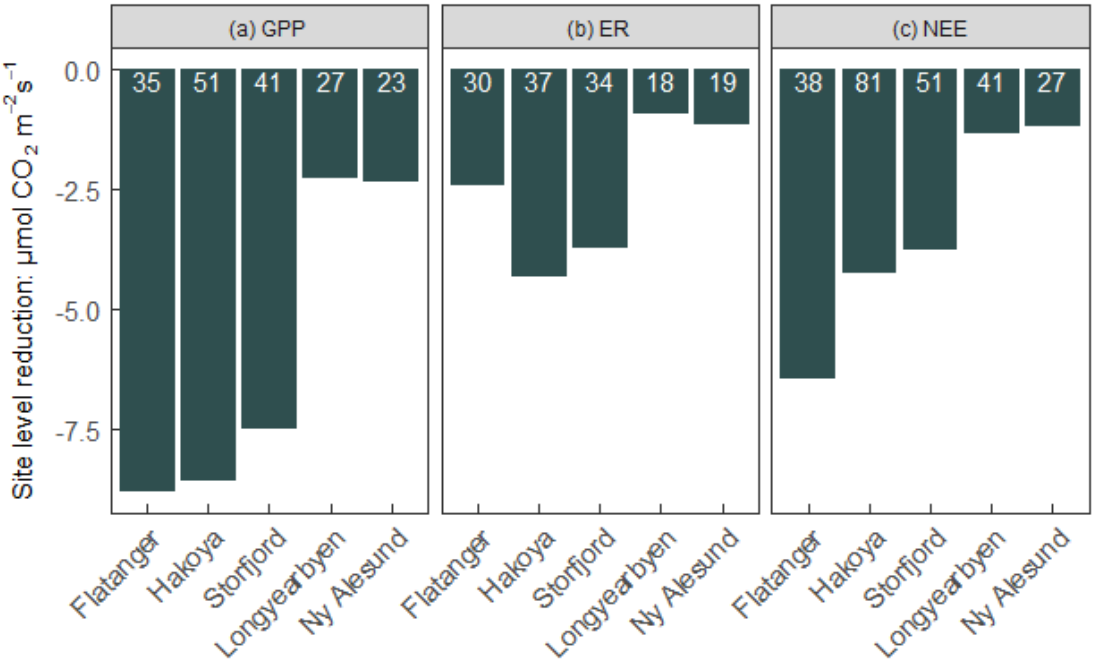

Figure 2.3: Reduction in (a) GPP_{600} (b) ecosystem respiration and (c) NEE_{600} at the mean percentage cover of browned vegetation for each site. Bar labels indicate the percentage of each flux in healthy vegetation at the same site that this reduction represents.

Site-level CO_2 uptake reductions according to mean percent browned at the sub-Arctic insect outbreak and frost-drought sites Håkøya_S_IO and Storfjord_S_FD were lower in absolute terms than at Flatanger_B_WW; however lower baseline productivity in the sub-Arctic region meant that reductions at these sites accounted for the largest proportion of the productivity of healthy vegetation, with GPP_{600} reduced by 51% and 41% and NEE_{600} by 81% and 61% at Håkøya_S_IO and Storfjord_S_FD respectively. R_{eco} was reduced by 35-37% according to mean percent browned at these sites.

Site-level reductions in CO_2 uptake according to mean percent browned were lower at High Arctic ice encapsulation sites compared with sub-Arctic and boreal regions. GPP_{600} was reduced by 27% at Longyearbyen_H_IE and 23% at Ny-Ålesund_H_IE. The smaller reductions here are partly due to lower mean percent browned values at High Arctic sites; at a

percent browned of 50%, GPP_{600} reductions at Longyearbyen_H_IE and Ny-Ålesund_H_IE are 36% and 49% respectively, comparable with values of between 41% and 53% at the other sites at the same level of browning.

2.4.3 Relationships between NDVI and fluxes

Strong linear relationships were identified between GPP_{600} and NDVI, with NDVI explaining 78% of variation in GPP_{600} at the boreal extreme winter warming site Flatanger_B_WW and 91% at the sub-Arctic insect outbreak site Håkøya_S_IO (Figure 2.4a; Flatanger_B_WW: R^2 = 0.783, fitted line: y = 3.537 + 30.158x, *DF* = 1,15, $p < 0.001$, Håkøya_S_IO: R^2 = 0.913, fitted line: y = -13.381 + 43.801x, *DF* = 1, 14, $p < 0.001$). A significant relationship explaining 49% of variation in GPP_{600} was maintained when data from both sites were combined (R^2 = 0.492, fitted line: y = -0.2321 + 27.707x, *DF* = 1, 31, $p < 0.001$). Significant relationships between NDVI and NEE_{600} also explained 67% and 80% of NEE_{600} at Flatanger_B_WW and Håkøya_S_IO respectively (Figure 2.4b; Flatanger_B_WW: R^2 = 0.671, fitted line: y = 1.252 + 22.456x, *DF* = 1, 31, $p < 0.001$, Håkøya_S_IO: R^2 = 0.796, fitted line: y = -10.775 + 23.844x, *DF* = 1,14, $p < 0.001$). However, although significant, the explanatory power of the NDVI - NEE_{600} relationship when data were combined was low comparative to when sites are treated separately (R^2 = 0.223).

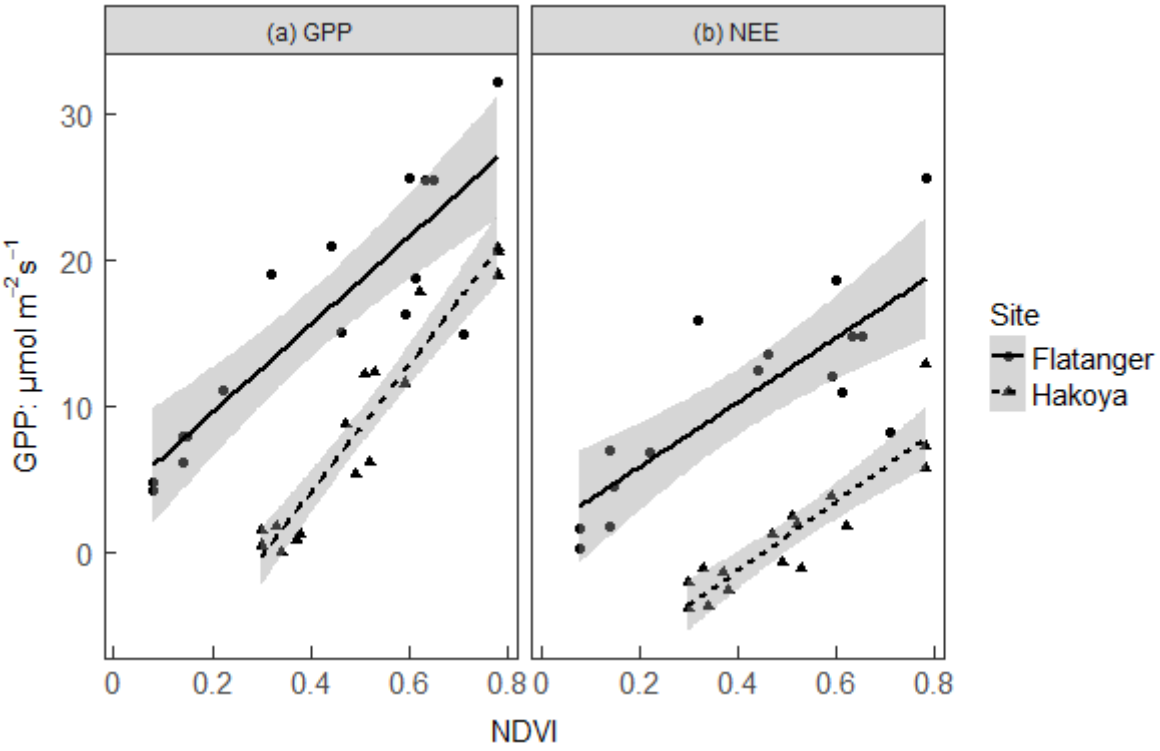

Figure 2.4: Linear correlations between NDVI and (a) GPP_{600} (Flatanger_B_WW: R^2 = 0.783, fitted line = 3.537 + 30.158x, *DF* = 1,15, p < 0.001, Håkøya_S_IO: R^2 = 0.913, fitted line: y = -13.381 + 43.801x, *DF* = 1, 14, *p* < 0.001) and (b) NEE_{600} (Flatanger_B_WW: R^2 = 0.671, fitted line = 1.252 + 22.456x, *DF* = 1, 31, *p* < 0.001, Håkøya_S_IO: R^2 = 0.796, fitted line: y = -10.775 + 23.844x, *DF* = 1,14, *p* < 0.001).

2.5 Discussion

This first detailed assessment of the consequences of extreme event-driven browning for ecosystem CO_2 fluxes has shown major impacts on GPP_{600}, R_{eco} and NEE_{600}, representing a substantial reduction in carbon sequestration capacity at peak biomass, when productivity should be at its highest. The magnitude of these impacts is clearly and predictably linked to the observed severity of damage. Fluxes were also closely coupled to NDVI (where measured at two sites), indicating potential to estimate extreme event impacts on CO_2 balance using remotely sensed NDVI.

2.5.1 Impact of damage on GPP

Significant linear declines in GPP_{600} with percent browned were ubiquitous, with GPP_{600} reductions clearly and consistently related to the severity of damage across the full range of sites. The relationships between GPP_{600} and percent browned were similar between sites, with inter-site differences that were observed (steeper slopes at more southerly sites) primarily driven by differences in productivity of undamaged vegetation associated with different dominant vegetation types: together, percent browned and dominant heathland species explained 69% of variation in GPP_{600} across all sites. This indicates a high commonality in the response of GPP (once vegetation differences in productivity are taken into account) to extreme event-driven browning, regardless of the specific driver of damage.

However, while there was a significant linear GPP_{600} - percent browned relationship at Ny-Ålesund_H_IE, a nonlinear model provided a better fit to the relationship at this site. This nonlinear relationship reflects larger reductions in CO_2 uptake at lower levels of percent browned compared with other sites, indicating that at this site, exposure to an extreme event

(ground icing) may have negatively impacted vegetation which has not been killed. This expands on previous studies which have shown that ice encapsulation can have physiological impacts on undamaged shoots, including by reducing flowering and berry production in some Arctic species (Preece et al., 2012; Preece & Phoenix, 2013; Milner et al., 2016). Here, the nonlinear relationship between GPP_{600} and percent browned suggests that physiological damage extends to photosynthetic capacity, reducing CO_2 uptake beyond what would be expected based on the observed level of mortality. This may be linked to a 'stress response' sometimes observed in surviving vegetation following extreme event exposure, visible as a deep red (anthocyanin) pigmentation (Bjerke et al., 2017).

When upscaled from site damage surveys, the decline in GPP_{600} with increasing damage translated to major overall reductions in productivity, which are similar to or greater than reductions suggested by initial assessments of climatic extreme events in similar regions (Bokhorst et al., 2011; Parmentier et al., 2018). The greatest reduction in absolute terms was at Flatanger_B_WW, where the productivity of undamaged vegetation was also highest. However, percent reductions were greatest at sub-Arctic sites. This is likely due to a combination of high leaf area relative to the high Arctic at sub-Arctic latitudes, facilitating substantial GPP reductions following damage, and lower productivity of healthy vegetation compared to boreal regions, meaning GPP reductions are of greater proportional importance. Heavily damaged vegetation at these sub-Arctic sites was even converted to a net CO_2 source, supporting previous work reporting major reductions in sink strength following insect defoliation (Kurz et. al., 2008; Heliasz et. al., 2011), and further suggesting that such substantial impacts can be expected following a broader range of extreme event types. That high levels of damage and corresponding GPP_{600} reductions are still evident at the sub-Arctic site Storfjord_S_FD, following three growing seasons of recovery, suggests a caveat to previous

work that showed recovery from event-driven browning can be quick (Bokhorst et. al., 2012): where damage is severe and results in extensive mortality - at the population as well as the plant shoot level - recovery may be slower, allowing landscape-level consequences for CO_2 uptake to persist over several years.

Although the effects of damage in the high Arctic, where GPP_{600} was reduced by 23-27%, are smaller than at other latitudes, these impacts remain important. Productivity at peak biomass is particularly crucial in the high Arctic due to the brevity of the growing season: as much as 80% of carbon fixation in Arctic heathland may occur between June and September (Larsen et al., 2007). Even a relatively small reduction in peak biomass GPP_{600} may therefore substantially alter annual CO_2 balance.

At all sites except Longyearbyen_H_IE, GPP_{600} was also positively correlated with the percent cover of green, healthy vegetation, which explained up to 88% of variation in GPP_{600}. This is clearly driven by the close relationship between GPP and leaf area established in healthy vegetation in Arctic ecosystems (Street et al., 2007; Shaver et al., 2013). However, that this relationship is maintained following extreme event driven damage is further indication that GPP reductions at these sites have been driven directly by a loss of live leaf area, and that any stress experienced by remaining green shoots has had a minimal impact on photosynthetic capacity (with the possible exception of Ny-Ålesund_H_IE).

2.5.2 Impact of damage on ecosystem respiration

Contrary to expectations, R_{eco} decreased at all sites with increasing percent browned (although this was not statistically significant at Longyearbyen_H_IE). R_{eco} was hypothesised to decrease due to reduced availability of carbon for respiration following a decline in GPP (Parker et al.,

2017). Alternatively, however, it was suggested that faster decomposition following increased litter inputs, warming of the soil surface, and (in the case of Håkøya_S_IO) high nutrient inputs in the form caterpillar frass and carcases (Baranchikov et al., 2002; Frost & Hunter, 2008; Kaukonen et. al., 2013) could increase R_{eco}. That reductions in R_{eco} were consistently observed with increasing damage suggests that substantial reduction in live leaf area and GPP, whether driven by insect outbreak or extreme climatic conditions, drive down R_{eco}. Certainly, reduced GPP will be the cause of any decline in autotrophic respiration (Litton et al., 2007). Any reduced allocation of carbon below ground is also likely to reduce heterotrophic respiration (Högberg et al., 2001). While heterotrophic and autotrophic respiration have not been separated in this study, the overall decline in R_{eco} may suggest that the effect of reduced carbon for heterotrophic respiration over-rides any possible effect of stimulated respiration from improved abiotic conditions (e.g. greater soil warmth and moisture due to exposure and reduce evapotranspiration) or increased litter inputs from dead plant material.

Stable or reduced R_{eco} following insect outbreak and frost events has previously been attributed to reduced leaf respiration and root growth, reduced microbial abundance and activity, and microbial mortality, resulting from decreased carbon transfer belowground (Grogan et al., 2004; Read et al., 2004; Christiansen et al., 2012; Zhao et al., 2017; Olsson et al., 2017; Parker et al., 2017). Parker et al. (2017) argue that where increased respiration is observed following insect outbreak (e.g. Frost & Hunter, 2004), this reflects increased belowground carbon allocation in an attempt to recover lost nitrogen, and is a response to comparatively mild defoliation damage. In contrast, Parker et al. (2017) shows that after total defoliation, belowground carbon allocation decreases, slowing soil processes including respiration. The results presented here support this, and suggest that climatic extreme events can result in a similar deceleration of soil processes, as is further indicated by observations of reduced root

growth and mycorrhizal biomass following an extreme winter warming field simulation (Bokhorst et al., 2009).

2.5.3 Impact of damage on NEE

Declines in NEE_{600} with damage were similar between sites, indicating a high commonality of response to different extreme event drivers of browning, similar to that seen for GPP_{600}. This consistency was particularly marked between Håkøya_S_IO and Storfjord_S_FD in the sub-Arctic, where the regression slopes of NEE_{600} and percent browned differed by < 0.001, despite the very different drivers of damage at these two sites (defoliating insect outbreak and frost-drought). This further suggests that any direct belowground effects specific to insect outbreaks as opposed to other event types (e.g. frass input), are relatively minor compared to impacts on vegetation with their above and belowground consequences, in terms of key ecosystem CO_2 fluxes.

Major site-level reductions in NEE_{600} were found at all sites. As for GPP_{600} these were most substantial in absolute terms at the boreal site Flatanger_B_WW, while percentage reductions were highest at the sub-Arctic sites, where NEE was more than halved. These changes represent substantial reductions in net CO_2 uptake capacity. That these impacts may even be comparable with the impact of wildfire in heathland vegetation is suggested by a small-scale assessment of CO_2 fluxes within an area of burned heathland adjacent to Flatanger_B_WW, which found that, less than 1 growing season after the fire, the average reduction in NEE_{600} compared to healthy vegetation was equal to that associated with 69% browned cover (unpublished data).

2.5.4 Relationships between NDVI and CO_2 fluxes

Highly significant linear relationships between NDVI and GPP_{600} were identified at both sites where NDVI was measured (R^2 = 0.78-0.91), and maintained when data from both sites were combined (R^2 = 0.49). Strong relationships were also found between NDVI and NEE_{600}, although when data were combined the explanatory power of this relationship was low (R^2 = 0.22). This suggests that with a simple characterisation of widespread Arctic heathland (e.g. dominant species), change in NDVI can provide a direct, accurate estimate of CO_2 uptake reduction following extreme event-driven browning: while an acceptable estimate of GPP reduction may be made even without such vegetation characterisation.

Previous work has found an exponential relationship between NDVI and GPP_{600}, explaining 75% of variation in GPP_{600} across multiple Arctic vegetation types (Street et al., 2007). That a linear, rather than an exponential, relationship is seen here may be linked to canopy structure (Steltzer & Welker, 2006). Arctic heathland has a homogenous canopy structure, meaning increases in greenness reflect proportional increases in leaf area. In contrast, across multiple Arctic vegetation types, NDVI increases at low values reflect increasing total vegetation cover, while NDVI increases at high values occur in plant communities where the canopy is already closed, and therefore reflect a comparatively greater increase in LAI. As LAI drives GPP, this means a linear NDVI - GPP_{600} relationship within a distinct vegetation type with a homogenous canopy structure is consistent with a nonlinear, pan-Arctic relationship across multiple vegetation types and canopy structures. For the same reason, a linear relationship between NDVI and GPP_{600} may be likely following browning within a given vegetation type: low NDVI values following browning represent a reduction in greenness, but without a change in canopy structure complexity.

These results indicate that established relationships between NDVI and CO_2 uptake are maintained following extreme event-driven browning, highlighting potential to use remotely sensed NDVI to upscale browning impacts. However this approach is challenging: suitability of satellite pixel-level NDVI for estimating CO_2 uptake can be reduced by factors such as vegetation heterogeneity, the contribution of mosses to the NDVI signal and confounding impacts of open water, clouds and low solar angles, particularly at high latitudes (Guay et al., 2014; Emmerton et al., 2015).

2.6 Conclusion

Extreme event-driven Arctic browning caused major reductions in key ecosystem CO_2 fluxes from boreal to high Arctic latitudes. Relationships between CO_2 fluxes and the extent of visible damage were consistent, demonstrating that net impacts are overwhelmingly determined by the severity of damage, regardless of the cause of browning. Furthermore, clear, linear relationships between CO_2 uptake and NDVI highlight potential to use remotely sensed vegetation indices, such as NDVI, to directly upscale the impacts of browning caused by multiple drivers on productivity in widespread dwarf shrub Arctic vegetation.

Given the considerable consequences for landscape CO_2 balance, there is a clear need to understand the regional and pan-Arctic importance of extreme event-driven browning. As many of the events causing vegetation damage occur more frequently with continuing climate change, it will become increasingly important to incorporate their effects into predictions of future vegetation change in the Arctic, and into estimations of Arctic carbon balance.

2.7 Appendix 1: Table 2.4

Table 2.4: Coefficients and summary statistics for linear regressions of percentage cover of green, undamaged vegetation against GPP_{600}, NEE_{600} and ecosystem respiration at each site.

Site	Flux											
	Gross Primary Productivity				Net Ecosystem Exchange				Ecosystem Respiration			
	Slope	Intercept	R^2	*p* value	Slope	Intercept	R^2	*p* value	Slope	Intercept	R^2	*p* value
Flatanger_B_WW	0.209	3.67	0.72	<0.001	0.150	1.46	0.60	<0.001	-0.055	-2.21	0.44	<0.01
Storfjord_S_FD	0.181	-0.14	0.67	<0.001	0.089	-1.76	0.50	<0.001	-0.092	-1.6	0.48	<0.001
Håkøya_S_IO	0.169	-0.51	0.88	<0.001	0.083	-3.99	0.64	<0.001	-0.085	-2.5	0.65	<0.001
Longyearbyen_H_IE	0.033	3.09	0.05	0.25	0.022	0.06	0.07	0.21	-0.011	-3.03	0.00	0.55
Ny-Ålesund_H_IE	0.123	0.85	0.78	<0.001	0.600	-0.34	0.56	<0.001	-0.063	-1.19	0.67	<0.001

2.8 Appendix 2: Figure 2.5

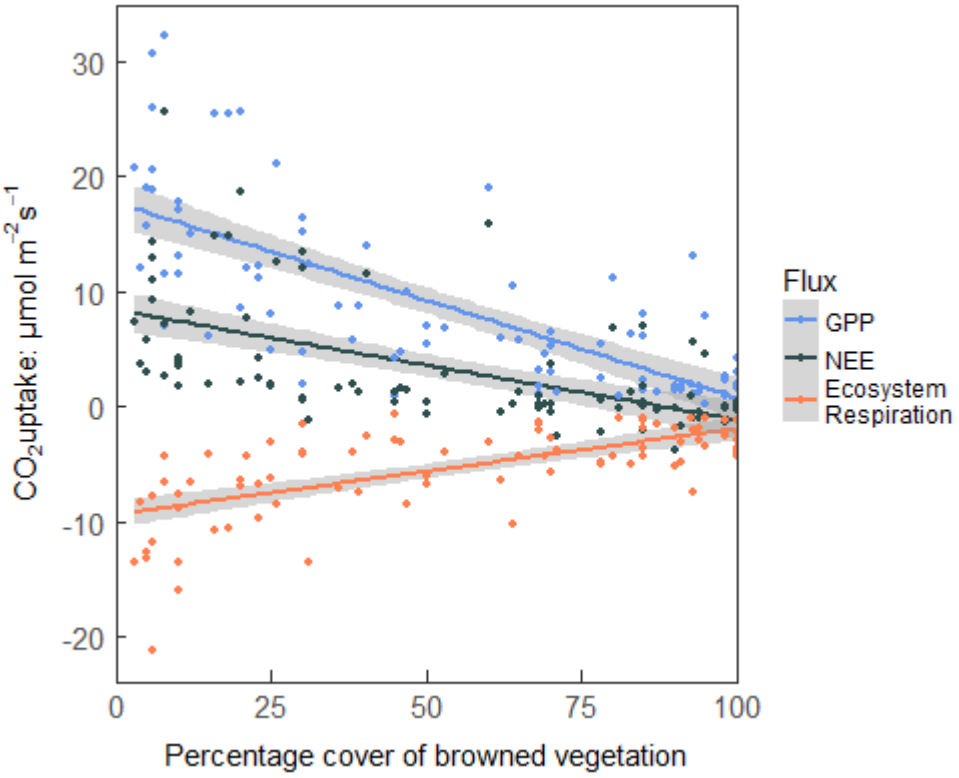

Figure 2.5: Linear regressions of percentage cover of browned vegetation against the CO_2 fluxes GPP600 (R^2 = 0.55, $p < 0.001$), NEE600 (R^2 = 0.33, $p < 0.001$) and R_{eco} (R^2 = 0.41, $p < 0.001$) when data from all sites is combined.

Chapter 3

Impacts of extreme climatic events on ecosystem CO_2 fluxes throughout the growing season

3.1 Summary

1. Extreme climatic events are among the drivers of recent declines in plant biomass and productivity observed across Arctic ecosystems, known as 'Arctic browning'.

2. These events can cause landscape scale vegetation damage, and so are likely to have major impacts on ecosystem CO_2 balance. However, there is little understanding of the impacts on carbon fluxes, especially across the growing season.

4. Furthermore, while widespread shoot mortality is commonly observed with browning events, recent observations show that shoot stress responses are also common, and manifest as high levels of persistent anthocyanin pigmentation. Whether or how this response impacts ecosystem CO_2 fluxes is not known.

5. A growing season assessment of browning impacts following frost drought and extreme winter warming (both extreme climatic events) on the key ecosystem CO_2 fluxes Net Ecosystem Exchange (NEE), Gross Primary Productivity (GPP), ecosystem respiration (R_{eco}) and soil respiration was carried out in widespread sub-Arctic dwarf shrub heathland, incorporating both mortality and stress responses.

6. Browning (mortality and stress responses combined) caused considerable site-level reductions in GPP and NEE (of up to 44%), with greatest impacts occurring at early and late season. Further, impacts on CO_2 fluxes associated with stress often equalled or exceeded those resulting from vegetation mortality.

7. This demonstrates that extreme events can have major impacts on ecosystem CO_2 balance, considerably reducing the carbon sink capacity of the ecosystem, even where vegetation is not killed.

8. Structural Equation Modelling and additional measurements, including of decomposition rates and leaf respiration, provided further insight into the mechanisms underlying impacts of mortality and stress on CO_2 fluxes.

9. The scale of reductions in ecosystem CO_2 uptake associated with both mortality and sub-lethal stress highlights the need for a process-based understanding of Arctic browning in order to predict how Arctic vegetation and CO_2 balance will respond to continuing climate change.

3.2 Introduction

The Arctic is warming twice as fast as the global average, with the most rapid temperature increases occurring during the winter months (AMAP, 2017; Richter-Menge et al., 2017). Warmer winters, in combination with greater temperature variability, are associated with increasingly frequent winter extreme climatic events that cause major disturbance in Arctic ecosystems (Beniston et al., 2011; Johansson et al., 2011; Vikhamar-Schuler et al., 2016; Graham et al., 2017). This disturbance includes severe vegetation damage and mortality, often at landscape or greater scales (Bokhorst et al., 2009; Bjerke et al., 2014; Phoenix & Bjerke, 2016).

Such extreme events are therefore among the key drivers of 'Arctic browning', the term used to describe the declining biomass and productivity observed at regional to pan-Arctic scales in recent years (Epstein et al., 2015, 2016; Miles & Esau, 2016; Phoenix & Bjerke, 2016). Only one previous study has made a full assessment of CO_2 fluxes following browning driven by an extreme climatic event in a northern peatland (Parmentier et al., 2018). While this work indicated a 12% reduction in GPP, full assessment of this event's effect on eddy covariance CO_2 fluxes was made challenging by large inter-annual variability in summer climate. Similarly, a single time-point measurement of GPP following browning driven by simulated extreme winter warming found a reduction of more than 50% (Bokhorst et al., 2011). However, despite the scale of the impacts suggested by this snap-shot of peak season CO_2 fluxes, measurements taken across the growing season are crucial to our understanding of how extreme events are impacting CO_2 balance. This is of particular importance in Arctic ecosystems, where the growing season and therefore the window of opportunity for substantial CO_2 fixation is short and dynamic (Larsen et al., 2007; Callaghan et al., 2011). In addition, while previous work has focussed on vegetation mortality driven by extreme events, sub-lethal stress

(indicated by high, persistent anthocyanin pigmentation, and an associated deep red-burgundy colouration) is also often observed following extreme events. Although this stress response has been observed in dwarf shrub ecosystems from boreal to high Arctic latitudes (Bjerke et al., 2017), it is not known whether it impacts shoot-level and ecosystem CO_2 fluxes.

Extreme event drivers of Arctic browning may be climatic, biological (e.g. defoliating insect outbreak) or physical (e.g. fire) (Bokhorst et al., 2008; Mack et al., 2011; Jepsen et al., 2013; Phoenix & Bjerke, 2016; Bjerke et al., 2017). Among the most damaging and frequently observed climatic extreme events is frost drought (Bjerke et al., 2014). Frost drought events arise from loss or absence of a protective snow layer in winter, either through low snow fall, anomalous winter warmth causing substantial snowmelt, or wind displacement. In these conditions, since soils remain frozen or near-frozen, plant water uptake is limited so that transpiration of exposed vegetation can result in desiccation injury (Tranquillini, 1982; Sakai & Larcher, 1987). This process is accelerated where exposure occurs in combination with high winds or irradiance (Hadley & Smith, 1986, 1989; Bjerke et al., 2014, 2017). Damage following frost drought is readily visible as partial to complete mortality of above ground shoots (i.e. "browning"), and hence this damage is similar to that caused by extreme winter warming events (another extreme event driver of browning), when winter snowmelt exposes vegetation to unseasonably warm temperatures sufficient to initiate premature dehardening, subsequently resulting in freeze damage on return of sub-zero winter temperatures (Phoenix & Lee, 2004; Bokhorst et al., 2010). It is of concern, therefore, that the frequency of mid-winter thaw episodes, the central characteristic of both extreme winter warming and frost drought events, may as much as double during this century in some Arctic regions (Johansson et al., 2011; Vikhamar-Schuler et al., 2016). These extreme events may therefore have an increasing influence over high-latitude vegetation.

Already, individual events such as these are causing landscape-level (>1000km^2) reductions in vegetation greenness (Bokhorst et al., 2009; Hansen et al., 2014; Phoenix & Bjerke, 2016). At the same time, increased browning trends (to which trend climate change, such as reduced summer warmth and delayed snow melt also contribute) have been observed across the Arctic (Bhatt et. al., 2013; Epstein et al., 2014, 2015; Bieniek et al., 2015). The severity of browning from extreme events can be considerable, as demonstrated when multiple extreme events in 2012, including frost drought and extreme winter warming, reduced Normalised Difference Vegetation Index (NDVI, a measure of greenness) to the lowest levels ever recorded across the Nordic Arctic Region (Bjerke et al., 2014).

These large-scale impacts reflect shoot mortality (Bokhorst et al., 2009, 2011), but likely also the sub-lethal stress response indicated by high, persistent anthocyanin pigmentation, that has nonetheless received limited attention to date (Bjerke et al., 2017). A plot-level assessment of areas affected by extreme climatic events from boreal to high arctic latitudes found this visible stress response affecting up to 75 % of *Calluna vulgaris* shoots, in addition to high levels of mortality observed in shoots of the evergreen shrubs *Calluna vulgaris* and *Cassiope tetragona* (up to 60 % and 50 % respectively) (Bjerke et al., 2017). Anthocyanin pigments fulfil a huge diversity of functions in plants; in addition to being associated with discrete developmental stages (such as autumn senescence in deciduous trees), they are involved in responses to a range of stressors including high light levels, cold temperatures and herbivory (Gould, 2004; Landi et al., 2015). Accumulation of anthocyanin pigments in leaves during and shortly after snowmelt is therefore common in many upland or high-latitude species (Oberbaeri & Starr, 2002). However, since synthesis of anthocyanins incurs a metabolic cost, and their presence reduces light capture by chlorophyll (Burger & Edwards, 1996; Steyn et al., 2002), their

accumulation is typically transient (Chalker-Scott, 1999; Mac Arthur & Malthus, 2012). In contrast, the unusually strong anthocyanin pigmentation observed after frost drought and extreme winter warming persists through much, or even all, of the growing season (personal observation).

Predicting the future impact of climate change in Arctic ecosystems will require not only quantification of the impacts of browning on ecosystem CO_2 fluxes, but also mechanistic insights into the processes driving these. For example changes in ecosystem respiration may be due to altered shoot-level respiration, or to changes in below-ground processes such as decomposition, which might be expected to accelerate following higher litter inputs or altered resource allocation following browning (Dahl et al., 2017; Parmentier et al., 2018), or decelerate due to reduced belowground carbon allocation (Parker et al., 2017). This process-based knowledge is critical to building Arctic browning into climate and vegetation models, many of which currently assume an arbitrary level of greening across the Arctic (Pearson et al., 2013).

To address these needs, we report the first detailed assessment of key ecosystem CO_2 fluxes across the growing season in a sub-Arctic heathland dominated by *Calluna vulgaris* in northern Norway, quantifying the impacts of both shoot mortality and visible stress following exposure to extreme winter conditions through direct comparison of affected and unaffected vegetation. Plot-level ecosystem CO_2 and soil fluxes were measured at plots dominated by either shoot mortality (‘damage’), dark red anthocyanin pigmentation (‘stress’) or green, healthy vegetation. Structural Equation Modelling (SEM) of these fluxes and plot-level measures of vegetation greenness, supported by additional measurements of shoot-level responses (growth, photosynthesis and respiration) and decomposition rates, facilitated more detailed

understanding of CO_2 flux changes associated with damage and stress, and the mechanisms underlying these. Finally, emergent relationships between CO_2 fluxes and overall browning were used to estimate the upscaled impact on CO_2 fluxes across the site.

It was hypothesised that i) NEE, GPP and R_{eco} would be reduced both in plots dominated by a visible stress response and, to a greater degree, in those dominated by shoot mortality, compared to green control plots; ii) reductions in these fluxes would diminish throughout the growing season (due to recovery and resprouting of evergreens and leaf-out of herbaceous species), most rapidly between early and mid-season, and more rapidly in plots primarily exhibiting stress compared to those exhibiting shoot mortality; iii) reductions in plot-level CO_2 fluxes would be associated with reduced shoot growth and slower decomposition rates; iv) ecosystem CO_2 fluxes would correlate negatively with overall browning throughout the growing season.

3.3 Methods

3.3.1 Study area

Field work was undertaken in 2016 in sub-Arctic heathland on the archipelago of Lofoten in northern Norway, at Storfjord (N 68˚ 9' 26.5" E 13˚ 45' 13.5"). This maritime, comparatively southern region typically experiences a mild winter climate with high levels of snowfall compared to other sub-Arctic regions (Førland et al., 2009). Vegetation at the site was dominated by the evergreen shrubs *Calluna vulgaris* (L.) Hull (54 % ± 21 %) and *Empetrum nigrum* (L.) (37 % ± 22 %). *Vaccinium* species were also common and near-continuous ground cover was provided by feather moss species *Hylocomium splendens* (Hedw.) Schimp and *Pleurozium schreberi* (Brid.) Mitt. The site was on a gentle, undulating slope with no tree canopy.

A large region of extensive shoot mortality in heathland throughout central and northern Norway, including in the Lofoten Archipelago, was observed following the 2013/2014 winter (Bjerke et al., 2017). This was attributed to frost drought: following an unusually mild December, extremely dry conditions exposed vegetation to cold temperatures and desiccation during January, February and early March 2014. Although some recovery occurred after 2014, significant shoot mortality was still present at smaller scales in many regions following this frost drought event, hence allowing the selection of our study site within this region.

In addition, during the 2015/2016 winter, snow cover and temperature data (accessed from publicly available databases senorge.no and eklima.no) indicate the region experienced a winter warming event with unusual warmth throughout much of December 2015 (weekly mean temperature elevated by up to 4.2 ˚C compared to normal December mean of -1.2 ˚C), leading

to total loss of snow cover. This thaw event was followed by a rapid temperature drop of more than 7˚C from 1 – 3 January 2016. Snow cover remained absent or shallow throughout January. In May 2016, around 1 month after spring snowmelt, heavy anthocyanin pigmentation (deep dark red colouration) was observed in widespread *Calluna vulgaris* heathland in multiple locations across the Lofoten region (personal observation).

We selected the Storfjord site based on presence of both shoot mortality following frost drought in winter 2013/14 and of heavy anthocyanin pigmentation following winter 2015/16, hence allowing us to study and compare both.

Data was collected in the growing season of 2016, during three measurement periods. Early season measurements were taken between 25 May and 10 June, peak season measurements between 12 and 23 July and late season measurements between 17 and 29 August.

3.3.2 Plot selection

Nineteen 50 x 50 cm plots were selected within a 25 x 60 m study area. Cover of dominant ericaceous dwarf shrubs was 75% or more at all plots. Of these plots, six 50 x 50 cm were control plots in healthy, green vegetation, a further six were 'damaged plots' in vegetation dominated by past browning (identifiable as dead grey leaves and shoots), and seven were 'stressed plots' in vegetation showing high anthocyanin production (identifiable as a deep dark red pigmentation in leaves and shoots). Of these, 16 were selected for flux measurements (six of damaged, five of stressed, and five healthy, green plots). We used 16 rather than all 19 plots for flux measurements simply because of time constraints on gathering flux measurements (see "*Ecosystem CO_2 flux measurements*"). Plots were marked to enable measurements to be repeated throughout the growing season.

Within each flux plot, percentage cover of browning and dominant species was recorded using a 50 x 50 cm quadrat. Browning was assessed visually (Fig. 3.1) by recording percentage cover of green (healthy), grey (shoot mortality from which all pigmentation has leached, indicating damage is from a previous year), brown (fresh shoot mortality from the winter preceding the measurement season) and dark red vegetation (stress, indicated by high anthocyanin pigmentation).

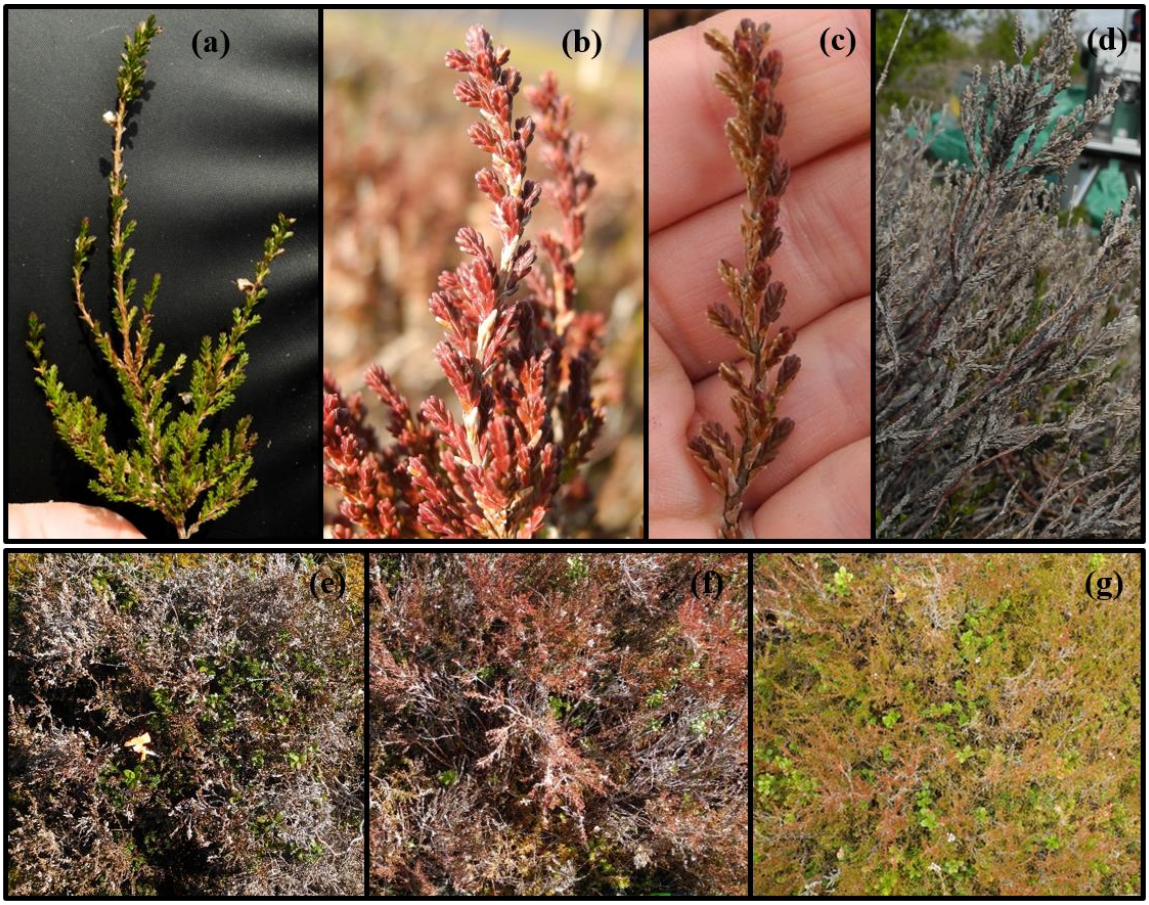

Figure 3.1: Distinguishing leaf colours at the shoot level (a-c) and plot level (e-g). At the shoot level, green (a), dark red (b; anthocyanin pigmentation, indicative of stress) and grey (d; past mortality) leaf area are all readily distinguishable. Closer examination is needed to separate red (c; right hand side of shoot) and brown (c; fresh mortality; left hand side of shoot) leaf area, which frequently occur on the same shoots. At the plot level, green control plots (e), plots dominated by dard red coloured C. vulgaris (f; anthocyanin pigmentation, indicative of stress) and plots dominated by grey coloured C. vulgaris (g; past mortality) are clearly distinguishable. However, distinguishing between dark red leaf area and brown leaf area (fresh mortality) within a plot requires careful and time consuming examination.

3.3.3 GPP, NEE and R_{eco}

At each flux plot (i.e. 16 of the 19 plots), CO_2 fluxes were measured both within the central 50 x 50 cm and the adjacent, associated 20 x 20 cm moss plot. Moss plot fluxes were measured immediately before or after the central 50 x 50 cm area.

NEE was measured using a LiCor LI-6400 system (LiCor, Bad Homburg, Germany) and a custom 50 x 50 x 25cm transparent acrylic vegetation chamber. Following this, light response curves of NEE and GPP were fitted, including calculation of a modelled term for R_{eco}, and allowing NEE and GPP to be standardised at a PAR of 600 µmols PPFD m^{-2} s^{-1}. Full methods are described in Chapter 2 ("*Ecosystem CO_2 flux measurements*").

Surface temperature was recorded concurrently with CO_2 concentration data using a temperature probe inserted into the enclosed ground layer vegetation (bryophyte/lichen) or leaf litter. Air temperature was recorded by the LI-6400. Moss layer and (in the case of 50 x 50 cm plots) soil surface moisture were recorded after each measurement set using a Delta-T HH2 moisture meter with a Theta probe (Delta-T, Cambridge, UK) inserted first at the surface of the moss layer and secondly at the soil surface at the same point, following removal of the moss layer. Height of the understory canopy within the plot was measured from the ground at three randomly chosen points following each measurement set.

Plot-scale measurements of ecosystem CO_2 fluxes were supported by a small dataset of shoot-level measurements of photosynthesis and respiration taken at peak season in stressed and controls plots (Appendix 1).

3.3.4 Soil respiration

An 11 cm diameter soil collar was inserted to a depth of 8 cm adjacent to each 50 x 50 cm flux plot. Vascular vegetation and the green bryophyte layer were clipped to the soil surface before each soil collar was inserted using a serrated cutting blade and mallet. Collars were inserted at the beginning of the early season measurement period and left to stabilise for a minimum of three days before measurements were taken (LiCor, 1997). When measurements were not being taken, a patch of moss was replaced on top of the collar to minimise soil surface heating and drying due to exposure.

Soil respiration measurements were taken using a LiCor LI-6400 system connected to a LI-6400-09 soil respiration chamber (LiCor, Bad Homburg, Germany). The 991 cm^3 chamber was placed on the soil collar with a foam gasket ensuring a good seal. Before each flux measurement, CO_2 was scrubbed to 15-20 ppm (dependent on flux) below ambient. Flux was then calculated and recorded as CO_2 concentration increased from 15-20 ppm below to 15-20 ppm above ambient. This cycle was repeated three times for each measurement and an average value calculated.

3.3.5 Shoot growth

Apical shoot growth was also assessed in each plot using retrospective growth analysis. Three live shoots of *Calluna vulgaris* were chosen at random within each plot and new growth was measured from shoot tips to the bud scar laid down the previous year. Growth was measured in this way at peak and late season only, as little shoot growth had taken place at the start of the early season measurement period.

3.3.6 Decomposition

Decomposition and litter stabilisation (the proportion of material that becomes recalcitrant during initial decomposition) were assessed using commercially available green and rooibos tea bags, following Keuskamp et al., (2013) and the Tundra Tea project (2018). In brief, two tea bags of each type were weighed before being buried in separate holes at a depth of 8 cm in an area of vegetation adjacent to and comparable with each plot at the beginning of the early season measurement period. They were then retrieved three months later, dried at 70 ˚C for 48 hours and reweighed. Fraction decomposed was calculated incorporating a correction for ambient moisture prior to burial.

3.3.7 Assessment of change in anthocyanin pigmentation

This was done on apical shoots across the growing season specifically in stressed and control plots. Two shoots within each stressed plot and one within each control plot were tagged at early season. On each shoot the percentage of total leaf area showing green (healthy), grey (mortality from a previous year), brown (fresh mortality) and dark red (anthocyanin pigmentation) colouration was estimated by eye twice during early season and once during peak and late season measurement periods. The height of these shoots from the ground to the previous year's bud scar were also recorded. Shoots were randomly selected, but only from those shoots within each plot which had not experienced total shoot mortality (i.e. live shoots). This additional shoot-level damage assessment was used to assess the difference in anthocyanin pigmentation of live vegetation between stressed and damaged plots, and the extent and speed with which pigmented leaf area recovered greenness, or alternatively experienced mortality (i.e. becoming brown), over the course of the growing season in each plot type.

3.3.8 Assessment of site-level browning

To estimate site-level browning two 15-18 m transects were completed during each measurement period with percentage cover recorded in a 1 m x 1 m area at 3 m intervals. Percentage cover of stress and damage, as well as cover of dominant species, was assessed visually (see Appendix 2 for more detail).

3.3.9 Statistical analyses and structural equation modelling

Changes in CO_2 fluxes across the growing season as a whole were assessed using repeated measures ANOVA with linear mixed effects models, incorporating plot number as a random effect. Differences between plot types (damaged, stressed and healthy controls) at each point during the growing season were assessed in more detail using one way ANOVA and Tukey multiple comparison tests.

One way ANOVA and Tukey multiple comparison tests were used to assess differences in shoot growth and litter decomposition. T-tests were used to assess differences in shoot-level CO_2 fluxes between stressed and healthy green shoots. Linear regression was used to assess changes in site-level (transect) browning and shoot-level anthocyanin pigmentation and other browning throughout the growing season.

Within each measurement period linear regression was also used to assess site-level correlations between percentage cover of total browned vegetation (including stress and damage) and GPP_{600}, R_{eco} and NEE_{600}. This approach was used to look for emergent relationships between total browned vegetation and CO_2 fluxes across the growing season and to investigate how differences in the CO_2 flux impacts of stress and damage might affect these

overall relationships. Linear regression of total browning and each CO_2 flux was compared with multiple regression using separate terms for previous damage (grey) and for fresh damage (brown) combined with stress (dark red). All statistical analyses were carried out in RStudio (R Core Team, 2015).

These analyses were supported by Structural Equation Modelling (SEM) using the lavaan package in RStudio (Rosseel, 2012; R Core Team, 2015). SEM provides a framework for multivariate analysis of networks and paths (Grace et al., 2010, 2012). SEM is also a robust approach to provide meaningful analysis of data collected using a survey-like approach, such as that used here, where variables are likely to be correlated and where both direct and indirect effects may be present (Graham et al., 2003; Grace, 2006). SEM was used here to add weight to conventional statistical tests and to guide inference as to the ecological processes underlying correlations identified through these tests. SEM was initiated by defining an *a priori* set of theoretically justified paths between variables, guided by the above conventional analyses. This core model was then used to address secondary hypotheses by incorporating additional variables (cover of herbaceous species and canopy height) into the model. SEM included one latent variable. Latent variables are unmeasured constructs, described by correlated indicator variables with an underlying common causal influence. Here, the latent variable 'Browning Severity' was used which combined percentage cover of browned vegetation (both mortality and stress) and cover of remaining green ericaceous (i.e. dwarf shrub) vegetation to indicate the overall severity of browning to the dominant ericoid vegetation in each plot. The chi-square test, the standard measure of fit in SEM, was used as a primary indicator of whether model fit was acceptable. The Comparative Fit Index (CFI), Root Square Mean Error of Approximation (RMSEA) and Standardized Mean Square Error of Approximation (SRMR) were used to provide additional assessment of model fit.

3.4 Results

3.4.1 Gross Primary Productivity

Across the growing season as a whole, mean GPP_{600} in both damaged and stressed plots was significantly reduced compared to controls by 37% and 23% respectively (F = 8.52, DF = 2, 42, $p < 0.001$, Tukey HSD $p < 0.05$). Within early season GPP_{600} was significantly affected by plot type (Fig. 3.2a; F= 5.19, DF = 2,12, $p < 0.05$), with GPP_{600} in damaged plots reduced by an average of 55 % (Tukey HSD $p < 0.05$). At peak season, differences between plot types were not significant. By late season, GPP_{600} was significantly affected, with GPP_{600} in damaged plots reduced by an average of 43% (Tukey HSD $p < 0.05$).

3.4.2 Ecosystem and soil respiration

Across the season as a whole R_{eco} was significantly affected by plot type (F= 3.44, DF = 2,42, $p < 0.05$). R_{eco} was increased in stressed plots across the growing season compared to damaged plots (Tukey HSD $p < 0.05$), particularly at peak season, when R_{eco} in stressed plots was almost double that in damaged plots (though not statistically significantly so; Fig 3.2b). Similarly, at peak season there was some evidence for elevated dark respiration in apical shoots from stressed plots (Appendix 1). In damaged plots and, most markedly, in stressed plots, there was a significant increase in R_{eco} from early to peak season (stressed plots: F= 7.565, DF = 2,11, $p < 0.01$, damaged plots: F= 10.56, DF = 2,15, $p < 0.01$), while in control plots R_{eco} did not change significantly between measurement periods.

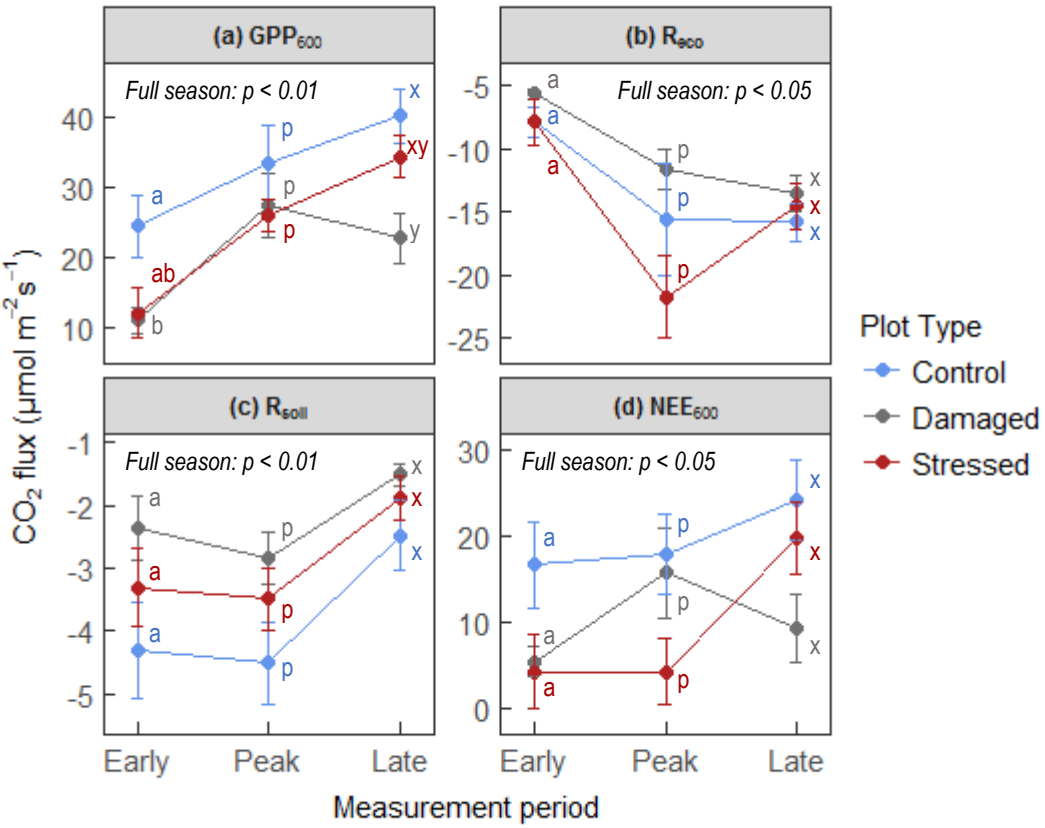

Fig. 3.2: Change throughout the growing season in key ecosystem CO_2 fluxes; (a) $GPP_{600;}$ (b) ecosystem respiration (dark CO_2 release from soil and vegetation); (c) R_{soil} and (d) NEE_{600} in damaged (dominated by previous mortality, grey coloured), stressed (dominated by high anthocyanin pigmentation, dark red coloured) and control (green) plots. Positive values represent CO_2 uptake (µmol m^{-2} s^{-1}). Straight lines between data points are not intended to indicate a known linear transition between times of year, but are used to help link plot type across the year. Error bars represent one standard error. Letters represent significant differences as assessed by Tukey Honest Significant Differences; tests apply within measurement periods. 'Full season' p values show differences between plot types across all time points. N=16 within each measurement period.

R_{soil} was significantly affected by plot type across the season as a whole (Fig. 3.2c, $F = 8.116$, $DF = 2,38$, $p < 0.01$), with a mean reduction in damaged plots of 40% (Tukey HSD $p < 0.01$) and a mean reduction of a near significant 23% in stressed plots (Tukey HSD $p = 0.057$). Despite these differences being apparent across all three measurement periods, they were not statistically different in Tukey multiple comparisons within each time period ($p < 0.05$). On average across all plots, R_{soil} was constant between early and peak season, after which it declined by just under half by late season ($F = 6.87$, $DF = 2,43$, $p < 0.01$).

3.4.3 Net ecosystem exchange

Differences in NEE_{600} between plot types (Fig. 3.2d) were similar to those seen for GPP_{600}. Across the full growing season plot type had a significant effect on NEE_{600} ($F = 4.718$, $DF = 2,42$, $p < 0.05$). Mean NEE_{600} overall was approximately halved in both stressed and damaged plots compared to controls (reductions of 50% and 48% respectively, Tukey HSD $p < 0.05$). The effect of plot type on NEE_{600} was near significant within early season ($F = 3.461$, $DF = 2,12$, $p < 0.065$), and within late season ($F = 3.43$, $DF = 2,12$, $p < 0.064$), with early season showing the most substantial reductions in mean NEE_{600} in both damaged and stressed plots of 74% and 67% respectively. Differences between plot types at peak season were not significant.

3.4.4 Shoot growth

The mean length of new shoot growth was significantly lower in both damaged plots and stressed plots compared to controls (38 % and 27 % lower respectively) at peak season (Fig. 3.3, $F = 16.76$, $DF = 2,54$, $p < 0.001$). Growth reductions in both plot types compared to controls remained significant at late season ($F = 24.89$, $DF = 2,52$, $p < 0.001$, Tukey HSD $p < 0.05$).

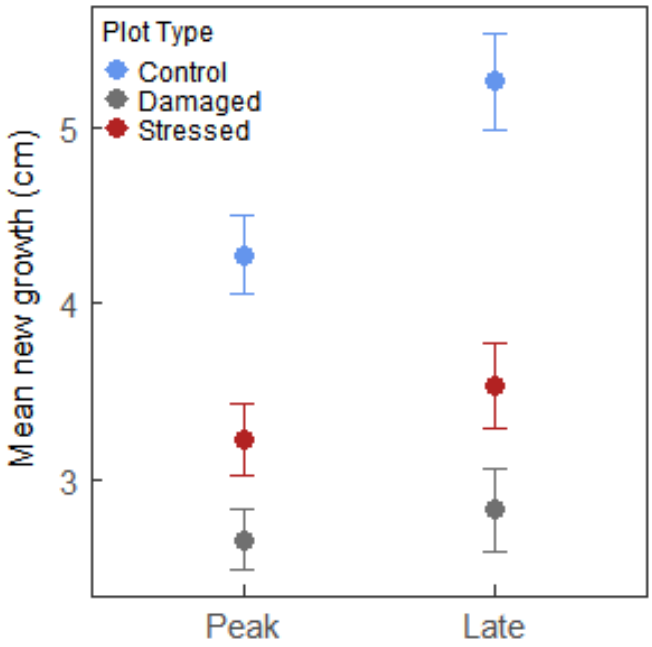

Figure 3.3: Mean new (first year) growth (cm) at shoot apices within each plot type (control plots, stressed plots dominated by dark red anthocyanin pigmentation, and damaged plots dominated by shoot mortality) at peak and at late season. Error bars represent one standard error.

3.4.5 Decomposition

No significant differences in fraction decomposed of rooibos tea were found between plot types. However there was a near significant difference in fraction decomposed of green tea between plots, with lower decomposition seen in damaged plots compared to control plots (Fig. 3.4, $F = 3.313$. $DF = 2,26$, $p = 0.052$, Tukey HSD $p = 0.053$). This difference corresponds to a near significant difference in litter stabilisation, which was higher in damaged plots when compared to controls ($F = 3.313$, $DF = 2,26$, $p = 0.052$, Tukey HSD $p = 0.053$).

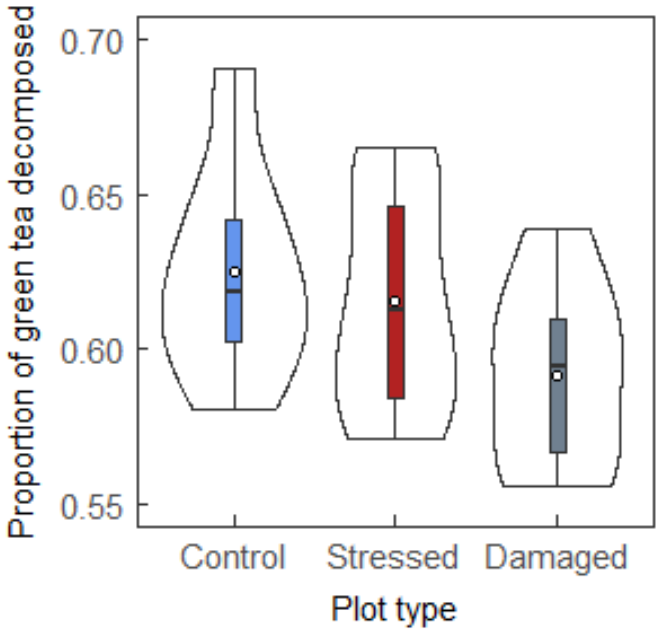

Figure 3.4: Mean proportion of green tea decomposed over three months in each plot type (control plots, stressed plots dominated by dark red anthocyanin pigmentation, and damaged plots dominated by shoot mortality). Outer shape surrounding each box plot is a mirrored density plot showing data distribution. White points show means and black bars show medians.

3.4.6 Change in anthocyanin pigmentation

Tagged shoot data (Fig. 3.5) showed high levels of anthocyanin pigmentation (dark red colouration) at early season in shoots located in stressed plots (mean of 63%) compared to those located in control plots (mean of 8%). Dark red anthocyanin pigmentation in shoots located in stressed plots fell significantly ($p < 0.05$) within the early season measurement period and from early to peak season. A slight, non-significant further decline was seen by late season. In control plots, levels of dark red pigmentation did not change significantly, but were highest at the start of the growing season and lowest at peak season. Proportions of grey (past mortality)

and brown (fresh mortality) colouration did not change significantly throughout the season in either shoots located in control plots or stressed plots. However there was some increase in the proportion of brown colouration in both plot types; an increase of 7% from June to September in stressed plots and of 4% in control plots.

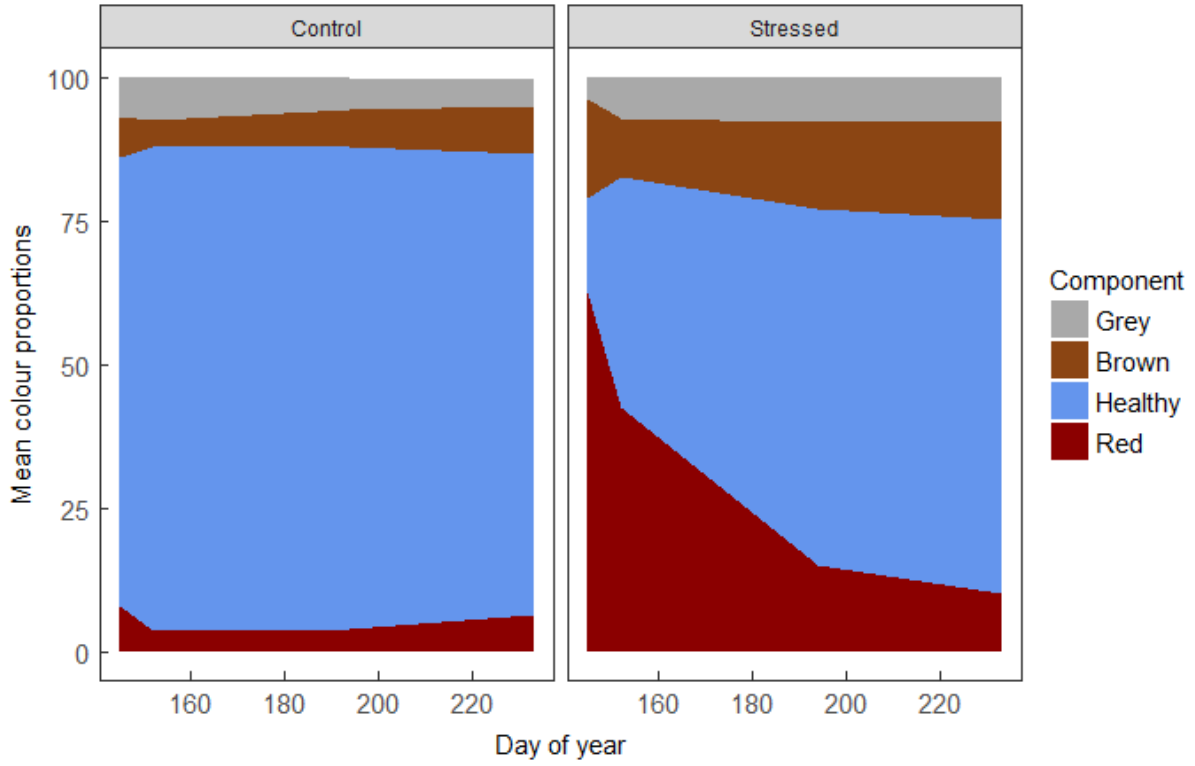

Figure 3.5: Mean proportions of total leaf area of tagged apical shoots exhibiting different states, as reflected by leaf colour. Grey indicates leaf mortality from a previous growing season (followed by degradation of leaf pigment over winter), brown indicates fresh mortality, red indicates high anthocyanin pigmentation (signalling stress) and healthy green leaf area is shown here in blue.

3.4.7 Browning: CO_2 flux relationships across plots

GPP_{600}: Negative correlations between GPP_{600} and total cover of browned (stress and damage combined) vegetation across flux plots were present throughout the growing season (Fig. 3.6). These correlations were highly significant at early and late season (early: $F = 13.41$, $DF = 1,13$,

$p < 0.01$, late: $F = 15.88$, $DF = 1,14$, $p < 0.01$) and near significant at peak season ($F = 4.312$, $DF = 1.14$, $p = 0.057$).

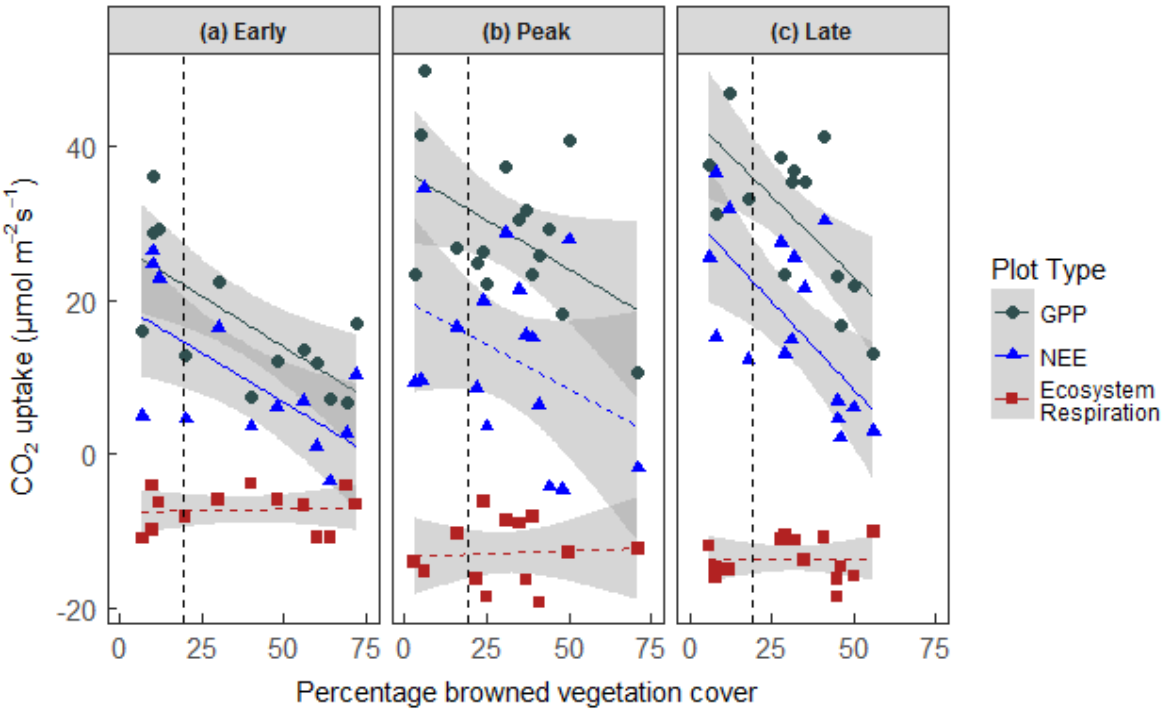

Figure 3.6: Correlations between total browned vegetation cover (including previous and fresh mortality and anthocyanin pigmentation stress response) and key ecosystem CO_2 fluxes GPP_{600} (grey), NEE_{600} (blue) and R_{eco} (red) during early, peak and late season. Positive values represent CO_2 uptake. Solid lines indicate statistically significant correlations. While these data represent CO_2 flux measurements repeated at the same plots across the growing season, cover of damaged vegetation changes throughout the season due to recovery and change in cover of herbaceous species. Thus the percentage cover of browning in each plot varies throughout the season.

Correlations between GPP_{600} and total browning correspond to substantial reductions in productivity at mean cover of total browning across the site, as assessed by transect surveys (Appendix 2). During early season, GPP_{600} at mean site-level browning was reduced by an estimated 34 % compared to that in undamaged vegetation, with a 15 % reduction seen at peak season and a 20 % reduction at late season. Multiple regression using separate terms for past

damage (grey shoot mortality) and recent browning (brown fresh shoot mortality and dark red pigmentation) was also significant at early and late season, but did not provide significantly improved model fit compared to linear regression.

R_{eco} and soil respiration: R_{eco} did not correlate with total browned cover at any point during the season (Fig. 3.6). Soil respiration declined with increasing area of total browned vegetation throughout the growing season (Fig. 3.7). This correlation was significant at early season (F = 6.02, DF = 1,11, $p < 0.05$) and near significant at peak (F = 4.12, DF = 1,14, p = 0.062) and late (F = 4.16, DF = 1,12, p = 0.064) season. Soil respiration at mean cover of total browning was reduced by between 26 % at early season and 16 % at peak season. Multiple correlations using separate terms for past damage and recent browning were not significant.

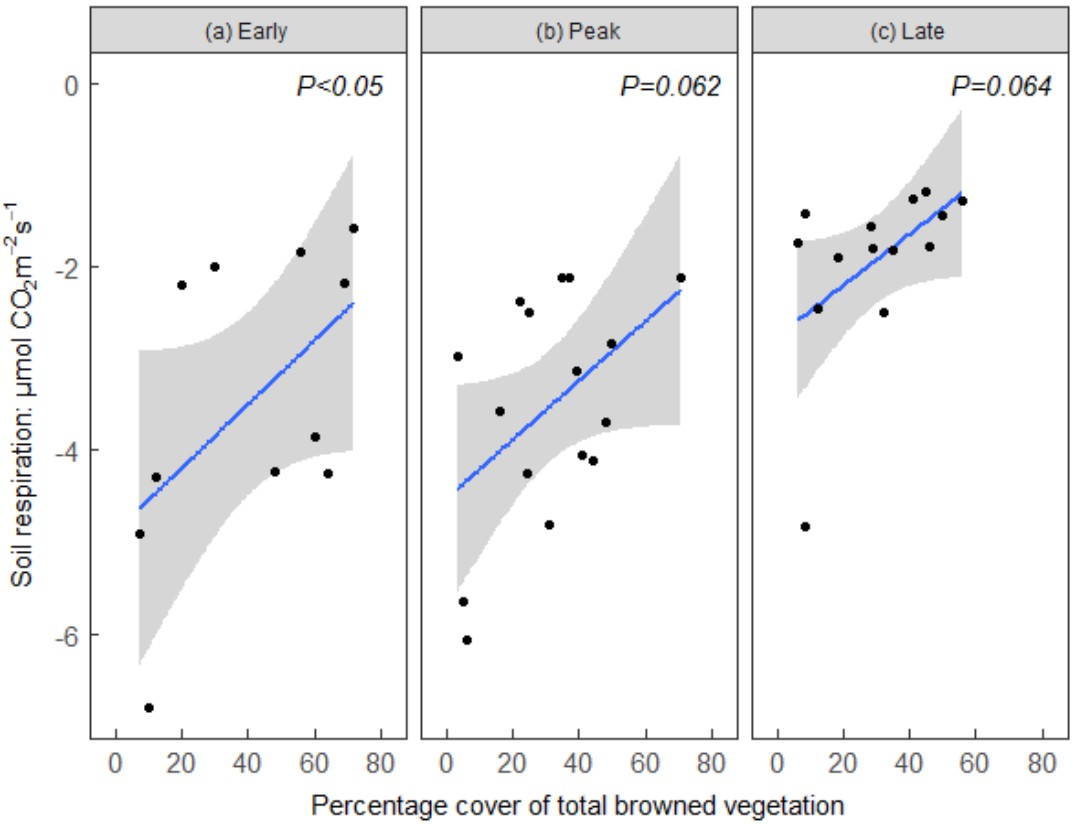

Figure 3.7: Correlations between total browned vegetation cover (including previous and fresh mortality and anthocyanin pigmentation stress response) and soil respiration during early, peak and late season. Negative values represent CO_2 release.

***NEE_{600}*:** NEE_{600} was negatively correlated with total cover of browned vegetation (including mortality and stress) during early (Fig. 3.6a, F = 10.34, DF = 1,13, $p < 0.01$) and late season (Fig. 3.6c, F = 10.76, DF = 1,14, p = 0.01), but not during peak season (Fig. 3.6b). These correlations corresponded with substantial estimated site-level NEE_{600} reductions when combined with mean cover of total browning across the site (Appendix 2), from a reduction of 44 % compared to healthy vegetation during early season to 28 % during late season. Multiple correlations using separate terms for past damage and recent browning were also significant at early and late season, resulting in higher estimated NEE_{600} reductions (reaching 52 % at early

season), and were marginally significant at peak season, providing an estimated site-level NEE_{600} reduction of 29 %.

3.4.8 Structural Equation Modelling

SEM supported the above analyses. 'Browning Severity', a latent, unmeasured variable (see methods) combining percentage cover of total browned vegetation (positive effect on Browning Severity) and remaining green ericaceous vegetation (negative effect on Browning Severity), had a strong, negative impact on both GPP_{600} and soil respiration throughout the growing season (Fig. 3.8). As conventional analyses found no site-level relationship between total browning and R_{eco}, this relationship was not included in SEM. However, since comparisons between plot types indicated a difference in the response of R_{eco} to browning associated with past mortality (grey coloured) compared with stress (dark red), an indirect relationship was modelled between Browning Severity and R_{eco} via the proportion of total browning associated with stress (as measured during early season). This showed that until late season (a) the proportion of browning initially associated with stress had a highly significant, positive relationship with R_{eco} (in agreement with comparisons between plot types, Fig 3.2c), (b) the proportion of browning associated with stress had a highly significant, negative relationship with Browning Severity; meaning the most heavily damaged plots were dominated by past mortality (grey coloured shoots), rather than recent stress (dark red anthocyanin pigmentation), and (c) there was a significant, negative indirect relationship between Browning Severity and $R_{eco;}$ meaning that when a high proportion of browning was associated with past mortality, R_{eco} was reduced. This indirect relationship was not significant at late season.

Conventional analysis also showed that damaged plots contained significantly greater cover of herbaceous species compared to controls (data not shown). It was hypothesised that this greater

cover of herbaceous species with high productivity in more heavily damaged ericaceous vegetation may contribute to the weaker overall GPP_{600}-browning correlation seen at peak season (following leaf-out of herbaceous species), compared to early and late season. Greater herbaceous cover could result from either altered conditions (e.g. higher soil moisture or reduced competition for space, light or nutrients due to reduced cover of dominant evergreen dwarf shrubs) following browning, or from the established tendency for taller vegetation both to facilitate co-occurring species, for example by reducing wind speeds and temperature variability during spring, and simultaneously to be more vulnerable to the effects of winter extreme events (Goetz et al., 2005; Brooks et al., 2011; Bjerke et al., 2014). This distinction is significant; the latter implies a process arising from patch-scale heterogeneity which may reduce the mean impact of browning on productivity, but is likely to vary in importance with vegetation structure and to operate at small scales, while the former implies a broader scale mechanism arising directly from browning through which reductions in productivity following browning may be slightly, but consistently, ameliorated. These ideas were explored via modification of the core SEM through the addition of a variable for green herbaceous cover and of paths between this new variable and both Browning Severity and canopy height (representing regressions on green herbaceous cover). The modified SEM was an acceptable fit at early and peak season and indicated a near significant ($p=0.052$) positive effect of canopy height on herbaceous cover at early season. However there was no significant correlation between Browning Severity and cover of green herbaceous species.

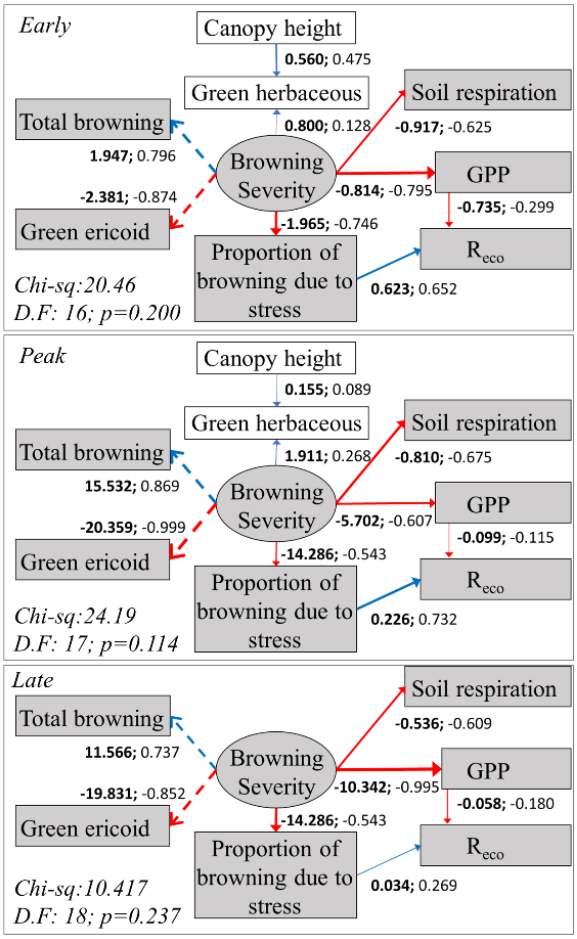

Figure 3.8: Structural Equation Models of early (top), peak (centre) and late (bottom) season data, showing the relationships between 'Browning severity' (a latent variable representing the impact of extreme conditions on the cover of the dominant ericoid vegetation), and CO_2 fluxes (GPP_{600}, R_{eco} and soil respiration). Core model is shown in grey with modifications in white (see methods). Measured variables are shown as squares, latent variables as circles, and paths between indicator variables and the latent variable they describe as dashed lines. Red lines indicate negative and blue lines positive effects, with annotations showing unstandardized (bold) and standardised coefficients. During late season modification of the established core model with cover of herbaceous species and canopy height was rejected ($p < 0.001$). Statistically significant model fit in SEM is indicated by $p > 0.05$.

3.5 Discussion

This detailed assessment of the impacts of climatic extreme event-driven Arctic browning on ecosystem CO_2 fluxes has shown that these events can considerably reduce ecosystem CO_2 uptake, with substantial consequences for soil processes and carbon sink capacity. Furthermore, the magnitude of impact was similar between mortality damage and stress responses such that both need to be considered when quantifying the impacts of extreme event browning in Arctic ecosystem CO_2 balance.

3.5.1 Gross primary productivity and growth

Mean GPP_{600} (gross Primary Productivity standardised at 600µmol m^{-2} s^{-1}; a moderate light level) was significantly lower in damaged and stressed plots across the growing season as a whole compared to control plots.

When measurement periods are considered individually, GPP_{600} in damaged plots was lower compared to control plots at early and late season, but not at peak season. This is contrary to the hypothesis that reductions in CO_2 fluxes associated with browning would diminish throughout the growing season; instead suggesting that the greatest impacts on ecosystem CO_2 uptake may occur towards the shoulder seasons. The lack of significant differences between plot types at peak season is likely due to a combination of factors including re-sprouting and recovery of damaged vegetation, and leaf-out of highly productive herbaceous species. Browned plots contained significantly more herbaceous cover compared to controls, meaning that leaf-out of these species will have had a larger positive impact on productivity in these plots. Structural Equation Modelling (SEM) indicated that this difference in herbaceous cover between plot types is linked to canopy height (Fig. 3.8); previous work has shown that taller

vegetation is more severely damaged following winter extreme events (Bjerke et al., 2017), while SEM showed that during early season taller vegetation also supported more herbaceous species (including graminoids). This is likely due to the facilitative effects of a taller canopy, such as reducing spring wind speeds (Sturm et al., 2005; Goetz et al., 2005; Brooks et al., 2011). Thus, higher herbaceous cover in damaged plots is probably not a result of browning, but rather a pre-existing co-variate of canopy height. This could indicate a mechanism providing some mitigation of the impact of browning on GPP within a landscape.

Although reductions in GPP_{600} within measurement periods were significant only where driven by mortality, mean GPP_{600} reductions associated with stress were of a similar magnitude to those driven by mortality at early and peak season. While previous work has shown anthocyanin production can reduce photosynthetic capacity (Burger & Edwards, 1996; Steyn et al., 2002), it is nonetheless surprising that stress resulted in such considerable reductions in plot-level CO_2 uptake. These reductions in productivity are reflected in first-year growth of live shoots, which was reduced in stressed and damaged plots, possibly due to delayed bud burst (Bokhorst *et al.*, 2008), transient physiological damage (Bokhorst et al., 2010), or the metabolic cost of anthocyanin synthesis (Zangerl et al., 1997).

3.5.2 Soil and ecosystem respiration

Overall, R_{soil} (dark CO_2 release from soil) was reduced in damaged and, with near significance (p = 0.057), in stressed plots across the three measurement periods. This supports previous work showing that vegetation damage following climatic and biological extreme events reduces R_{soil} (Moore et al., 2013; Olsson et al., 2017; Zhao et al., 2017), and further demonstrates that vegetation stress may have qualitatively similar effects to damage (albeit of a lesser magnitude). Reductions in R_{soil} following vegetation damage have previously been

attributed to diminished microbial activity and deceleration of soil processes due to reduced transfer of carbon below ground (Litton et al., 2007; Parker et al., 2017). Here, decomposition data is consistent with this mechanism, given that decomposed fraction of green tea (labile litter) was lower in damaged plots, indicating reduced microbial activity.

The respective impacts of vegetation stress and damage on R_{eco} (dark ecosystem CO_2 release, including from soils and vegetation) are less consistent. In stressed plots R_{eco} was increased across the growing season compared to damaged plots (in which R_{eco} was slightly, but not significantly, lower than in controls). Reduced soil respiration implies that this increase was driven by increased respiration of vegetation, an effect which SEM analysis indicates was greatest at peak season. That increased vegetation respiration is directly linked to stress, as indicated by the high anthocyanin pigmentation observed in *C. vulgaris*, is supported by a marginally significant increase in dark respiration of visibly pigmented shoots compared to green shoots (Appendix 1). Stress associated with exposure to winter extreme events thus appears to increase respiration, likely reflecting greater maintenance and repair needs, as documented following drought, herbivory and mechanical damage (Zangerl et al., 1997; Strauss et al., 2002; Flexas et al., 2005).

3.5.3 Net ecosystem exchange

Major impacts on NEE_{600}, (net ecosystem CO_2 exchange standardised at 600µmol m^{-2} s^{-1}; a moderate light level) which varied substantially across the growing season, were seen in both stressed and damaged plots. Mean NEE_{600} was reduced by 48% and 50% across the growing season in damaged and stressed plots respectively compared to controls. NEE_{600} is the primary measure of ecosystem carbon balance; this therefore represents a substantial impact on sequestration capacity, particularly in an ecosystem in which vegetation is typically snow-

covered for most of the year, and annual carbon sequestration therefore depends on a short, dynamic growing season (Larsen et al., 2007).

The considerable reductions in NEE_{600} across the growing season are remarkably similar in damaged and stressed plots. While in damaged plots these impacts follow two growing seasons of recovery, in contrast to stressed plots in which impacts are likely to be more transient, this nonetheless highlights the importance of considering sub-lethal responses to extreme event exposure.

Differences in NEE_{600} between plot types at individual measurement periods were not significant. However, the magnitude of differences in mean NEE_{600} between stressed and damaged plots at peak season, combined with contrasting impacts of stress and damage on R_{eco}, indicate potentially important differences in how stress and damage affect NEE_{600}. Specifically, while mean NEE_{600} in damaged plots increased substantially between early and peak season, mean NEE_{600} in stressed plots did not (due to the rapid increase in respiration of stressed vegetation discussed above), and was therefore 73% lower than in damaged plots at peak season. By this point, a substantial proportion of stressed vegetation had 're-greened' following break-down of anthocyanin pigments. Future work should therefore consider this potential difference in peak season impacts of stress and damage on NEE_{600}, and the possibility that where substantial stress follows extreme event exposure, impacts on NEE_{600} may not be predictably related to loss of greenness at peak season, and therefore be harder to detect.

3.5.4 Change in anthocyanin pigmentation

In shoots from stressed plots, the mean proportion of leaf area exhibiting stress (dark red anthocyanin pigmentation) remained at more than 40% in early June, and more than 15% at

peak season. This is markedly higher compared to both control shoots (mean 3.8% dark red in June), and to previous observations of spring pigmentation in evergreen dwarf shrubs, which typically falls to its lowest levels by early – mid June and/or shortly after snowmelt (Starr & Oberbauer, 2003; MacArthur & Malthus, 2012), demonstrating that this response is beyond usual levels of pigmentation following snowmelt. Dark red pigmentation in stressed shoots diminished rapidly early in the season, dropping from 63% in May to 43% in June. This is in accordance with recovery of the dwarf shrub *Cassiope tetragona* on Svalbard during summer 2015 (Anderson et al., 2016) from frost injury caused by lack of sufficient winter snow cover the previous winter (Callaghan et al., 1989). While the rapid decline in the mean proportion of dark red leaf area observed here largely reflects breakdown of anthocyanin pigments and a resulting increase in green leaf area, there is also evidence of mortality occurring in highly pigmented leaves (resulting in conversion from dark red leaf area to brown), as the mean proportion of leaf area showing fresh mortality (brown) increases across the growing season. This suggests that while *C. vulgaris* exhibiting high anthocyanin pigmentation following stress is largely able to 're-green', it also experiences increased leaf mortality across the season compared to unaffected vegetation. While anthocyanins are known to be synthesised to provide plant protection (Gould, 2004; Landi et al., 2015), the possibility that persistent pigmentation may signal plant damage and be followed by elevated mortality is little understood.

3.5.5 Browning: CO_2 flux relationships across plots

GPP_{600} was negatively correlated with percentage cover of total browned vegetation throughout the growing season, demonstrating for the first time that the extent of visible browning was clearly and consistently related to the impact on plot-level CO_2 uptake, regardless of whether browning was primarily a result of mortality or stress. This adds to previous work identifying emergent relationships to help simplify the heterogeneity of vegetation distribution and

productivity in Arctic regions, which are crucial to regional estimates of carbon balance and its response to climate change (Street et. al., 2007, Shaver et. al., 2007). When scaled to the site level, these linear negative correlations of GPP_{600} to browning translated to substantial reductions in GPP_{600} at site-level of up to 34%.

Soil respiration was negatively correlated with total browning, further reflecting the slow-down in belowground processes which follows a reduction in above-ground productivity (Litton et al., 2007; Parker et al., 2017). However, no overall correlation between total browning and R_{eco} was identified. As evidenced by plot comparisons, this is due to the opposing impacts on vegetation respiration of mortality and stress, which decrease and increase vegetation respiration respectively. This is further supported by SEM, which indicated that browning severity had a negative impact on R_{eco} when the influence of vegetation stress was controlled for.

As was seen with GPP_{600}, NEE_{600} correlated linearly and negatively with total browning at early and late season, irrespective of browning type, translating to site-level reductions of between 25% and 44% across the growing season. However, at peak season there was no correlation between NEE_{600} and total browning, due to the contrasting impacts of damage and stress on vegetation respiration. Furthermore, multiple regression of peak season NEE_{600} against peak season past damage (grey mortality) and early season – rather than peak season - stress and fresh damage (brown mortality) provided a significant correlation. This demonstrates that peak season NEE_{600} in stressed vegetation is not linearly related to visible greenness at peak season, but rather is subject to a legacy effect of stress-related browning visible only earlier in the season. This may be an important caveat to the use of simplified relationships with vegetation greenness to predict carbon balance (Street *et. al.*, 2007, Shaver *et. al.*, 2007);

where winter extreme events cause substantial vegetation stress, assessing their impacts according to peak season greenness alone could substantially underestimate the reduction in net CO_2 uptake capacity – by almost 10% in this case.

The extreme conditions during winter 2013/14 winter which caused mortality at this site resulted in similar damage across the Lofoten region, and even other regions of sub-Arctic and boreal Norway as much as ~600km south of our study site (Bjerke & Tømmervik, personal communication), indicating that these vegetation responses are increasingly relevant even at regional scales.

3.6 Conclusion

Overall, this work shows that both stress and mortality following exposure to winter climatic extreme events can have major impacts on plant physiology and ecosystem function, including significantly reducing ecosystem CO_2 uptake. While these impacts can persist through much of, or even all of the growing season, often they are most substantial early or late in the season. This highlights the need to support peak season measurements with full season assessments, and adds to an increased appreciation of the role of shoulder seasons in Arctic biogeochemical cycling (Oechel et al., 1997; Grogan & Jonasson, 2005, 2006). Importantly, over a single growing season, stress indicated by dark red pigmentation was just as important for reducing net CO_2 uptake as mortality, and continued to reduce CO_2 sequestration (due to ongoing greater respiration) following recovery of greenness. This adds an additional challenge to detecting and upscaling the impacts of vegetation stress on CO_2 uptake on a regional or global scale using remote sensing (Park et al., 2016). Furthermore, the extensive mortality and visible stress are both common responses following exposure to extreme events such as frost drought, icing and extreme winter warming, which are predicted to increase in frequency with climate change (Johansson et al., 2011; Vikhamar-Schuler et al., 2016). The impacts of mortality and stress on ecosystem CO_2 fluxes, and the scale of their impacts across the growing season, highlight a clear need for process-based understanding of the impacts of such events on Arctic vegetation and CO_2 balance. This understanding is central to predicting both how vegetation will respond to continuing rapid climate change at high latitudes, and how these responses may feedback to climate.

3.7 Appendix 1: Shoot level CO_2 exchange

3.7.1 Methods

During the peak season measurement period, shoot level CO_2 exchange was measured on shoots adjacent to and showing a similar level of anthocyanin colouration to tagged shoots (see '*assessment of change in anthocyanin pigmentation*) in 5 control plots and 5 stressed plots, using an LI-6400 system connected to a LI-6400-05 transparent conifer chamber. PAR was recorded using a LiCor Quantum sensor mounted on an acrylic shelf outside the conifer chamber. Shoot CO_2 exchange was recorded at 5 light levels, beginning with full light and adding three successive levels of shading, achieved using optically neutral shade clothes, before ending in darkness achieved using a tarpaulin. Shoot photosynthetic rate (µmol CO_2 m^{-2} s^{-1}) was allowed to stabilise at each light level (indicated by a coefficient of variation of photosynthetic rate of <0.1). Photosynthetic rate was converted to net CO_2 flux per unit leaf area and modelled as a rectangular hyperbola with a term for respiration. Subtraction of the latter from CO_2 flux enabled a light response curve of GPP to be fitted, and thus GPP to be standardised at a PAR of 600µmols PPFD m^{-2} s^{-1} (GPP_{600}).

After measurements were complete, the extent of the shoot sealed within the conifer chamber was marked and clipped. Clipped shoot sections were stored in high humidity conditions provided by damp kitchen roll in polythene bags for 5 days to prevent drying and shrinkage, after which leaves and stems were separated. The leaves from each shoot were then scanned on a flatbed scanner and the resulting image analysed in Image J (Schneider et al., 2012) to obtain total leaf area for each shoot level measurement.

3.7.2 Results

There were no significant differences in photosynthetic activity between shoots from stressed and control plots (Fig. 3.9a). Shoots from stressed plots on average respired at a higher rate compared to those from control plots (Fig. 3.9b). Although this difference is not statistically significant (t = 1.96, DF = 5.83, p = 0.099), it may nonetheless indicate elevated respiration in stressed shoots, particularly given the small sample size of this supporting dataset (n = 9).

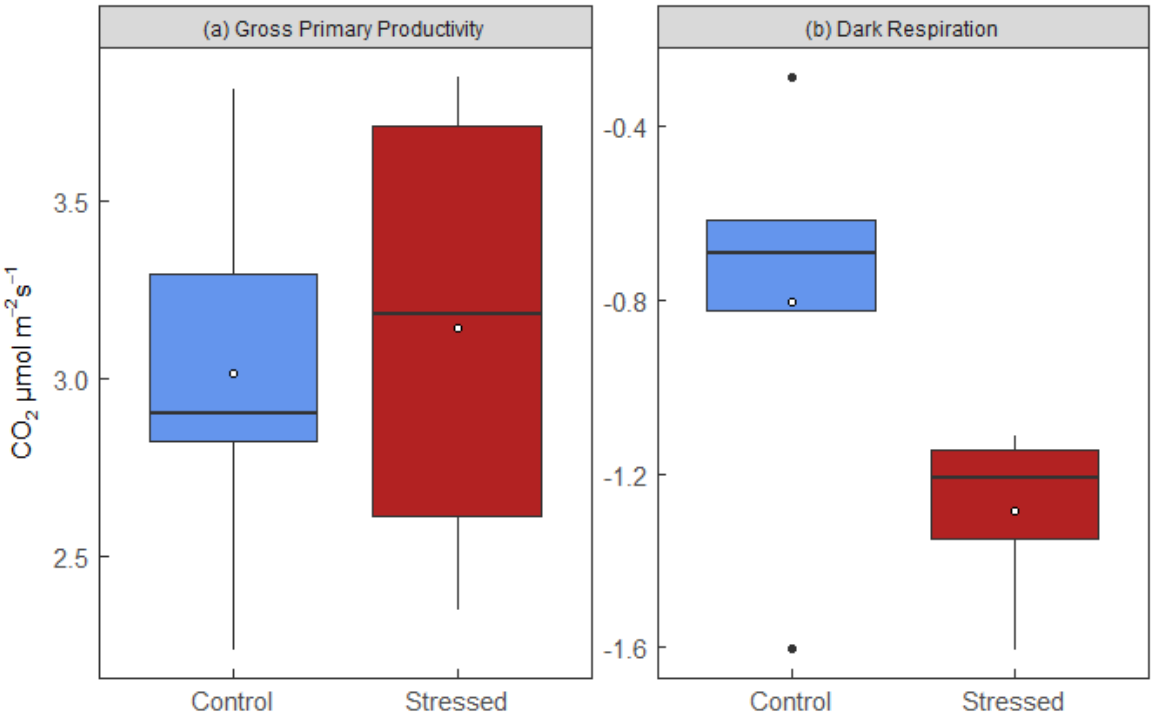

Figure 3.9: (a) Mean Gross Primary Productivity and (b) mean dark respiration at 600 µmol PPFD m^{-2} s^{-1} in *C. vulgaris* shoots from green control plots and from stressed plots dominated by red/black anthocyanin pigmentation.

3.8 Appendix 2: Assessment of site-level browning

3.8.1 Methods

To estimate site-level browning (including both stress and damage), two 15-18m transects were completed during each measurement period with percentage cover recorded in a 1m x 1m area using four 50 x 50cm quadrats at intervals of three metres. In each quadrat damage was assessed visually, along with percentage cover of dominant species, by recording percentage cover of green (healthy), grey (shoot mortality from which all pigmentation has leached, indicating damage is from a previous year), brown (fresh shoot mortality) and red/black vegetation (high anthocyanin pigmentation, indicating stress). While all three categories of browning (grey, brown, red/black) are readily distinguishable by eye at a shoot level (Fig. 3.1) close examination can be required to distinguish between fresh shoot mortality (brown) and anthocyanin pigmentation (red/black) at the plot level. The time consuming nature of the process of distinguishing between percentage cover of brown (fresh mortality) and red/black (stress) leaf area at the plot-level meant that these two damage types were recorded in combination (i.e. total damage) during transect surveys.

3.8.2 Results

Site transects showed substantial total browning (previous and fresh shoot mortality and high anthocyanin pigmentation combined) during the early season measurement period, with >50% cover of browning recorded at a quarter of plots. Significant browning remained visible by late season (Fig. 3.10). Within total browning, mean cover of fresh shoot mortality and high anthocyanin pigmentation combined (brown and red/black respectively) was 15.2% during early season. This fell significantly to 10.3% between early and peak season ($t = 3.0773$, $DF = 63.913$, $p < 0.01$), before a further slight decrease to 9.5% by late season. Mean cover of

previous shoot mortality (grey standing dead shoots from 2013-14 winter frost drought) was 22.2% during early season, falling significantly to 11.7% by peak season (t = 5.5789, DF = 78.486, $p < 0.001$) with a further non-significant decrease by late season, likely due to fresh growth overtopping and obscuring dead material. Mean cover of apparently healthy, green vegetation increased from 70.3% during early season to 106.4% by mid-season, partly accounted for by a significant 15.2% increase in mean cover of herbaceous species (t = -6.1303, DF = 111.806, $p < 0.001$).

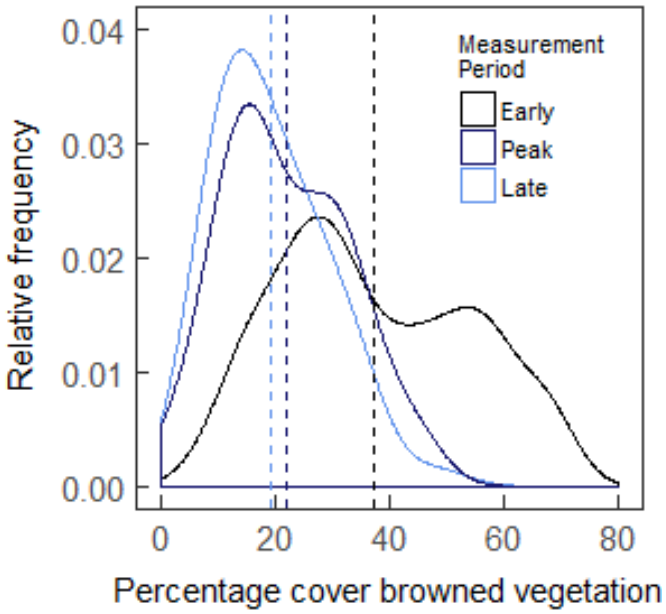

Figure 3.10: Frequency polygon showing seasonal change in total percentage cover of all types of browned vegetation combined (including previous and fresh shoot mortality and anthocyanin pigmentation stress response), as recorded by transect surveys.

Chapter 4

Impacts of extreme climatic events on moss growth and CO_2 fluxes across the growing season

4.1 Summary

1. Rapid climate change is leading to more frequent extreme events in Arctic regions. These can cause severe damage to heathland communities by driving shoot mortality and visible stress responses. This damage, or 'browning', has major implications for ecosystem CO_2 fluxes.

2. Mosses are a key component of these high latitude heathland communities, accounting for as much as 50% of total biomass and contributing substantially to productivity.

3. Past work has shown reduced moss growth and photosynthesis following simulated extreme winter warming. However, these responses have been assessed only at peak season, and the impacts of other events, such as frost drought, are completely unknown.

4. Therefore, a full growing season assessment of moss responses to two successive extreme events - frost drought and extreme winter warming – was carried out in sub-Arctic dwarf shrub heathland. Gross Primary Production (GPP), respiration and net CO_2 exchange were measured on moss (primarily *Hylocomium splendens*) forming the ground layer of plots where vascular vegetation was dominated by shoot mortality ('damage'), visible stress, or healthy, unaffected shoots. This CO_2 flux assessment was supported with measurements of moss growth, nutrient content, and the temperature and moisture conditions in the moss layer.

5. Growth was reduced by up to 27% and 15% in moss associated with damaged and stressed plots respectively. Substantial differences in CO_2 fluxes were also identified in these plots, with net CO_2 exchange reduced by up to 36% across the growing season compared to controls, despite increased GPP in damaged plots at early season.

6. This shows that extreme events, including frost drought, can negatively impact moss growth and CO_2 balance. That GPP can be temporarily increased, alongside these negative impacts, may further indicate that indirect consequences of browning (for example higher light penetration to the moss layer) could to some extent ameliorate the effects of direct physiological damage.

7. The major impacts of two extreme events on moss physiology and CO_2 fluxes reported here demonstrate that moss responses play a significant role in determining net ecosystem impacts, and suggest that predicted increases in extreme event frequency may influence the responses to moss to continuing climate change.

4.2 Introduction

Winter climate in high latitude ecosystems is changing rapidly (AMAP, 2017). With warmer winters comes an increased frequency of extreme climatic events (Vikhamar-Schuler et al., 2016; Graham et al., 2017). These cause stress and mortality in vascular species of widespread dwarf shrub heathland communities, often at landscape scales (Bokhorst et al., 2009; Bjerke et al., 2017). This extreme-event driven 'Arctic browning' leads to major reductions in ecosystem CO_2 uptake (Chapters 1 and 2). However, although recent work shows that mosses can also be damaged following exposure to extreme events (Bjerke et al., 2011, 2013, 2017b), understanding still falls well short of our level of knowledge of vascular plant responses. We also have little understanding of their contribution to CO_2 fluxes following browning.

Mosses are a key component of high latitude communities, in terms of biomass, diversity and ecological function. They typically comprise 20-50% of total aboveground biomass at high latitudes (Hobbie & Chapin, 1998; Campioli et al., 2009; Turetsky et al., 2010) and contribute substantially to primary productivity, accounting for an average of around 30-60% of ecosystem carbon uptake (Chapin et al., 1995; Douma et al., 2007; Campioli et al., 2009; Turetsky et al., 2012). In some ecosystems, or at certain times in the growing season, this contribution may reach 90% or more (Douma et al., 2007; Street et al., 2012). In addition, mosses have a significant influence over nutrient cycling and availability to vascular plant species, particularly of nitrogen. This is due to their low nitrogen-use efficiency and high rates of nitrogen interception and retention in the moss layer, as well as their slow decomposition rates (Galloway et al., 2004; Cornelissen et al., 2007; Turetsky et al., 2010). Similarly, the moss layer influences environmental conditions; in dry conditions moss is a good insulator, while in wet conditions it is both moisture retentive and conductive to heat (Longton, 1997; Gornall et al., 2007). As a result, moss reduces fluctuations in soil temperature and moisture. Common

feathermoss species such as *Hylocomium splendens* and *Pleurozium schreberi* are also nitrogen fixers (DeLuca et al., 2002).

Mosses are therefore central to the function of high latitude ecosystems. However their winter ecology is little understood (Cornelissen et al., 2007; Bjerke et al., 2011). In addition, their responses to global change, including rapid winter climate change, are likely to be different to those of vascular species. This is in part because bryophytes lack a belowground root system or protective cuticle, leaving them more dependent on the availability of water in their immediate environment compared to vascular species (Proctor et al., 2007; Cornelissen et al., 2007). They are therefore adapted to readily switch between metabolic activity and dormancy, allowing them to survive long periods of desiccation following which they can recover without physiological damage upon rehydration (known as poikilohydry).

Mosses are generally thought to respond negatively to gradual summer warming as an indirect result of increases in productivity, leaf area and stature seen in vascular vegetation. Termed 'Arctic greening', this vascular vegetation response primarily reflects expansion of shrubs (Sturm et. al., 2005; Tape et. al., 2006; Elmendorf et. al., 2012; Macias-Fauria et. al., 2012). While mosses are typically shade-adapted, with low photosynthesis compensation and saturation points, further shading from a denser, taller understory canopy can slow moss productivity and growth (Arndal et al., 2009; Alatalo et al., 2014). However, this response is by no means universal. Other work has suggested that warming could directly stimulate moss productivity, causing vascular species to grow taller to avoid being overtopped by moss (Keuper et al., 2011; Turetsky et al., 2012; He et al., 2016). The dependence of bryophytes on their immediate external environment, and particularly on water availability, is likely to make

responses to increased average temperature variable between species, latitude and even micro topography and climate (Douma et al., 2007; Uchida et al., 2010; Elumeeva et al., 2011).

The impacts on bryophytes of winter climate change, and in particular of winter extreme climatic events, are poorly understood, and lack the knowledge base now established for vascular plants. Of the little work on bryophytes conducted to date, negative impacts have been observed following extreme winter warming events, with growing season reductions in growth and photosynthesis reaching up to 52% and 48% respectively in *H. splendens* following events simulated in the field (Bjerke et al., 2017b, 2013, 2011). Extreme winter warming events are characterised by abrupt, short-lived periods of warmth which cause partial or total snowmelt, exposing vegetation adapted to a stable sub-nivean environment. In vascular vegetation, this exposure to a transient increase in temperature results in damage by stimulating premature dehardening and even budburst, following which a return to sub-zero temperature inflicts freezing damage (Bokhorst et al., 2010). Similarly, exposure of *H. splendens* during winter causes it to quickly become active and reach optimal rates of photosynthesis (Bjerke et al., 2013). It is thought that such premature activity stimulates the development of frost-sensitive shoot apices, which are then damaged following a return to cold temperatures (Bjerke et al., 2017b). Most of this understanding, however, relies almost entirely upon this single assessment of the impacts of simulated extreme winter warming events on *H. splendens* at the peak of the growing season.

Measurements taken across the growing season are also critical to a full understanding of how bryophytes respond to these events. Considering impacts across the season is of particular importance in this case given the comparatively long growing season experienced by Arctic bryophytes (*cf* vascular plants), which remain capable of substantial photosynthesis late into

the Arctic summer after vascular species have senesced (Arndal et al., 2009), and also because of their potential to have greatest metabolic activity in early and late season when moist, rather than in the drier mid-season.

Such differences in the responses of bryophytes to environmental conditions compared to vascular vegetation mean the impacts they experience are likely to vary with event intensity, event type and with the severity of impacts on the vascular understory. For example, an extreme winter warming event may be of sufficient intensity to damage vascular vegetation without causing full exposure of the moss layer and so may not initiate moss shoot growth and neither therefore result in any physiological damage. Similarly, while the impacts of other common types of winter extreme climatic event on vascular vegetation are very similar to those of extreme winter warming (Chapter 1), impacts on moss may differ more between event types. In particular 'frost drought' events, common in many high latitude regions, occur when vegetation is exposed, through either snowmelt following a warm period, snow removal following high winds, or a combination of these (Bjerke et al., 2014). In this case damage to vascular vegetation results from desiccation following exposure to winds and irradiance in combination with frozen soils. As bryophytes are highly desiccation tolerant (Proctor et al., 2007), they may not sustain physiological damage following frost drought. Winter extreme climatic events which result in damage to the vascular understory but do not cause physiological damage to moss during the event, might even be expected to favour moss photosynthesis and growth, by reducing shading and increasing availability of moisture and nutrients (Gornall et al., 2011; Turetsky et al., 2012). Mosses may therefore have the potential to alleviate the consequences of extreme events, for instance in compensating for loss of carbon gain by vascular plants.

We therefore carried out a full growing season assessment in 2016 of *in situ* moss CO_2 fluxes in widespread sub-Arctic dwarf shrub heathland which experienced extreme climatic events in the winters of 2013/14 (frost drought) and 2015/16 (extreme winter warming) (Chapter 3). CO_2 flux measurements were carried out on the moss layer of plots where vascular vegetation was primarily either damaged (shoot mortality following 2013/14 frost drought), stressed (unusually high, persistent anthocyanin pigmentation, visible as deep red/black colouration, following 2015/16 extreme winter warming) or healthy (control plots). Surface temperature and moisture were measured concurrently with moss CO_2 fluxes at each plot, and segment growth and nitrogen content of shoots of the dominant moss species (*Hylocomium splendens*) from each plot were also assessed. This allowed the impact of exposure to two natural extreme events on activity of the moss layer to be assessed, and provided an insight into the drivers of identified differences.

It was hypothesised that i) moss productivity (GPP and NEE) would be increased in damaged plots compared to controls, but not in stressed plots, ii) this increase would be linked to increased temperature, moisture or nutrient content of the moss layer in damaged plots, iii) this increase would be more pronounced during early and late season compared to peak season, iv) first year segment growth (growth throughout the growing season during which measurements were taken) would be reduced in stressed and damaged plots. It was further hypothesised that v) second year segment growth would be unchanged between plot types, because this growth will have taken place in the growing season preceding the measurement year, and therefore prior to the extreme winter warming event and with one year of recovery after exposure to the frost drought event.

4.3 Methods

4.3.1 Study area

Field work was undertaken in 2016 in sub-Arctic heathland on the archipelago of Lofoten in northern Norway, at Storfjord (N 68˚ 9' 26.5" E 13˚ 45' 13.5"). This site is the same as described in Chapter 3 (3.3.1; "*Study area*"); fieldwork for Chapter 3 and Chapter 4 was completed in parallel. In brief, vegetation at this site was dominated by the evergreen shrubs *Calluna vulgaris* (L.) Hull (54 % ± 21 %) and *Empetrum nigrum* (L.) (37 % ± 22 %), and near-continuous ground cover was provided by feather moss species *Hylocomium splendens* (Hedw.) Schimp and *Pleurozium schreberi* (Brid.) Mitt. The site was affected by a frost drought event in the 2013/14 winter which resulted in extensive shoot mortality in evergreen dwarf shrubs throughout central and northern Norway (Bjerke et al., 2017). In addition to this event, snow cover and temperature data (accessed from publicly available databases senorge.no and eklima.no) indicate the region experienced a winter warming event during the 2015/2016 winter. In May 2016, around 1 month after spring snowmelt, heavy anthocyanin pigmentation (deep dark red colouration) was observed in widespread *Calluna vulgaris* heathland in multiple locations across the Lofoten region (personal observation).

This particular site at Storfjord was chosen based on presence of both shoot mortality following frost drought in winter 2013/14 and of heavy anthocyanin pigmentation following winter 2015/16, hence allowing us to study and compare both. Data was collected in the growing season of 2016, during three measurement periods. Early season measurements were taken between 25 May and 10 June, peak season measurements between 12 and 23 July and late season measurements between 17 and 29 August.

4.3.2 Plot selection

As described in Chapter 3 (3.3.2; "*Plot selection*") nineteen 50 x 50 cm plots with high (75% or more) cover of dominant ericaceous dwarf shrubs were selected within a 25 x 60 m study area. Of these plots, six were control plots in healthy, green vegetation, a further six were 'damaged plots' in vegetation dominated by past browning (identifiable as dead grey leaves and shoots), and seven were 'stressed plots' in vegetation showing high anthocyanin production (identifiable as a deep dark red pigmentation in leaves and shoots). Of these, 16 were selected for flux measurements (six of damaged, five of stressed, and five healthy, green plots). 16 rather than all 19 plots were used for flux measurements simply because of time constraints on gathering flux measurements (3.3.3; "*GPP, NEE and R_{eco}*"). Adjacent to each flux plot, an additional 20 x 20 cm moss flux plot was selected. These plots were located in the 20 x 20 cm area with near-continuous moss cover and minimal vascular vegetation cover which was nearest (within 1 m) to each vascular vegetation flux plot. Any substantial vascular vegetation encroaching into moss plots was clipped to the moss surface. Each of the 16 moss flux plots was marked to enable measurements to be repeated throughout the growing season. Percentage cover of moss species within each plot was estimated by eye.

4.3.3 Net moss CO_2 exchange, GPP and respiration

Net Ecosystem Exchange (NEE) was measured within each 20 x 20 cm moss flux plot using a LiCor LI-6400 system (LiCor, Bad Homburg, Germany) and a custom 20 x 20 x 15 cm transparent acrylic vegetation chamber. Light response curves of NEE and GPP were fitted, including calculation of a modelled term for R_{eco}, and allowing NEE and GPP to be standardised at a PAR of 600 µmol PPFD m^{-2} s^{-1}. Full flux and calculation methods are described in Chapter 3 (3.3.3; "*GPP, NEE and R_{eco}*"). From measurements of NEE and R_{eco}, net

CO_2 exchange and respiration specifically of the moss layer were calculated by subtracting soil respiration values measured adjacent to each plot (see below). Total respiration and moss CO_2 exchange, respiration and GPP were subsequently analysed.

In addition to these *in situ* measurements, net moss CO_2 exchange, GPP and respiration were measured on two excised moss plots at late season for comparison with more methodologically challenging *in situ* measurements (Appendix 1). The full 20 x 20 cm plot area of moss was cut from the surrounding moss layer using a serrated blade, and removed as a turf to prevent disruption of the moss layer structure. Organic matter was trimmed from the base of the turf using a serrated blade and clippers to leave the brown and green moss layer. Each excised moss plot was then placed on an acrylic surface and sealed inside the transparent acrylic chamber used for *in situ* measurements (seal provided by a foam gasket). Net CO_2 exchange, GPP and respiration were then measured following the same procedure used for *in situ* plots.

4.3.4 Soil respiration

Soil respiration data was used to estimate the contribution specifically of moss respiration to total respiration (see above). Soil respiration data is that described in Chapter 3 (3.3.4 and 3.4.2; methods and results respectively). In brief, soil respiration was measured at 11 cm diameter soil collars inserted to a depth of 8 cm adjacent to each plot using a LiCor LI-6400 system connected to a LI-6400-09 soil respiration chamber (LiCor, Bad Homburg, Germany). Moss respiration was calculated by subtracting soil respiration (CO_2 m^{-2} s^{-1}) from chamber measurements of total respiration (CO_2 m^{-2} s_{-2}).

4.3.5 Abiotic conditions (temperature and moisture)

The temperature of the moss surface was recorded concurrently with CO_2 concentration data using a temperature probe inserted into the enclosed moss layer. Air temperature was recorded by the LI-6400. The moisture content of the moss layer was recorded after each NEE measurement set using a Delta-T HH2 moisture meter with a Theta probe (Delta-T, Cambridge, UK) inserted at the surface of the moss layer.

4.3.6 Segment growth

Five or more shoots of *H. splendens* from each plot were collected at the end of each measurement period. These were clipped to the uppermost, green portion and air dried. The growth form of *H. splendens* in sub-Arctic regions is typically sympodial and composed of annually formed segments which are clearly distinguishable by eye (Fig. 4.1; Callaghan et al., 1997; Ross et al., 1998; Salemaa et al., 2008). The lengths of current year growth segments (growth laid down during the 2016 growing season during which measurements were taken) and previous year segment growth (growth laid down the 2015 growing season, one year before measurements were taken) were measured on five shoots from each plot using callipers. This approach has previously been used effectively for air dried samples (Bjerke et al., 2017). As the 2013/14 frost drought event occurred three years prior to measurements being taken, three growth segments have been laid down following possible moss exposure to this event. Therefore, both current year and previous year growth segments could be affected by this event. The 2015/16 extreme winter warming event occurred immediately prior to measurements being taken; therefore only current year growth could have been affected by this event.

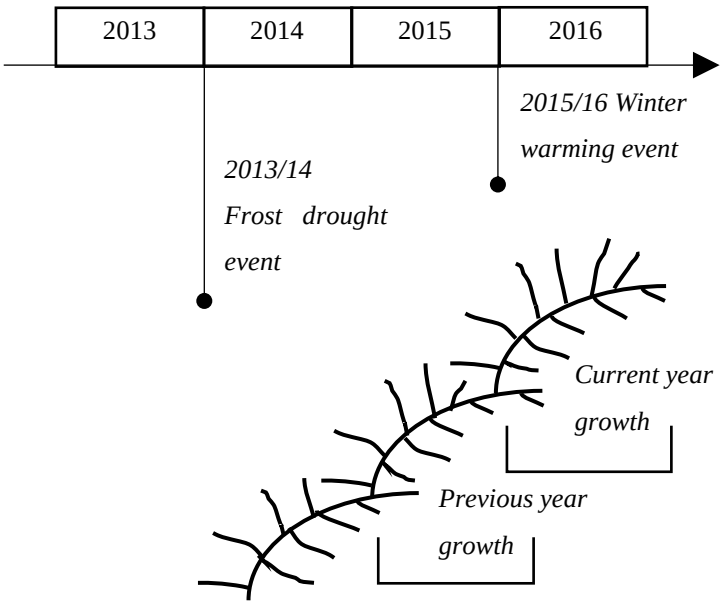

Figure 4.1: Schematic showing sympodial growth of *Hylocomium splendens*, with current year growth segment (growth laid down during the growing season in which measurements were taken) and previous year segment (growth laid down the growing season before that in which measurements were taken) indicated by square brackets. A timeline is also show, indicating how the timing of the two extreme events corresponds with segment growth.

4.3.7 Nitrogen content analysis

Air dry *H. splendens* samples from each plot (as described above) were homogenised by grinding. Prepared samples were redried and analysed for percentage nitrogen content using a C:N analyser (Vario EL Cube, Elementar, Hanau, Germany).

4.3.8 Statistical analyses

Changes in moss CO_2 fluxes, temperature and moisture across the growing season as a whole were assessed using repeated measures ANOVA with linear mixed effects models, incorporating plot number as a random effect. Differences between plot types (damaged, stressed and healthy controls) at each time point during the growing season were assessed in more detail using one way ANOVA and Tukey multiple comparison tests. At late season,

measurements of soil respiration at two stressed plots failed. Therefore, stressed plots at late season were not included in data analysis and net moss CO_2 exchange and respiration were compared only between control and damaged plots, using T Tests. For data visualisation purposes, a mean of soil respiration across other stressed plots at late season was used to provide estimate of net moss CO_2 exchange and respiration in stressed plots at late season.

Differences in temperature variation between plots were assessed using F tests of equality of variances, and correlation between temperature and moisture variables and CO_2 fluxes (net moss CO_2 exchange, moss respiration and GPP) were investigated by linear regression.

Differences in first year segment growth and nitrogen content between plot types were assessed using repeated measures ANOVA. Differences in first and second year second year segment growth were also assessed using one way ANOVA and Tukey multiple comparison tests. All statistical analyses were carried out in RStudio (R Core Team, 2017).

4.4 Results

4.4.1 CO_2 fluxes

Overall, moss layer GPP_{600} increased significantly throughout the growing season, with mean GPP_{600} increasing by 82% between early and late season (Fig. 4.2a; $F = 7.12$, $DF = 1, 38$, $p < 0.05$). At early season, there was a near significant effect of plot type on GPP_{600} ($F = 3.224$, $DF = 2, 10$, $p = 0.083$), with GPP_{600} in damaged plots (those where vascular vegetation was dominated by previous mortality) elevated by 102% compared to controls (Tukey HSD: $p < 0.05$).

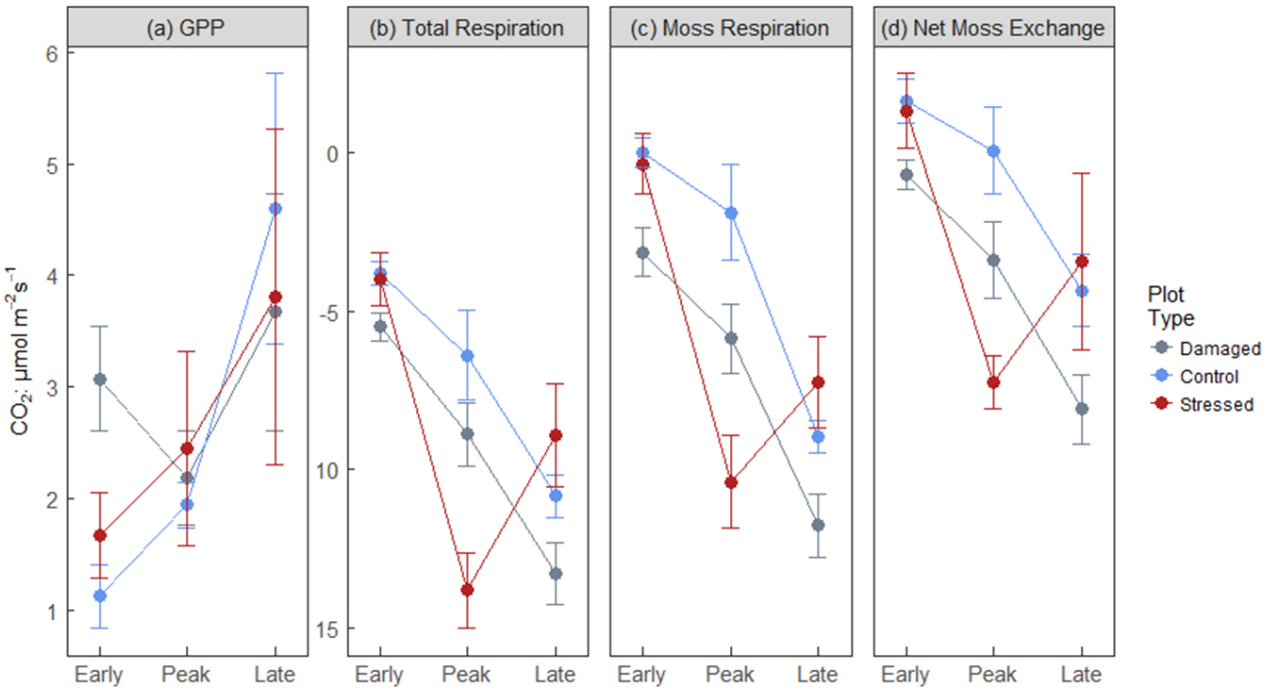

Figure 4.2: Moss layer CO_2 fluxes: (a) Gross Primary Productivity, (b) Total respiration, including CO_2 release from the moss layer and from the soil, (c) Moss respiration, an \estimate of respiration from the moss layer alone with soil respiration (measured separately) subtracted) and (d) Net moss CO_2 exchange, the net product of GPP and moss respiration. Positive values represent CO_2 uptake and negative values represent CO_2 release. Fluxes are shown for control, damaged (vascular vegetation dominated by shoot mortality), and stressed (vascular vegetation dominated by high anthocyanin pigmentation) plots during early, peak and late season. Straight lines between data points are not intended to indicate a known linear transition between times of year, but are used to help link plot type across the year. Error bars represent one standard error. Letters represent significant differences as assessed by Tukey Honest Significant Differences; tests apply within measurement periods. NSD = no significant differences. Error bars represent one standard error.

Across the growing season there was a near significant increase in total respiration, which includes CO_2 release from soil as well as the moss layer, in damaged plots compared to controls (F = 2.92, DF = 2, 35, p = 0.067, Tukey HSD: p = 0.064). Within early season, plot type had a significant effect on total respiration (Fig. 4.2b; F = 4.63, DF = 2, 10, $p < 0.05$), again reflecting a near significant greater CO_2 release from damaged plots compared to controls (Tukey HSD: p = 0.055). Between early and peak season there was an increase in total respiration across all plots (F = 19.72, DF = 2, 37, $p < 0.001$, Tukey HSD: $p < 0.001$). This increase in CO_2 release was particularly rapid in stressed plots, with mean total respiration more than 230% higher in these plots by peak season compared to early season (F = 20.88, DF = 2, 8, $p < 0.001$, Tukey HSD: $p < 0.001$). As a result, peak season respiration in stressed plots was significantly greater than in either control or damaged plots (F = 9.35, DF = 2, 11, $p < 0.01$, Tukey HSD: $p < 0.05$). By late season, mean respiration in stressed plots fell by 33% compared to peak season values, and a near significant impact of plot type on total respiration primarily reflects greater CO_2 release from damaged plots (F = 4.03, DF = 2, 10, p = 0.052, Tukey HSD: $p < 0.05$).

Moss respiration was calculated by subtracting soil respiration, measured separately at each plot, from total respiration. Across the growing season as a whole there was a significant effect of plot type on moss respiration (Fig. 4.2c; F = 5.90, DF = 2, 33, $p < 0.01$), with respiration in both damaged and stressed plots significantly higher (reflecting greater CO_2 release) than in control plots (Tukey HSD: $p < 0.05$). When measurement periods are considered separately, moss respiration shows a similar pattern to that described for total respiration; at early season, damaged plots respired around 50 times more rapidly than controls plots (F = 13.07, DF = 2, 10, $p < 0.01$, Tukey: < 0.01), while at peak season respiration was significantly (425%) higher in stressed plots compared to controls and damaged plots (F = 9.00, DF = 2, 11, $p < 0.01$, Tukey: < 0.05). At late season moss respiration in damaged plots was significantly (31%)

higher than in control plots (stressed plots not included in analysis due to lack of replicates: t = 2.4855, *DF* = 7.0647, $p < 0.05$).

Net moss exchange (calculated by subtracting soil respiration from plot NEE) increased significantly across the growing season from a small CO_2 sink on average during early season to a CO_2 source by peak and late season (Fig. 4.2d; $F = 12.97$, $DF = 2, 35$, $p < 0.001$). Across the growing season as a whole, there was a significant effect of plot type on net moss exchange ($F = 5.23$, $DF = 2, 33$, $p < 0.05$), with greater net exchange (reflecting greater CO_2 release) in damaged plots compared to controls (Tukey HSD: $p < 0.01$) and a near significant increase in stressed plots compared to controls (Tukey HSD: $p = 0.067$). Differences between plots within early season were not significant, but at peak season net moss exchange was greater (and a net CO_2 source) in stressed plots and damaged plots compared to controls, which were a net CO_2 sink ($F = 8.52$, $DF = 2, 11$, $p < 0.01$; Tukey HSD: $p < 0.01$). At late season net moss exchange remained greater, and a net CO_2 source, in damaged plots compared to controls ($F = 5.99$, $DF = 2, 8$, $p < 0.05$; Tukey HSD: $p < 0.05$).

4.4.2 Shoot growth

Current year growth increased throughout the growing season (Fig. 4.3a; $F = 47.48$, $DF = 2, 41$, $p < 0.001$), as would be expected for an ongoing growth process. Mean length of current year growth was not significantly different between plot types during early and peak season. However, by late season, when the growth segments laid down during that season are likely to be nearing their maximum lengths, shoots had grown significantly less in damaged and stressed plots compared to controls ($F = 4.08$, $DF = 2, 13$, $p < 0.05$), with current year growth on average 27% and 15% lower in damaged and stressed plots respectively.

Across the growing season, plot type had a significant effect on previous year growth (length of segments laid down during the growing season before the year of measurements), which was significantly (24%) lower in damaged plots (Fig. 4.3b; $F = 3.73$, $DF = 2, 39$, $p < 0.05$) compared to controls (Fig. 4b) As expected, previous year growth did not increase significantly throughout the growing season (i.e. old growth did not grow any more, data not shown).

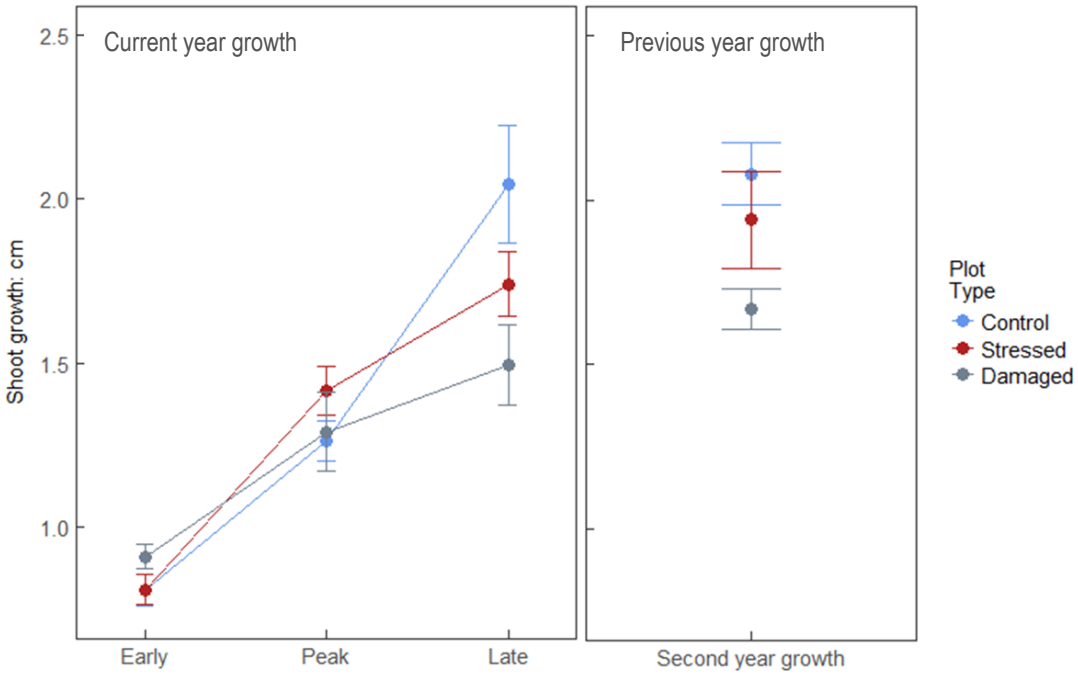

Figure 4.3: Length of (a) current year growth segments (growth of these segments is ongoing throughout the growing season) and (b) previous year segments (in which growth, laid down the previous year, is complete) of *Hylocomium splendens* for control, stressed (vascular vegetation dominated by high anthocyanin pigmentation) and damaged (vascular vegetation dominated by shoot mortality) plots. First year segment growth is shown progressively during early, peak and late season, while second year growth is from the full growing season. Error bars represent one standard error.

There was a significant positive correlation between first year growth and GPP_{600} when all plot data was combined (Fig. 4.4; $F = 4.80$, $DF = 1, 32$, $p < 0.05$, $R^2 = 0.13$). When plot types are treated separately, a strong positive correlation was maintained in control plots ($F = 19.12$, *DF*

= 1, 9, $p < 0.01$, $R^2 = 0.67$). However there was no relationship between first year growth and GPP_{600} in either damaged or stressed plots when analysed separately.

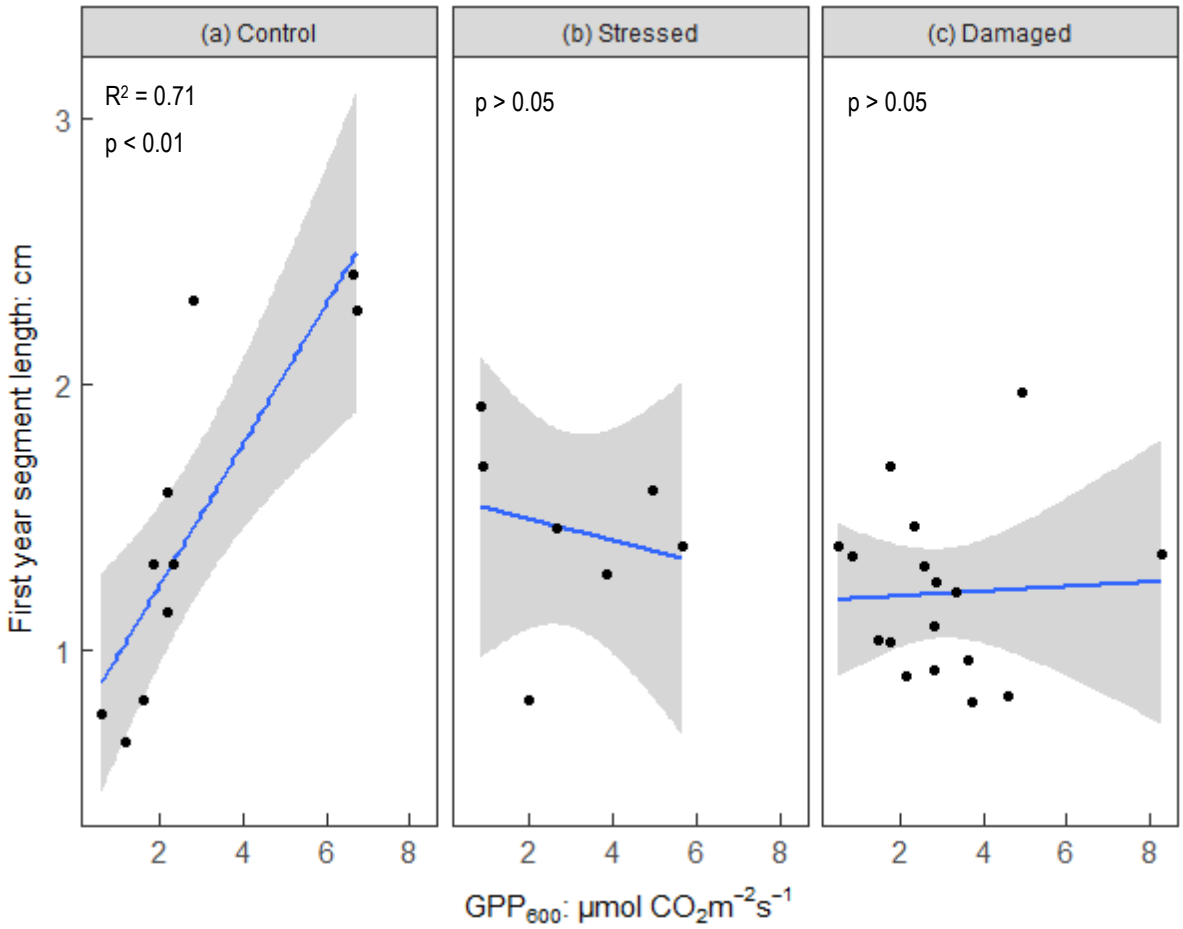

Figure 4.4: Correlations between first year segment length and GPP_{600} in (a) control plots (b) stressed plots and (c) damaged plots. Confidence intervals show one standard error.

4.4.3 Environmental conditions

The environmental variables assessed were air temperature, surface temperature (the temperature of the moss surface), and surface moisture content.

There were no significant differences in any environmental variable between plot types, although visual assessment suggests surface moisture content was slightly lower in control plots compared to stressed and damaged plots (Fig. 4.5).

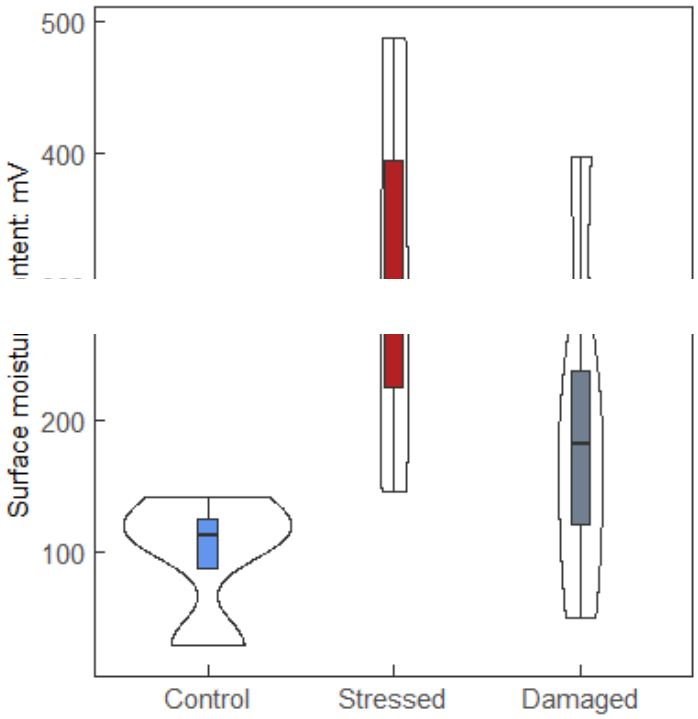

Figure 4.5: Moisture content of the moss surface in control, stressed and damaged plots. Outer shape surrounding each box plot is a mirrored density plot showing data distribution. White points show means and black bars show medians. No significant differences shown.

No environmental variable correlated with GPP_{600} across the growing season as a whole. However, there was a significant negative correlation between air temperature and GPP_{600} at early season (F = 6.76, DF = 1, 11, $p < 0.05$), with warmer air temperatures associated with lower GPP_{600}.

Air temperature also correlated positively with net moss CO_2 exchange, both across the growing season as a whole (F = 14.44, DF = 1, 34, $p < 0.001$), and at peak season (F = 8.35, DF = 1, 12, $p < 0.05$). In both cases warmer air temperatures were associated with greater net moss exchange (reflecting greater CO_2 release).

Moss respiration was positively correlated with air temperature both across the growing season as a whole (F = 7.55, DF = 1, 34, $p < 0.01$), and at peak season (F = 11.29, DF = 1, 12, $p < 0.01$), with warmer air temperatures corresponding to greater CO_2 release. Neither surface temperature nor surface conductivity correlate with any CO_2 flux.

4.4.4 Nitrogen content

Percentage nitrogen content was significantly (19%) greater in damaged plots compared to control plots (Fig. 4.6; $F = 3.95$, $DF = 2, 41$, $p < 0.05$, Tukey HSD: $p < 0.05$).

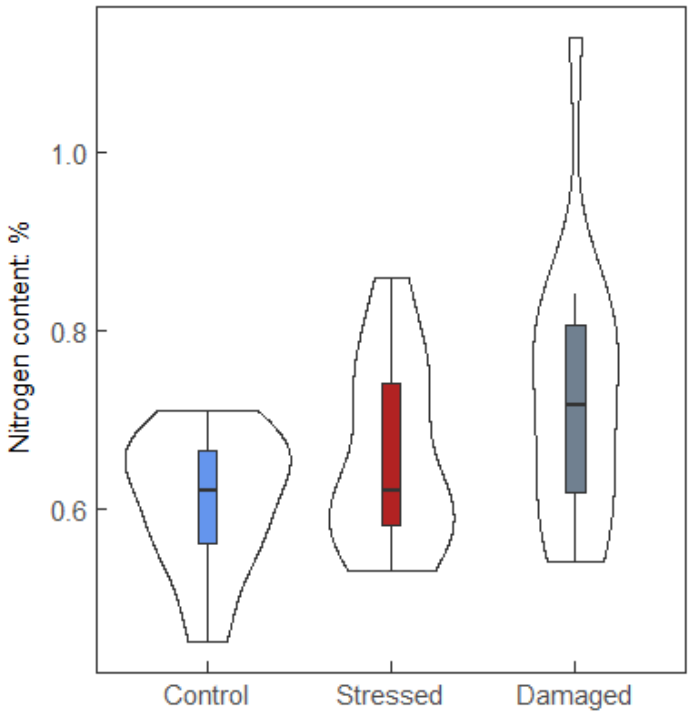

Figure 4.6: Percentage nitrogen content of moss samples in control, stressed and damaged plots. Outer shape surrounding each box plot is a mirrored density plot showing data distribution. White points show means and black bars show medians.

4.5 Discussion

This assessment of the impacts of extreme winter climatic events on the moss layer in a heathland ecosystem has shown that such events can impact productivity and growth of a widespread feather moss species. It has shown that some of these impacts change substantially across the growing season, with reductions in first year growth in this case only detectable by late season. Importantly, it has also indicated that direct and indirect impacts may differ, with reduced segment growth and increased GPP both occurring in plots where vascular vegetation is dominated by shoot mortality.

4.5.1 Impacts on CO_2 fluxes and growth

There were substantial differences in the key CO_2 fluxes GPP, net CO_2 exchange and respiration between moss plots associated with damaged, stressed and healthy control vascular vegetation. Most notably, at early season, GPP_{600} in damaged plots was more than 100% higher than in controls. Despite this increase in moss productivity in damaged plots, exposure to extreme events nonetheless appears to have had a negative physiological impact on the moss layer. This is indicated by measurements of segment growth. Previous year growth (reflecting growth of segments laid down in the summer before measurements were taken – in the second growing season following the 2013/14 frost drought event) was significantly lower in moss from damaged plots compared to control plots, suggesting that even after one growing season of recovery, moss exposed to the 2013/14 frost drought event is experiencing negative impacts. Further, current year growth was also lower in these plots compared to controls; this could reflect a negative impact of the 2013/14 frost drought event, the 2015/16 extreme winter warming event which occurred the winter before current year growth was laid down, or a combined impact of both. This suggests that, in line with previous work, these extreme winter

events have had negative impacts on the moss layer, reducing growth rates and increasing respiratory costs, possibly as a result of damage to sensitive shoot apices during winter (Bjerke et al., 2011, 2017b).

This evidence of physiological damage, alongside the increase in GPP_{600} seen in the same plots specifically at early season, suggests that increased GPP_{600} is an indirect result of altered environmental conditions in these plots, resulting from the loss of leaf area in the vascular canopy - rather than a direct consequence of extreme event exposure. For example, it is possible that while new or young moss shoots are damaged by extreme winter conditions, causing their growth to be slowed or prevented, moss segments laid down in previous years may be less susceptible to damage from frost, desiccation or high irradiance, and are able to photosynthesise at a higher rate under more favourable environmental conditions associated with browning of the vascular understory (e.g. higher light or moisture availability). This is further supported by the strong positive correlation between first year growth and GPP_{600} found in moss from control plots, and the breakdown of this relationship in moss exposed to extreme winter events (stressed or damaged plots). The increase in GPP reported here appears to contrast with previous work reporting reduced photosynthetic rates in moss following extreme winter warming (Bjerke et al., 2011). This is likely to be because previous work measured moss photosynthesis *ex situ*, on individual dried and rehydrated shoots, eliminating the influence of differences in environmental conditions and focussing specifically on the effects of shoot-level physiological change.

Moss respiration and net CO_2 exchange were also elevated in damaged plots, with consistently higher CO_2 release from the moss layer in these plots compared to controls throughout the growing season. At early season, higher moss respiration may be linked to higher productivity

and an overall increase in metabolic activity (Flexas et al., 2005, 2006), although, the consistent increase in respiration, compared to the elevation of GPP_{600} at early season alone, implies that higher respiration could also be associated with recovery, for example increased maintenance and repair costs, in moss exposed to two extreme winter events (Kirschbaum., 1988; Bokhorst et al., 2010). However, as the methodology used here is not able to exclude the contribution of vascular plant roots to total or to moss respiration, the attribution of differences in CO_2 release between plot types to the moss layer should be treated with caution, and requires further work (see below).

In stressed plots (plots where vascular plants showed little shoot mortality, but instead a pronounced dark red pigmentation), GPP_{600} was similar to that in control plots throughout the growing season. Reduced first year growth in these stressed plots indicates that moss in these plots also sustained some physiological damage following exposure to extreme events. Moss respiration in these plots was significantly higher compared to controls at peak season. This may be due to increased metabolic activity associated with maintenance and repair following the extreme winter warming event the previous winter (Kirschbaum, 1988; Bokhorst et al., 2010) but, as a marked increase in the respiration of vascular vegetation in stressed plots was also recorded during this period (Chapter 3), this apparent increase in moss respiration is likely to be an artefact of increased respiration from roots of the vascular understory. This is an increase that will not have been apparent in the soil respiration data used in the calculation of moss respiration since many of the roots are likely to have been severed in soil respiration plots. Until that uncertainty is resolved, it cannot be ruled out that despite negative impacts on growth, exposure to extreme winter warming has had little impact on moss CO_2 fluxes in plots dominated by vascular vegetation stress.

In both stressed and damaged plots, substantial increases in moss respiration mean that net CO_2 exchange is also increased compared to controls, to the extent that moss in damaged plots is a net CO_2 source throughout the growing season, while moss in control plots is a net CO_2 sink until late season. Conclusions drawn from these absolute values should be treated with caution, as a small supporting dataset of excised moss turfs suggested that *in situ* moss respiration measurements (and therefore net CO_2 exchange) may be overestimated by a consistent margin across all plot types (Appendix 1). However, the substantial relative difference in net CO_2 exchange between plots exposed to extreme winter events and control plot is supported by excised moss data, and demonstrates the potential ecological importance of these effects.

4.5.2 Environmental conditions

There is some evidence for a small (although not statistically significant) increase in moisture content of the moss surface in damaged and stressed plots compared to controls at early season. Higher moisture content in these plots at early season could be due to reduced leaf area, and therefore reduced interception of rainfall, in the vascular understory canopy, causing a higher proportion of rainfall to reach the moss layer (Price et al., 1997). It could also result from greater snow accumulation (and thus increased snow melt volume) around taller shrubs, which are more likely to be exposed during winter and therefore more likely to be heavily browned (Bjerke et al., 2017). The significantly higher nitrogen concentrations found in moss from damaged plots may support the possibility of such a relationship between browning and moisture content, as feathermoss species in high latitude ecosystems obtain much of their nitrogen from rainfall and snowmelt (Woolgrove & Woodin, 1996).

Correlations between environmental variables and CO_2 fluxes show temperature is an important influence on both GPP and respiration in the moss layer. Warmer temperatures were

associated with lower moss productivity and increased CO_2 release. This is in line with reduced growth of *Hylocomium splendens* observed following warming treatments (Potter et al., 1995). However, there is no evidence that any influence of temperature on moss CO_2 fluxes is mediated or affected directly by browning, so temperature is unlikely to be a major determining factor of the differences in CO_2 fluxes observed between damaged and control plots here.

An additional environmental factor likely to be affected by browning which is not considered here is light availability. Although feather mosses such as *Hylocomium splendens* are highly shade tolerant (Bergamini et al., 2001), reduced competition for light can nonetheless result in increased moss biomass (van der Wal et al., 2005), and light availability is thought to be a primary cause of negative relationships between moss biomass and that of vascular understory species (Bergamini et al., 2001). Given this important role of light availability, it is likely that the reductions in shading following considerable loss of canopy leaf area have some impact on productivity in the moss layer.

It is not possible to definitively attribute the higher moss GPP observed here in damaged plots to any one environmental driver or change. However, it is likely that multiple interacting factors contribute. For example, while elevated nitrogen content in damaged plots may to some extent promote GPP directly, it is also a strong indication that more nitrogen has been intercepted from precipitation in these plots. Increased moisture inputs are highly likely to promote productivity, as the water content of *Hylocomium splendens* is heavily dependent on the availability of moisture in its environment (Proctor et al., 2007). Similarly, it is likely that a substantial reduction in the leaf area of the understory canopy will reduce shading of the moss layer. However, the resulting increase in light availability may only have a positive effect when

moisture levels are high and temperatures are low (as is the case during early season), and the moss layer is therefore less likely to desiccate under increased irradiance.

4.6 Conclusion

This study supports the previous small body of work showing that extreme winter climatic events can negatively impact mosses; a key component of heathland communities at high latitudes. Further, the results reported here provide the first evidence that frost drought events specifically can reduce growth and alter CO_2 fluxes in the moss layer. This is somewhat surprising, as frost drought damages vascular vegetation through desiccation, and moss species including *Hylocomium splendens* are known to be highly desiccation tolerant.

This work also highlights that the direct physiological consequences of exposure to extreme events, and the indirect impacts of altered environmental conditions following the event, may contrast. In particular, it is shown here that moss patches which appear to have sustained damage following extreme event exposure (as indicated by growth reductions), may be more productive compared to moss not exposed to an event. Possibly, these contrasting impacts are due to different impacts on different components of the moss layer; for example physiological damage in new or young moss shoots, alongside increased productivity in older, more resilient, moss segments which may benefit from altered environmental conditions following browning of vascular vegetation. It appears likely that these altered environmental conditions which may promote increased productivity include improved moisture status, and an associated increase in nitrogen content. Other factors not assessed here, such as light availability, may also contribute.

Increased moss productivity following browning may help to ameliorate the more direct negative consequences of extreme winter events, both on the moss layer and heathland communities as a whole (Bjerke et al., 2011). However, despite the substantial elevation of early season productivity in moss from damaged plots, large and consistent increases in respiration meant that moss in these plots appeared to be a CO_2 source throughout the growing season, compared to moss from control plots, which was a net CO_2 sink during early and peak season. Given the scale of these impacts, further work is needed to understand both the mechanisms through which extreme winter events such as frost drought cause damage to feathermoss species, despite their tolerance of desiccation, and the mechanisms via which changing environmental conditions may, to some extent, ameliorate the negative effects of these events on moss CO_2 uptake.

4.7 Appendix 1: Comparison of in situ and excised plots

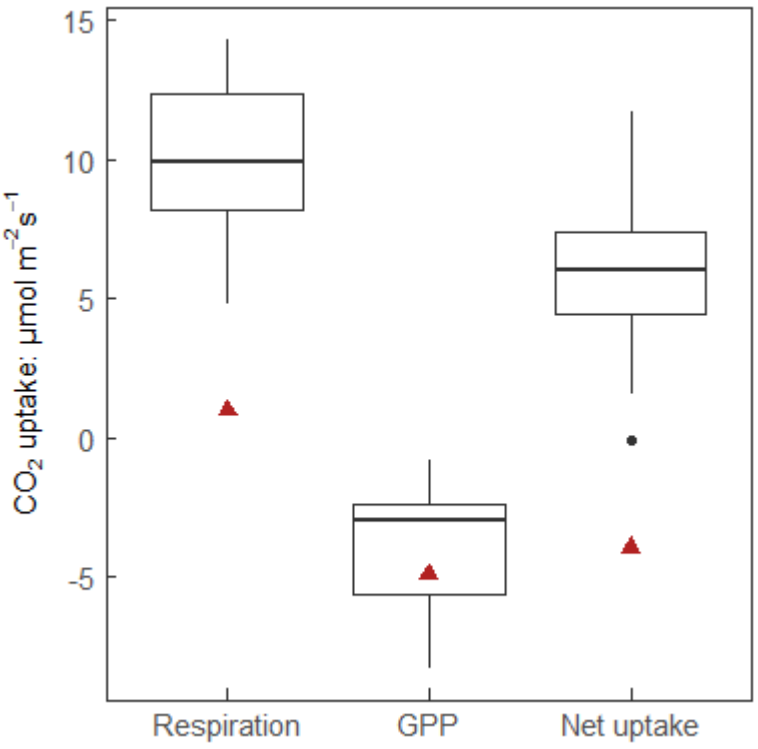

Figure 4.8: Boxplot showing mean fluxes from the moss layer (respiration, GPP and net CO_2 uptake from left to right) across all in situ plots at late season. Black bars indicate mean values. Mean values from excised plots (n=3, 1 from each plot type) are overlaid as red triangle points.

Chapter 5

Developing new metrics to assess and quantify climatic drivers of extreme event driven Arctic browning.

5.1 Summary

1. Rapid climate change in Arctic regions, particularly during winter months, is resulting in more frequent and severe extreme climatic events. These events can cause major reductions in vegetation biomass and productivity, and are therefore among the key drivers of browning trends observed across Arctic regions in recent years.

2. Extreme events which cause browning are complex. They are driven by multiple interacting climate variables, rather than by the crossing of any single climatological threshold. They are therefore defined by their ecological impact – typically plant mortality or a visible stress response.

3. Quantifying the climatic causes of these multivariate, ecologically defined events is challenging. Existing work has therefore typically focussed on event impacts and assessed climatic drivers on a case-by-case basis in a descriptive, unsystematic manner.

4. While this approach has developed an important qualitative understanding of the mechanisms underlying extreme event driven browning, it cannot definitively link browning to specific climatic variables, or predict how change in these variables, or in event timing, will influence the severity of subsequent browning. It is therefore not yet possible to quantify the contribution of extreme climatic events to regional scale browning, or to predict how increasing event frequency will influence the responses of Arctic ecosystems to climate change.

5. To address this, a quantitative framework for assessing event drivers and correlating these to observed responses is needed.

6. Novel, process-based climate metrics that can be used to quantify and systematically compare extreme event drivers were therefore developed using publically available snow depth and air temperature data (two of the main climate variables implicated in browning) in combination with plot-level observations of Normalised Difference Vegetation Index (NDVI;

a measure of greenness) and visible vegetation damage at sites across boreal and sub-Arctic Norway. These metrics explained up to 63% of variation in NDVI at these sites.

7. These metrics were then scaled up across the Norwegian Arctic Region and compared to change in remotely sensed NDVI. Significant correlations between these climate metrics and NDVI provided novel, much-needed insight into how different climatic variables and the interactions between them determine the severity of browning. They also demonstrated potential to use simple metrics to assess the contribution of extreme events to Arctic browning at regional scales, and to improve understanding of how winter climate change will affect biomass and productivity in Arctic regions.

5.2 Introduction

More climatic extreme events are among the most marked consequences of climate change (IPCC, 2017). The frequency, severity, duration and intensity of these events is predicted to increase, and in many cases substantial change is already being observed (Easterling et al., 2001, Ummenhofer & Meehl 2017). Although traditionally, climate change research has focussed on changes in mean conditions, it is now recognised that extreme events can have major impacts on ecosystems (Zscheischler et al., 2014, Solow, 2017). These impacts include considerable changes to plant communities in terms of biomass, productivity, phenology and community composition (Bokhorst et al., 2008, Jepsen et al., 2013, Reichstein et al., 2013).

In the Arctic, climate change is progressing faster than almost anywhere else in the world, and especially so during winter (AMAP, 2017). Increases in a number of extreme events particularly associated with winter climate are therefore being observed in the Arctic (Vikhamar-Schuler et al., 2016, Graham et al., 2017). These include frost drought (Chapter 3), extreme winter warming, ground icing and outbreaks of defoliating insects (Chapter 2). Already, such events are causing major disturbance in the form of sudden mortality and extreme stress in widespread Arctic and sub-Arctic plant communities - even resulting in record low productivity across the Nordic Arctic Region in 2012, attributed to the combined effects of 14 extreme events (Bokhorst et al., 2009, Bjerke et al., 2014, 2017). They are therefore an important driver of 'Arctic browning', a decline in biomass and productivity observed across Arctic regions in recent years (Epstein et al., 2015, 2016, Phoenix & Bjerke, 2016). However, while the climatic drivers of extreme events which drive browning are qualitatively understood, existing work does not allow us to quantify these drivers, to link them to damage severity, or therefore to make accurate predictions about how changing Arctic winters will impact vegetation communities and ecosystem carbon balance.

Extreme events are challenging to study. This is in part because they are by nature rare and often stochastic (Frank et al., 2015), but also because there is no single universally accepted definition for an extreme event (van de Pol et al., 2017). Extreme events are typically defined using climatological thresholds, or using an impact-orientated or biological definition. The latter two, for example, may define an extreme event as one where the ability of an organism to acclimate is substantially exceeded (Gutschick & BassiriRad, 2003) or as a climatologically rare event that alters ecosystem structure or function outside the bounds of normal variability (Smith, 2011). Impact orientated definitions may be more appropriate for assessing the drivers of extreme biological responses (in contrast to the impacts of a climate extreme) or for 'compound events'; events driven by combinations of interacting variables which separately may not trigger an extreme response, but, together, cross ecological thresholds to trigger an extreme response (van de Pol et al., 2017).

Extreme climatic events which drive Arctic browning, such as frost-drought and extreme winter warming, are examples of compound events. For instance, an extreme winter warming event is comprised of multiple conditions which interact together to trigger vegetation damage: snowmelt and associated ecosystem exposure, unseasonable warmth sufficient to initiate premature dehardening (loss of freeze tolerance), and a subsequent rapid return to sub-zero temperatures that kills buds and shoots (Bokhorst et al., 2009). These events have therefore so far been defined by their biological impacts; most clearly vegetation mortality (Bokhorst et al., 2011; Chapter 2 & 3) or a marked visible stress response indicated by persistent anthocyanin accumulation, visible as deep red pigmentation (Bjerke et al., 2017, Chapter 3).

Events such as these which are defined by an ecological impact and driven by a combination of multiple climatic variables are especially complex to quantify, compare or predict (Easterling et al., 2000). This complexity is compounded when the physiological thresholds beyond which an extreme response is triggered are likely to differ not just between species, but with event timing, preceding conditions and the occurrence of successive events (Knapp et al., 2015, Sippel et al, 2016, Wolf et al, 2016, Ummenhofer & Meehl 2017). This is particularly relevant in Arctic regions, where the depth and extent of insulating snow cover determines whether vegetation is exposed to ambient conditions such as air temperature (Williams et al., 2014; Bokhorst et al., 2016), where event timing may drastically change the conditions to which vegetation is exposed, such as light intensity, and where susceptibility to an extreme response may be heavily dependent on preconditioning, such as the duration of chilling prior to an extreme winter warming event, which could determine susceptibility to premature dehardening during the warming event.

In common with much extreme event literature (Bailey & van de Pol, 2015, Altwegg et al., 2017), assessment of the multivariate climatic drivers in studies of extreme event driven Arctic browning is therefore typically descriptive and unsystematic, dealing with a single event or a few, often differing, events. None-the-less, these studies have provided critical insights into the extreme events which drive Arctic browning, including a qualitative understanding of event drivers and quantification of major impacts on both vegetation growth, phenology and productivity, and on ecosystem CO_2 fluxes (Bokhorst et al., 2008, 2009, 2011; Bjerke et al., 2014, 2017; Parmentier 2018, Chapters 2-4). However their ability to attribute these measured responses definitively to specific hypothesised climatic drivers is limited. In addition, this approach cannot determine where response thresholds lie, or therefore predict how the severity

of the browning response could scale with different climate variables, or when specific conditions might be expected to result in vegetation damage.

This is of concern given the scale of observed browning impacts, which include substantial loss of biomass at landscape or greater scales (Bjerke et al., 2014, 2017) and, as shown in Chapters 2-4, large changes in ecosystem CO_2 fluxes with significant implications for landscape-level carbon balance. Furthermore, as the frequency of many types of extreme climatic event is predicted to increase in Arctic regions as climate change progresses, the scale and extent of these impacts are likely to increase (Vikhamar-Schuler et al., 2016, Graham et al., 2017). To fully understand how these events will influence the responses of Arctic ecosystems to climate change, a more systematic approach is needed; correlating measured response to specific, process-based climatic variables. As a first step, a framework to quantify the drivers of extreme event-driven Arctic browning, and the interactions between them, is required to understand how variation in these drivers influences the severity of response in vegetation communities, and ultimately drives browning. This quantitative understanding is critical to identify the contribution of extreme events to Arctic browning trends at regional scales, and to fully understand how winter climate change will impact Arctic plant communities.

Therefore, the aims of this work were to apply established ecological understanding about the drivers of specific instances of extreme event driven browning to (a) identify simple, process-based, quantitative climate metrics that can be used to quantify extreme winter conditions in a systematic, comparable way and (b) assess the relationship between these metrics and changes in the Normalised Difference Vegetation Index (NDVI) at regional scales. NDVI is a measure of greenness and a well-established indicator of biomass and productivity (Pettorelli et al.,

2005). However, while it can be used effectively to (for example) assess the extent of known extreme-event driven browning events, it alone cannot distinguish between extreme event driven browning and other browning drivers (such as changes in the length of the growing season). Therefore, the development of appropriate climate metrics in this analysis initially utilised a dataset of plot-level measurements of NDVI and visible vegetation damage (proportion of browned vegetation) in areas known to have been affected by extreme winter climatic events (primarily frost drought and extreme winter warming experienced during the 2013/14 winter) and subsequent browning. This observed data covered 19 sites with a total of 357 observations of browning across boreal and sub-Arctic Norway. Following this, national meteorological and modelled snow cover datasets were used to compare climate metrics with remotely sensed NDVI across the Norwegian Arctic Region (the Norwegian mainland north of the Arctic Circle and extending east to the northernmost point of the Nordic Arctic Region). It was hypothesised that (a) simple climate metrics will be identified that correlate with NDVI in areas known to have been affected by browning, (b) these metrics will reflect ecological understanding about the mechanisms underlying extreme climatic event driven browning, and (c) these metrics will correlate with NDVI change at regional scales.

5.3 Methods

5.3.1 Developing climate metrics using plot-scale analysis

5.3.1.1 Plot-level NDVI

Widespread browning of evergreen shrubs across boreal and sub-Arctic regions of Norway was observed following the 2013/14 winter, attributed to extreme winter weather conditions (Meisingset et al., 2015; Bjerke et al. 2017). For this plot-scale analysis, observations of browning recorded in the growing seasons of 2014 or 2015 were collated from 19 sites (Fig. 5.1) in boreal and sub-Arctic Norway. Browning at the majority of these sites was driven by the extreme conditions during the 2013/14 winter, with remaining sites browned during previous winters (2011/12 at the earliest). Observations consisted of NDVI measurements taken using digital cameras converted to record Red-Green-Blue (Llewellyn Data Processing, New Jersey) or a commercial GreenSeeker NDVI sensor (Trimble, California) and/or visual assessments of plant damage (mortality; observed browning). The latter were recorded either as percentage cover of browned vegetation, or the proportion of the dominant species affected by browning (own data and data provided by J. Bjerke). As NDVI and observed browning (plot survey) were significantly correlated ($p < 0.05$), these correlations (calculated separately across plots within each county) were used to predict plot-level NDVI at plots where observed browning alone, and not NDVI, was recorded. The number of NDVI measurements available for each site ranged from 1 to 143 (with a mean of 19).

To provide controls, a 'pre-browning' NDVI value was estimated for each site. To do this, linear regressions of NDVI and observed browning were calculated separately for each county ($p < 0.05$) and used to predict NDVI in vegetation with no observed browning. This approach produced ecologically reasonable estimates for healthy dwarf-shrub heathland NDVI of

between 0.67 and 0.75. At two sites, NDVI values in adjacent undamaged vegetation (in addition to observed browning plots) were recorded; in these cases recorded NDVI values in undamaged vegetation were averaged to estimate pre-browning values for those sites. Pre-browning NDVI values were assigned to the growing season preceding the winter during which browning occurred (i.e. 2013 for the majority of sites).

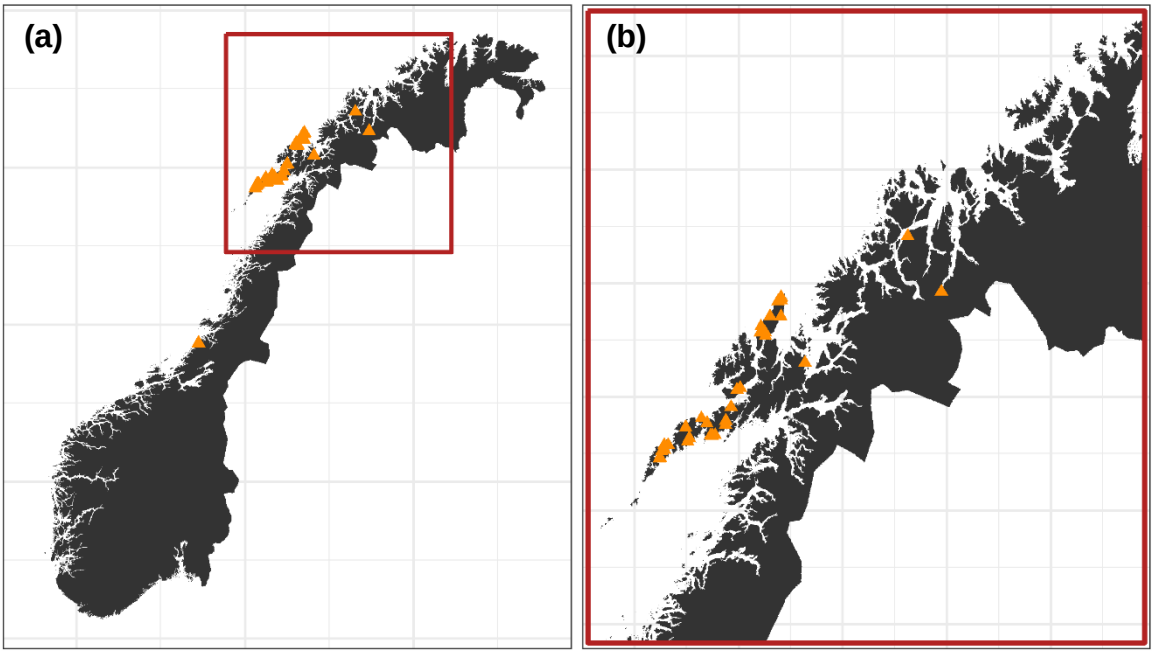

Figure 5.1: (a) Map of Norway showing locations of 19 sites (orange triangles) where extreme event-driven browning was observed and plot-level NDVI was measured. The Norwegian Arctic Region, the area used for regional level analysis, is outlined in

5.3.1.2 Climate data

Snow depth maps of Norway with a daily temporal and 1 x 1 km spatial resolution were obtained from The Norwegian Water Resources and Energy Directorate (NVE). This publically available data is produced using the SeNorge snow model (http://www.senorge.no), which is forced by daily observations of temperature and precipitation and performs well in Norway (Saloranta, 2012).

From SeNorge snow maps, daily snow depth values were extracted from each pixel which contained plot-level browning observations in the dataset described above. This data was extracted for each winter between 2011 and 2015. Daily snow depth values were then averaged for each site.

Daily mean, minimum and maximum air temperature was obtained from the Norwegian Meterological Institute via the publically available eklima.no web portal. Data for 2011 – 2015 was downloaded from the weather stations closest to each site at an elevation of < 200m (as sites were located in relatively low-lying areas). Based on the quality and availability of air temperature data from these stations, data from 14 stations was subsequently analysed.

5.3.1.3 Development of metrics

Snow and air temperature data was combined into a single dataset. Only data from the winter period was used to develop climate metrics, to avoid any confounding effect of occasional late spring or summer snowfall. To identify an appropriate window for this winter period during which snow cover and cold temperatures could reasonably be expected, and therefore during which warmth and exposure may have ecological consequences, first winter snow fall and final spring snow melt for each winter (2011/12 – 2014/15) were identified. This was done by

selecting all periods of absent snow cover (0 mm snow depth) throughout the year; first winter snow fall and final spring melt were recorded as the dates following and preceding the long summer exposure period in consecutive years. Winter was thus defined from Day of Year 305 (Day of Winter 1) to Day of Year 120 (Day of Winter 181 or 182).

Within each winter a set of approaches were used to extract 'events' which may have influenced NDVI. These were 'exposure events' based on absent snow cover (0 mm snow depth) or 'warming events' based on warm winter temperatures (> 2 ˚C). A 2 ˚C threshold for warming events was chosen based on visual assessment of temperature data during warming events known to have resulted in browning, and aimed to ensure the full duration of any warming events was considered, while differentiation between short, relatively mild warming events and prolonged periods of high temperatures was facilitated by the intensity metric (below and Table 5.1). Periods of exposure or warming occurring before initial winter snowfall or cold temperatures were excluded. For exposure events, event duration, start date and mean air temperature were recorded. For warming events, a wider range of variables were recorded (Table 5.1). Metrics for each event type were chosen based on the mechanism of damage particularly associated with either winter warming (i.e. premature dehardening and initiation of spring-like bud burst), followed by frost damage on the return of cold temperatures) or frost drought (loss of snow cover and subsequent exposure, leading to gradual desiccation as transpiration exceeds uptake from frozen or near-frozen soils) (Table 5.1). These two processes account for the majority of extreme climatic event driven browning in mainland Norway (J. Bjerke, personal communication).

Using this approach, several events were extracted for each year. To select those most likely to influence growing season NDVI, up to 4 events were selected for each year. These were (a) the

warming event with the highest 'Intensity' (air temperature*duration; Table 5.1), (b) the warming event with the greatest 24 hour temperature drop following the final day of the event, (c) the maximum duration exposure event (i.e. no snow cover) (d) the warmest exposure (no snow cover) event.

Table 5.1: Variables (climate metrics) recorded for each event type (either warming events based on consecutive daily air temperatures of >2˚C, or exposure events based on consecutive days of absent (0mm) snow cover) as extracted from snow depth and air temperature data.

Variable	Meaning	Event type
Count	Event duration (days).	Warming; exposure
Start date	Date (Day Of Winter) of the first day of the event.	Warming; exposure
Intensity	Cumulative mean daily air temperature (˚C) linearly weighted by duration throughout the event. E.G. for a 3 day event with daily mean air temperatures of 4˚C, 6˚C and 3˚C, Value = (4*1) + (6*2) + (3*3) = 25.	Warming
Mean snow depth	Mean snow depth (mm) during the event.	Warming
Mean air temperature	Mean air temperature (˚C) during the event.	Exposure
End minimum temperature	Minimum temperature 24 hours following the final day of the event (˚C).	Warming
24 hour temperature drop	Difference between mean daily air temperature on the last day of the event and minimum air temperature 24 hours later (˚C).	Warming
5 day temperature mean	Mean daily air temperature over the 5 days following the event (˚C).	Warming

5.3.1.4 Satellite NDVI

Remotely sensed NDVI data were extracted from the publically available MOD13Q1 version 6 dataset. MOD13Q1 provides level 3 16 day composites of vegetation indices at 250m resolution in a sinusoidal projection. Tiles were downloaded for DOY 193 in 2015, the nearest date to when plot-level measurements were recorded, using USGS Earth Explorer. These tiles were re-projected to the UTM Zone 33 projection using the NASA HDF-EOS To GeoTIFF Conversion Tool (HEG) and mosaicked to encompass the full extent of plot-level data.

5.3.1.5 Statistical analysis

Correlations between metrics representing selected events and subsequent growing season NDVI were assessed by multiple regression. Selection of metrics with high explanatory power for use in multiple regression was initially guided by tree based regression analysis, following which interactions included in multiple regression of each event type (a – d, see '*5.3.1.3 Development of metrics'*) against NDVI were based on a priori knowledge and predictions relating to the mechanisms through which each event may cause browning. Terms and interactions without a significant correlation with NDVI change were removed step wise. A maximum of three terms was included in each multiple regression. Plot-level and MODIS NDVI were compared by linear regression.

5.3.2 Applying climate metrics at regional scales

The Norwegian Arctic region (Fig. 5.1) was selected for upscaling as a clearly definable region encompassing the majority of sites used for plot-level analysis. This area extends southwards to the Arctic Circle and eastwards to the longitude of Magerøya, Finnmark; the most northerly point of the Nordic Arctic Region (NAR, Bjerke et al., 2014).

5.3.2.1 Satellite NDVI

Remotely sensed NDVI data were extracted from the publically available MOD13Q1 version 6 dataset described above from the beginning of May (DOY 129) to the end of August (DOY 241). Tiles were extracted for this period in 2014, as the most marked and widespread browning observed at plot-level occurred during the 2013/2014 winter (see "*5.3.1.1 Plot-level NDVI*"), and from 2005 to 2010 (inclusive) to create a baseline period for comparison. Tiles were re-projected and mosaicked as described above. Un-vegetated areas (NDVI < 0.12) were masked out. Images were aggregated (by mean) to a 1km resolution to facilitate comparison with climate data.

From this May-August NDVI dataset, time-integrated NDVI (TI-NDVI; the sum of NDVI values during this period) was calculated for 2014 and the 2005-2010 baseline period. Change detection was then carried out between 2014 and the 2005-2010 baseline period, producing TI-NDVI change. This process was also carried out for mean July (approximately peak biomass) NDVI.

5.3.2.2 Climate data

Data was obtained from The Norwegian Water Resources and Energy Directorate (NVE) and the Norwegian Meteorological Institute as described above. To provide air temperature data continuously across the Norwegian Arctic region, data was downloaded from every Norwegian Meteorological Institute weather station with an elevation of < 200m in the counties of Nordland, Troms and Finnmark; a total of 77 stations. The 200m cut-off was used since above this, weather stations tended to be on mountainsides, where data may be less representative of the broader surrounding landscape and so be less suitable for interpolation (the majority of the heathland vegetation typically affected by browning is in low lying regions). Mean daily air

temperature from each station was interpolated across these three counties using Inverse Distance Weighted interpolation, before the resulting air temperature map was cropped to the Norwegian Arctic region. Climate data (both air temperature maps and SeNorge snow maps) were resampled using nearest neighbour assignment resampling to correspond to each other and to MODIS data.

5.3.2.3 Climate metrics

Maximum intensity warming events and maximum duration exposure events were chosen to investigate further in this analysis due to their high explanatory power in the plot-level analysis. Extreme event metrics for these two event types were calculated as described above for the 2013/2014 winter within each 1km pixel.

5.3.2.4 Statistical analysis

Multiple regressions of the parameters for each event type were carried out using Generalised Least Squares against TI-NDVI change. This was also done for July NDVI change (change in mid-season NDVI). All regressions were carried out at a 4km resolution to reduce computational intensity. As the Moran's I test indicated significant spatial autocorrelation in model residuals, this was accounted for by using correlated error structures (exponential, Gaussian, linear, spherical and rational quadratic) and selecting the appropriate model error structure (rational quadratic for TI-NDVI and exponential for July NDVI) according to the AIC criterion.

5.4 Results

5.4.1 Developing climate metrics using plot-scale analysis

Climatic events described by simple metrics were closely correlated with plot-level NDVI. 'Maximum intensity warming events' were calculate as the greatest value within a pixel of sum of daily mean air temperature multiplied by event duration (i.e. intensity) in periods of consistently warm (> 2˚C) winter air temperatures. The start day in winter , mean snow cover and intensity of these events explained more than 60% of variation in plot-level NDVI in multiple regression (Fig 5.2a; $F = 14.26$, D.F. = 4, 27, $p < 0.001$, $R^2 = 0.63$), with high intensity, later start day and lower mean snow cover corresponding to lower NDVI values. 'Temperature drop warming events' were calculated as the periods of consistently warm air temperature (> 2^{o}C) with the greatest drop in temperature during the 24 hours following the final day of the event. The start day and intensity of these events explained almost 50% of variation in NDVI in multiple regression (Fig 5.2b; $F = 10.81$, D.F. = 3, 33, $p < 0.001$, $R^2 = 0.45$). Again, high intensity and later start day were associated with lower NDVI. For both warming event types (maximum intensity warming events and temperature drop warming events) there was a significant interaction between intensity and start day ($p < 0.05$). Tree-based regression analysis (Appendix 1) of metrics calculated for warming events also highlighted the 24 hour temperature drop following an event as a metric with high explanatory power for variation in NDVI; mean NDVI in plots which had experienced a maximum intensity warming event with a 24 hour temperature drop of more than 5.7˚C was 0.2 (NDVI) lower than in those which had not. While the importance of the 24 hour temperature drop is of interest and provides some insight into mechanisms underlying plant damage following warming events, its computational complexity (in particular its use of minimum as well as mean air temperature datasets) meant

that it was unsuitable for further analysis within this work and was therefore not included in multiple regression.

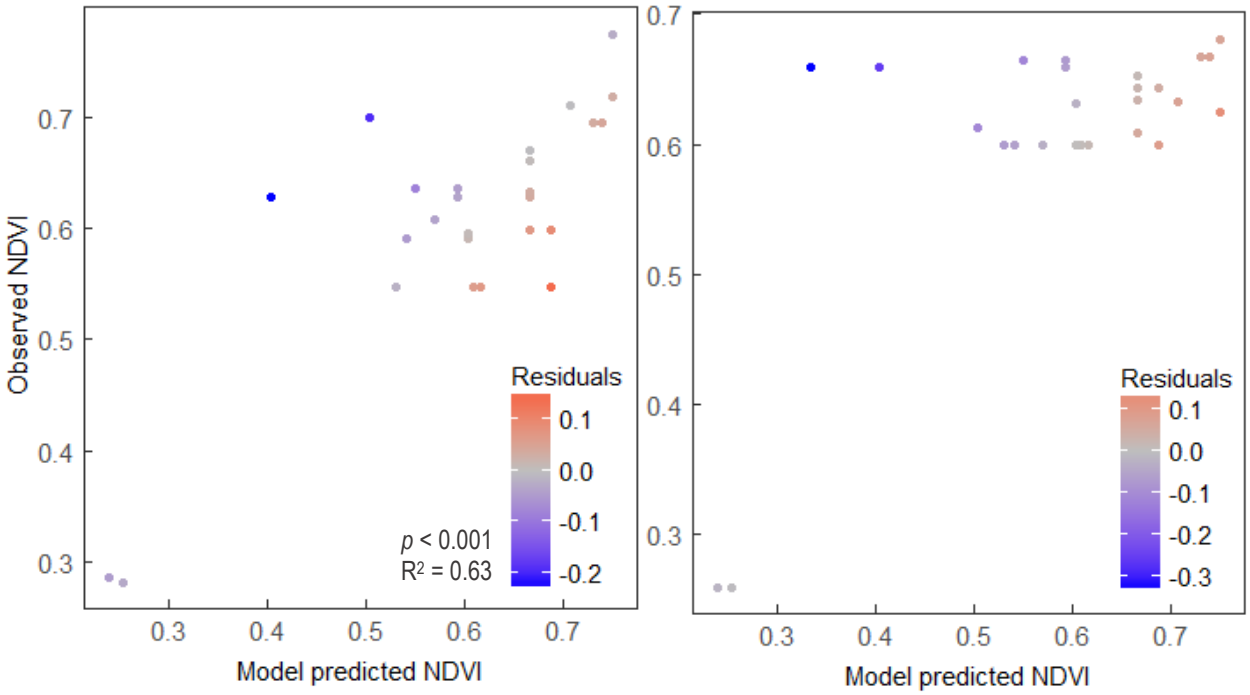

Figure 5.2: Correlations between plot-level NDVI as predicted by multiple regression models and plot-level NDVI observed in the field. Correlations are shown for (a) 'Maximum intensity warming events' and (b) 'Temperature drop warming events'. Points are coloured according to the value of residuals; warm colouring indicates that multiple regression predicted higher NDVI values than were observed in the field, while cold colouring indicates that multiple regression predicted lower NDVI values than observed.

'Maximum duration exposure events' were calculated as the periods of consistently absent snow cover (0 mm snow depth) with the longest duration in days during winter. The start day of and mean temperature during these events were highly correlated with NDVI in multiple regression (Fig 5.3a; $R^2 = 0.61$, $F = 17.87$, D.F. = 3, 29, $p < 0.001$). Maximum warmth exposure periods are the periods of consistently absent snow cover with the highest mean temperature. The start day and duration of these events were also significantly correlated with NDVI in multiple regression, albeit with a weaker R^2 (Fig 5.3b; $F = 3.802$, D.F. = 3, 29, $p < 0.05$, R^2 =

0.21). In both cases there was a significant interaction between the two model predictors (start day and mean temperature).

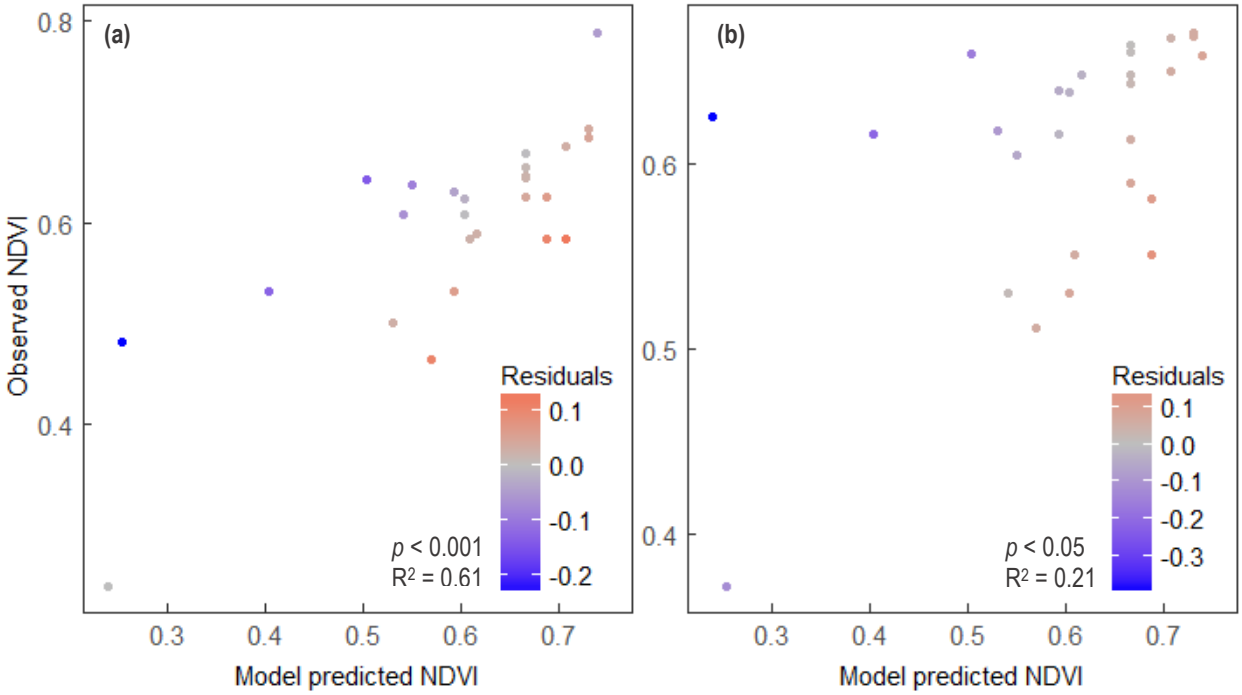

Figure 5.3: Correlations between plot-level NDVI as predicted by multiple regression models and plot-level NDVI observed in the field. Correlations are shown for (a) 'Maximum duration exposure events' and (b) 'Maximum warmth exposure events'. Points are coloured according to the value of residuals; warm colouring indicates that multiple regression predicted higher NDVI values than were observed in the field, while cold colouring indicates that multiple regression predicted lower NDVI values than observed.

5.4.2 Applying climate metrics at regional scales

Climate metrics calculated and mapped across the Norwegian Arctic implicate the processes underlying frost drought and extreme winter warming in MODIS NDVI change between the 2005-2010 baseline period and 2014. They also highlight interesting characteristics of winter climate and the conditions which lead to extreme climatic event driven browning.

5.4.3.1 Event characteristics

Maximum intensity warming event metrics (intensity, start day and mean snow cover) show that prolonged periods of warmth during winter were rare across the Norwegian Arctic region in the 2013/14 winter (indicated by low maximum intensity across much of the region; Fig 5.4a). Such rare occurrence is consistent with climatic conditions which can produce an ecologically extreme response (i.e. extreme events). The median observations in the 2013/14 winter was 61 across the entire Norwegian Arctic Region, compared to a median of 328 in observed browning sites. The wide variation inherent in this variable (with a range of 3 to 2440) means that when mapped, areas where events of especially high intensity took place – reflecting prolonged, unseasonable warmth –are clearly distinguishable by eye (Fig 5.4a). Visual comparison suggests these are most common in coastal areas, including on Vestvågøy, Lofoten Islands (Chapters 2 and 3 field site location). While most warming events across the region occurred in the first half of the winter period, with 60% occurring in January alone, events with the highest maximum intensity typically began later in the season (Fig 5.4; model: AIC = 53029.17, R.S.E = 187.24, D.F = 5265; start day: $t = 9.56$, S.E. = 0.07, D.F. = 5265, $p<0.001$). There was no significant correlation between event intensity and mean snow cover during the event.

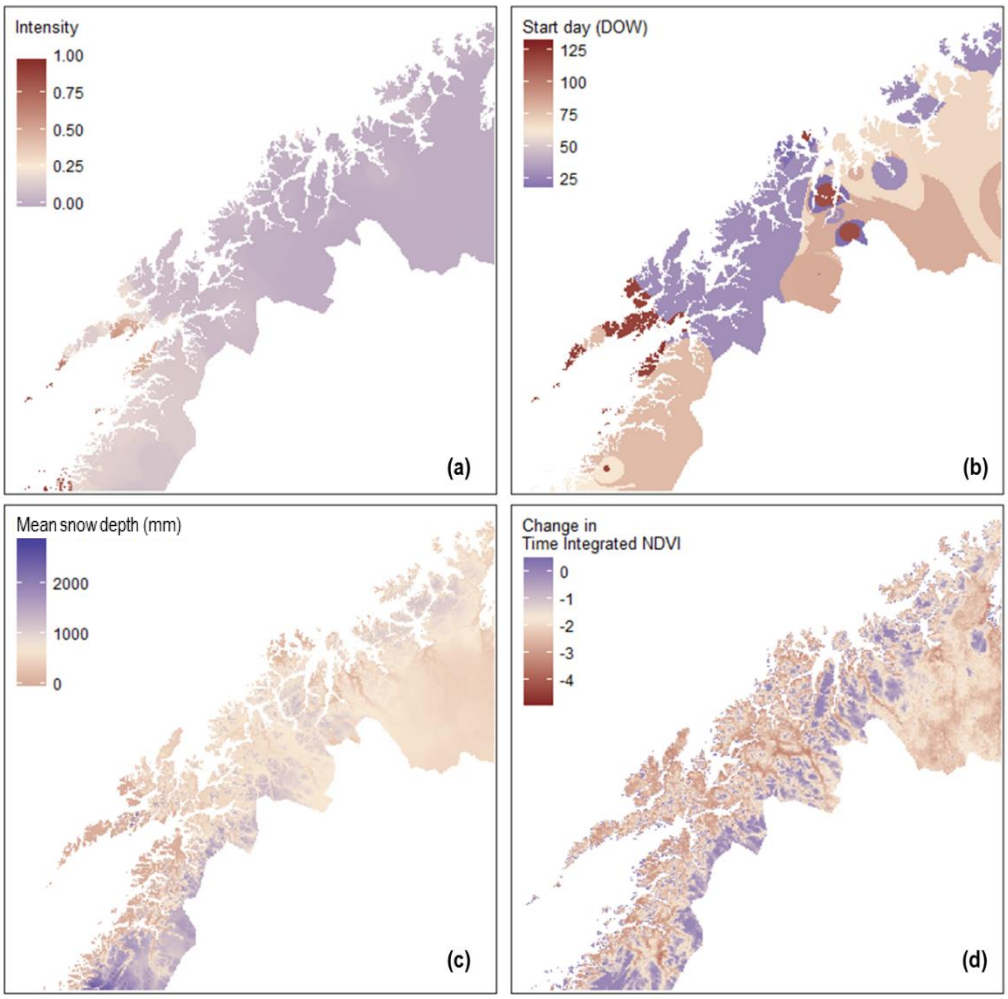

Figure 5.4: Climate metrics calculated for the warmth event with the highest intensity in each 1 km^2 pixel. Climate metrics shown are (a) intensity; cumulative warmth weighted linearly by event duration, here rescaled to a range of 0-1 for easier interpretation, (b) the start day of the event (Day Of Winter 1 equivalent to Day Of Year 305) and (c) mean snow depth (mm) during the event. The change in time integrated NDVI between the baseline 2005-2010 period and 2014 is shown (d) for comparison with the above potential climatic drivers.

Similarly, exposure event metrics show that exposure during winter was relatively rare across the Norwegian Arctic in the 2013/14 winter (Fig. 5.5a), and was limited primarily to coastal areas. Where exposure (snow depth = 0) events did take place further inland, visual comparison

suggests they typically began later in the winter compared to those taking place close to the coastline (Fig. 5.5b). All winter 2013/14 exposure events across observed browning sites plus the majority (59%) of exposure events across the Norwegian Arctic region were associated with a mean air temperature of more than 0˚C during the event. However, 21% of Norwegian Arctic-region exposure events were relatively cold, with mean air temperature below or equal to -2˚C. Visual comparison suggests these cold exposure events may be more common further inland. Timing of the longest exposure events across the region was relatively evenly spread throughout the majority of the winter period, although with a higher proportion (32%) of events occurring in April.

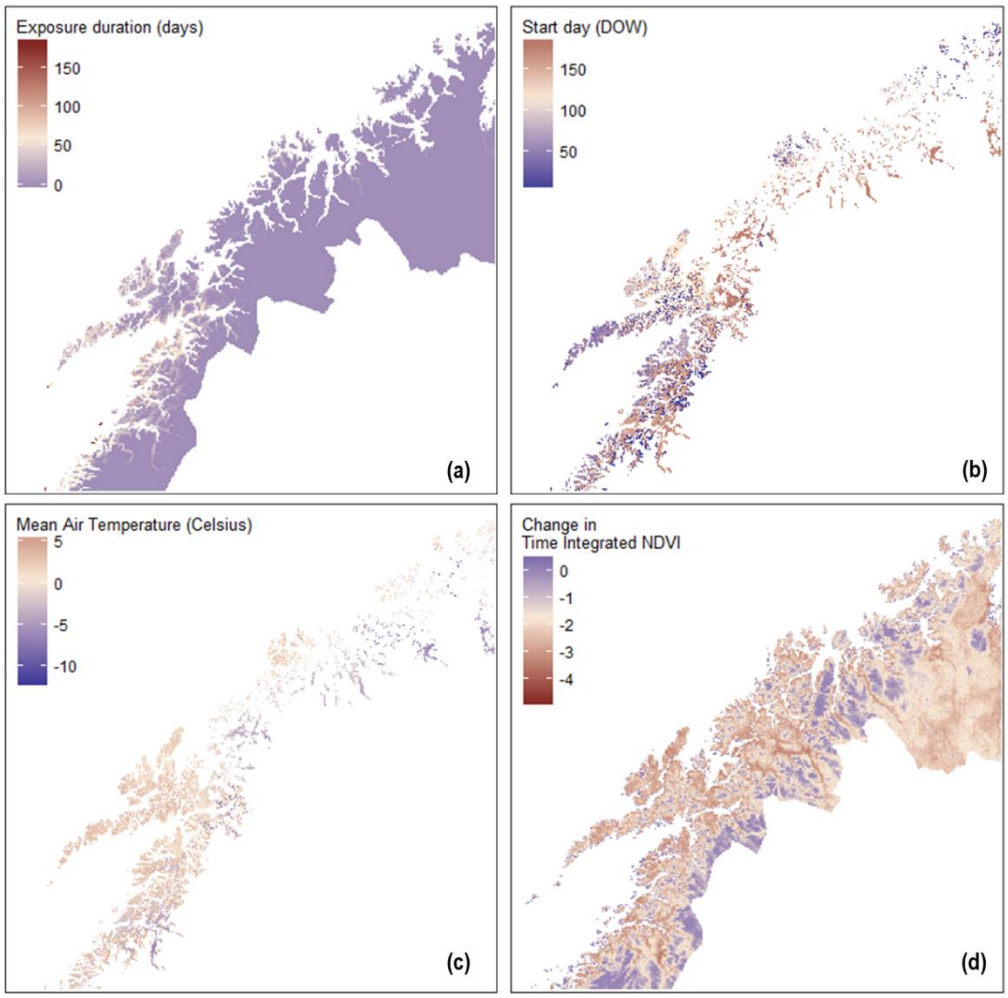

Figure 5.5: Climate metrics calculated for the exposure event with the longest duration in each 1 km^2 pixel. Climate metrics shown are (a) event duration (b) the start day of the event (Day Of Winter 1 equivalent to Day Of Year 305) and (c) mean air temperature (˚C) during the event. The change in time integrated NDVI between the baseline 2005-2010 period and 2014 is shown (d) for comparison with the above potential climatic drivers.

5.4.3.2 Correlation with MODIS NDVI

Maximum intensity warm events: both the intensity of the event (Fig. 5.4a), and the mean snow cover during the event (Fig. 5.4c) were significantly positively correlated with change in time integrated NDVI (TI-NDVI), i.e. cooler and shorter warming events with shallower snow resulted in greater negative change in TI-NDVI. (Fig. 5.4d; model: AIC = 5463, R.S.E. = 0.54, D.F. = 5259; intensity: t = 2.1, S.E. < 0.001, p < 0.05; mean snow cover: t = 13.9, S.E. < 0.001,

$p < 0.001$). There was also a significant negative interaction between intensity and mean snow cover ($t = -5.19$, S.E. <0.001, $p < 0.001$) and, while the start day of the event did not have a significant main effect, there was a significant positive three-way interaction between intensity, mean snow depth and start day (Fig. 5.6, $t = 2.56$, S.E. < 0.001, $p < 0.05$). Overall, these terms and interactions show that increasing event intensity (greater air temperature * duration) at the shallowest snow depths results in smaller TI-NDVI reductions (Fig. 5.6, 25cm line), while at the deepest snow depths increasing event intensity results in greater TI-NDVI reductions (Fig. 5.6, 100cm line). As winter progresses (moving left to right on Fig. 5.6), the slope of the relationship between TI-NDVI change and event intensity becomes more positive at any given snow depth; meaning that the threshold of snow depth above which this slope is negative increases.

There was no correlation between change in peak season (July) NDVI and any maximum intensity warm event metric.

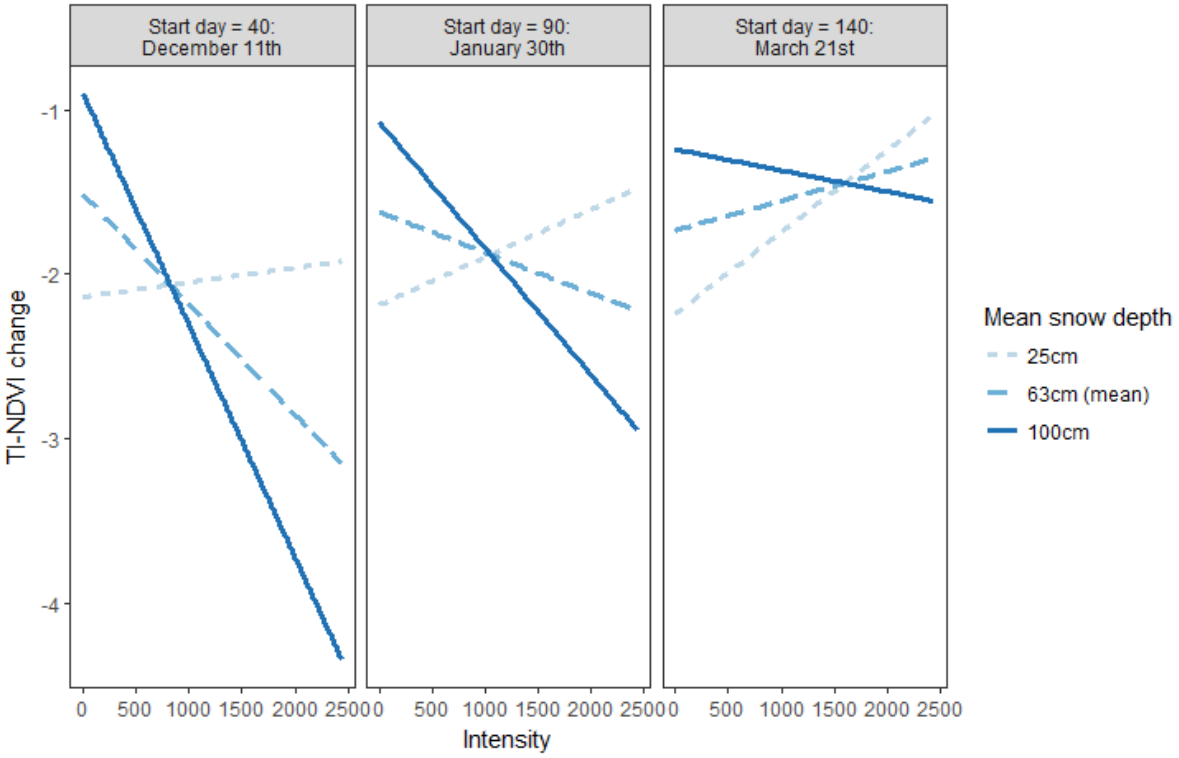

Figure 5.6: Three way interaction between intensity (the sum of air temperature multiplied by duration for each day of the event), start day, and mean snow depth in multiple regression of maximum intensity warmth events (the warming event within each pixel with the greatest intensity) with TI-NDVI change. Lines illustrate relationships between event intensity and TI-NDVI change at snow depths of 25cm (short dashed line), the mean value across the Norwegian Arctic Region of 63cm (long dashed line) and 100cm (solid line). Panels show these relationship at different time points during winter.

Maximum duration exposure events: Start day of the longest exposure event (Fig. 5.5b) was significantly negatively correlated with change in TI-NDVI, i.e. later longest exposure events resulted in greater negative NDVI change (model: AIC = 3299, R.S.E. = 0.57, D.F. = 2331; start day: $t = -3.91$, S.E. < 0.001, $p < 0.001$). The mean temperature of the event (Fig. 5.5c) was significantly positively correlated with change in TI-NDVI (greater negative TI-NDVI change with cooler events; $t = 3.29$, S.E. = 0.015, $p < 0.001$), while event duration (Fig. 5.5a) showed

no correlation. There was a significant interaction between start day and mean temperature, showing that the slope of the positive relationship between TI-NDVI change and mean temperature became shallower, and eventually became negative, as the winter progressed (Fig. 5.7; t = -3.5, S.E. < 0.001, p > 0.001).

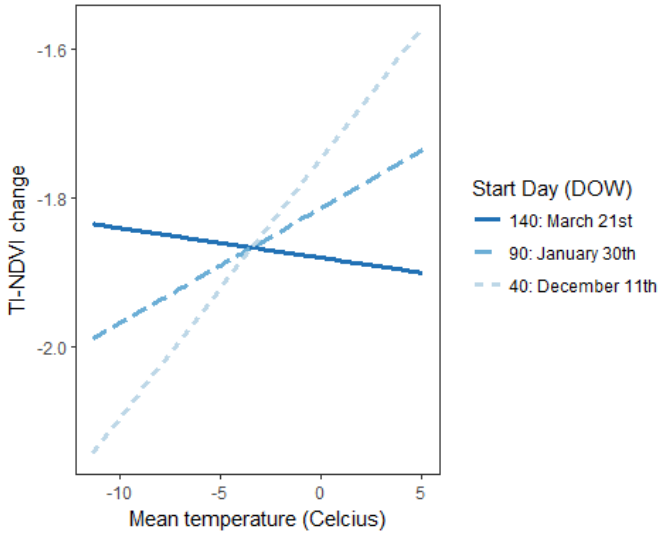

Figure 5.7: Two way interaction between the start day and mean air temperature of maximum duration exposure events (periods of consistently absent snow cover with the longest duration in each pixel). Lines illustrate relationships between mean temperature and TI-NDVI change on Day of Winter (DOW) 40 (December 11th; short dashed line), DOW 90 (January 30th; long dashed line) and DOW 140 (March 21st; solid line).

There were no correlations between any exposure event metric and change in July NDVI.

5.5 Discussion

We demonstrate that simple climate metrics can explain variation in NDVI (vegetation greenness) in areas known to have been affected by extreme event-driven Arctic browning. These process-based metrics (i) reinforce previous descriptive and qualitative assessments of the climatic drivers of browning, showing that periods of unusual warmth and low snow cover during winter are associated with loss of vegetation greenness (Hancock, 2008; Bjerke et al., 2014, 2017; Bokhorst et al., 2009; Meisingset et al., 2015), and (ii) provide much-needed insight into how variation in these climate drivers influence the severity of the browning observed. This work also suggests that such metrics, easily calculated from mean daily air temperature and snow depth, could be used to assess the contribution of winter climatic extreme events to Arctic browning at regional scales, and ultimately to improve predictions of how changing Arctic winters will affect the biomass and productivity of vegetation communities.

5.5.1 Plot-level analysis

Metrics representing both maximum intensity warming events (the period of consistently warm, > 2˚C, air temperature with the highest intensity in the plot's pixel, where intensity is the sum of daily mean air temperature multiplied by event duration) and maximum duration exposure events (the period of consistently absent snow cover, 0 mm snow depth, with the longest duration in days in the plot's pixel) explained a high proportion of variation in plot-level NDVI across observed browning sites. In analysis of maximum intensity warm events, high intensity, late start date and shallow snow depth were associated with low NDVI. This is consistent with NDVI and biomass reductions driven by extreme winter warming or frost drought events (Bokhorst et al., 2009, Bjerke et al., 2014; Meisingset et al., 2015). In the former, unusual winter warmth causes premature dehardening and initiation of spring-like bud-

burst following snow melt and exposure of vegetation to warmth, after which the rapid return of sub-zero temperatures causes frost damage (Phoenix & Lee, 2004; Bokhorst et al., 2008). It is likely that vegetation could be more prone to extreme winter warming damage later in winter, after a substantial cold period has already been experienced and when light levels are increasing, meaning any subsequent warm period is more likely to trigger premature de-hardening and bud-burst (Körner, 2016; Parmentier et al., 2018). Alternatively, frost drought occurs when vegetation is exposed and soils are frozen, which reduces the availability of free water and promotes winter desiccation (Sakai & Larcher, 2012; Tranquillini 1982). In late winter, soils are most likely to be closer to their coldest year-round temperature. Exposure events with a higher mean air temperature at this time may therefore encourage plant transpiration and water loss, but may not be sufficiently warm to initiate soil thaw and an increase in the availability of free water (Larcher & Siegwolf, 1987). Desiccation is likely to be further accelerated in late winter due to higher solar irradiance, which promotes physiological activity including transpiration, increasing water loss (Hadley & Smith, 1986, 1989). However, since there is a high explanatory power of the 24 hour drop in temperature following the end of the warm period, it appears likely that the browning observed at these sites is driven largely by extreme winter warming rather than frost drought.

In analysis of maximum duration exposure events, a late start day and comparatively warm mean air temperature (1.7˚C) was associated with lower plot-level NDVI, with the negative correlation between mean air temperature and NDVI steepening throughout the winter. Similarly to the above, this could either indicate frost drought or extreme winter warming. Regardless, it would appear that periods of warmth associated with snowmelt or shallow snow depth, particularly in late winter, are strong drivers of the NDVI reductions observed at these sites. This is also consistent with observations that reductions in *Vaccinium myrtillus* biomass

in the 2014 growing season in Northern Norway were associated primarily with winter warmth (Meisingset et al., 2015).

5.5.2 Regional scale analysis

Climate metrics calculated for both event types – maximum duration exposure events and maximum intensity warming events show that both prolonged, warm periods during winter and periods of winter exposure are rare across the Norwegian Arctic region; the majority of the region experienced low maximum intensity of warmth events and no periods of exposure during the 2013-14 winter. This is consistent with ecological theory that states that extreme events should be rare enough that organisms are not (or poorly) adapted to them, such that when these events do occur, an extreme ecological response is produced (Smith, 2011). As might be expected, the highest magnitudes of both event types occurred primarily along the coastline, where temperatures are warmer and the climate more variable. As both mean temperatures and temperature variability are expected to increase as climate change progresses (AMAP, 2017), this suggests that coastal areas may act as indicators of conditions likely to become more common as colder, inland areas warm, and supports predictions that the magnitude and frequency of these events will increase across Arctic regions as climate change progresses (Vikhamar-Schuler et al., 2016, Graham et al., 2017).

Climate metrics for both event types correlated with change in TI-NDVI. For maximum duration exposure events the strongest predictor of change in TI-NDVI was mean temperature during the exposure event. However, this relationship changes throughout the winter; the negative correlation between start day and change in NDVI (with later events associated with greater TI-NDVI reductions) is steeper where mean temperature is high. This means that early in the winter, cold exposure events are associated with greater TI-NDVI reductions, but in late

winter, from around March, it is warmer events that cause larger TI-NDVI reductions. It is these late winter, relatively warm events which contribute to the largest reductions in TI-NDVI overall. Similarly to the plot-level analysis, this could suggest that in late winter, when vegetation has already experienced cold winter temperatures and light availability is increasing, warm conditions may be more likely to initiate premature dehardening, driving extreme winter warming damage (Bokhorst et al., 2010). However there is also evidence that the impact of exposure events on change in TI-NDVI may be driven to some extent by frost drought. As described above, mild temperatures and high light levels in late winter could accelerate desiccation by encouraging transpiration and water loss before soils begin to thaw (Parmentier et al., 2018). The contrasting link between TI-NDVI reduction and colder temperatures in early winter suggest greater possibility of frost-drought as the driving mechanisms of damage: in early winter when normal air temperatures are higher and soils have had little time to chill, cold exposure events may accelerate or exacerbate soil freezing (Hancock, 2008; Zhao et al., 2017), promoting vegetation desiccation.

For maximum intensity warmth events the strongest predictor of change in TI-NDVI was mean snow depth during the event. Although, overall, maximum intensity warmth events with shallower snow depths were associated with greater TI-NDVI reductions, the relationship between the severity of these events and change in TI-NDVI was determined by interactions between mean snow depth, start day and the intensity of the event. In early winter, increasing event intensity was associated with greater reductions in TI-NDVI when the mean snow depth during those events was deeper. Also, as winter progresses, the relationship between intensity and TI-NDVI becomes shallower, and by late winter increasing event intensity is associated with greater loss of TI-NDVI only at relatively deep snow depths. This shows that at low temperatures, shallow snow depth and exposure were consistently associated with greater

reductions in TI-NDVI. However, these relationships may also reflect smaller impacts of increasingly severe warm spells in vegetation communities which typically experience shallow snow cover or periods of exposure during winter (for example coastal vegetation communities), compared to those where snow cover is typically deep and persistent (Bokhorst et al., 2016). For instance, where snow depth during warming events is very shallow or absent, warming events have no relationship with TI-NDVI change (early-mid winter) or positively impact it (late winter). Low mean snow depth in these areas may represent lower snow depth throughout winter, rather than snow melt associated with warming. In this case, vegetation in areas with normally low snow depth may be more adapted and resilient to fluctuations in winter temperature because they typically are (more likely to be) exposed above the snow (Kudo & Hirao, 2006, Bienau et al., 2014). Increasing warming event intensity in these vegetation communities may therefore have little effect. In contrast, an area with greater snow depth during a warming event may nonetheless have experienced substantial snow melt as a result of warming, which may cause vegetation exposure. If such areas are typically covered by deep snow throughout winter, vegetation may be much more sensitive to extreme temperature fluctuations and higher rates of water loss associated with exposure from the browning event. Further work should determine whether amount of snow melt (i.e. initial snow depth – final snow depth) during a warming event may be a more ecologically relevant metric than mean snow depth.

It is not clear why the relationship between change in TI-NDVI and event intensity is positive in late winter, even at mean snow depth (i.e. less negative TI-NDVI change with greater intensity). This may be related to the alleviation of water stress from snow melt-water, or to the impact of increased soil moisture following snowmelt on phenology (Vaganov et al., 1999; Barichivich et al., 2014). Alternatively, it may suggest that late in the winter, when mean air

temperatures are beginning to increase, warming events are less likely to be followed by the rapid drop in temperature which was highlighted by plot-level analysis as an important driver of NDVI decline. Without this temperature drop warming in later winter may simply encourage earlier spring snowmelt and accelerate phenology, without damaging effects (Meisingset et al., 2015). However, this appears to conflict with the association between large NDVI reductions and warm exposure events during late winter, but the reason for these apparently conflicting associations is not clear.

The regional scale findings arise from analyses of change in TI-NDVI [a proxy for total growing season productivity, Epstein et al., (2017)], yet regional scale climate metrics did not correlate with change in July NDVI (approximately peak biomass, or peak NDVI). This is likely to be in part a result of the influence of altitudinal, latitudinal and coast-inland variability in the peak NDVI timing combined with detection of this from just two MODIS images within a single month, meaning the genuine peak NDVI may be missed. TI-NDVI may make for better comparison of greenness among sites that have contrasting phenology and timing of peak biomass. In addition, while winter extreme climatic events can drive extensive vegetation mortality, and therefore biomass loss, they also frequently cause severe stress and delayed phenology (Bjerke et al., 2017). Subsequent recovery from stress (Chapter 3), and catch-up in phenology/growth (Koller, 2011), would reduce detection from peak season NDVI, while the initial stress and phenology impacts would be incorporated in (and likely detected in) TI-NDVI, which correlates with total growing season productivity (Epstein et al., 2017)

5.5.3. Plot-level compared with regional analyses

Analyses at plot-level and regional scales, combined with correlation between plot-level and remotely sensed NDVI (Appendix 2), indicated similar processes underlying the deepest

reductions in NDVI, in particular periods of unusual warmth and exposure during winter, and especially during late winter. However regional scale analysis showed more complexity compared to plot-level analysis; for example with colder temperatures during exposure periods associated with greater TI-NDVI reductions in early winter. This illustrates that, while the plot-level analysis focussed on the drivers of pre- and post-damage NDVI in observed browning sites, when these drivers are scaled up to regional analysis, a wider range of processes are involved in NDVI change. As TI-NDVI reflects cumulative productivity across the May – August growing season, reductions in this indicator could reflect altered phenology, and lower productivity in otherwise 'undamaged' vegetation, as well as the more extreme ecological responses associated with extreme event driven browning, such as mortality and visible stress responses. Assessing this greater range of conditions driving TI-NDVI change is necessary to investigate the drivers of reductions in greenness observed at landscape to pan-Arctic scales in recent years (Epstein et al., 2015, 2016; Phoenix & Bjerke, 2016). In addition, the additional complexity at regional compared to plot-scale highlights the challenges of linking between 'on the ground' and satellite scale data. These challenges include, for example, the contributions of multiple land cover types within a single satellite pixel, and the difficulty of distinguishing between processes which may similar trends in remotely sensed indices (such as changes in hydrology and in vegetation productivity). Using data of an appropriate resolution and using plot-level studies to inform analyses of remotely sensed or modelled data, as is done here, are key means of making regional-scale analyses more robust. None-the-less, having demonstrated that a small number of climate metrics explain a high proportion of variation in NDVI across sites affected by browning in the 2014 growing season, there is considerable potential for such simplified approaches requiring a limited range of climate datasets to attribute drivers of browning and be used in models to predict browning in the future. A clear opportunity to build on this potential is to apply these metrics to regions and years where extreme-event driven

browning has been both measured at plot-level, and mapped using remotely sensed data; in particular to the extensive browning reported across the Nordic Arctic Region following a combination of extreme event types during the 2011-2012 winter (Bjerke et al., 2014).

5.6 Conclusion

This analysis has demonstrated that the severity of NDVI reductions, both across sites where browning has been observed and at a regional scale, can be related to simple, process-based climate metrics. These metrics reinforce ecological theory about the drivers underlying winter climatic extreme event driven browning, showing that prolonged periods of unusual warmth and vegetation exposure during winter have negative consequences for NDVI. They also provide novel and much-needed insight into how different climatological variables and timing interact to produce more or less severe browning. Looking forward, with further development, simple climate metrics could be used to assess the impact of winter extreme climatic event driven-browning on productivity at regional scales, and improve predictions of changes in browning frequency in the future.

5.7 Appendix 1: tree-based regression analysis

Multivariate regression trees (Fig. 5.6) were used to guide the development of multiple regression analysis by highlighting the climatic variables which explained a substantial amount of the variation in plot-level NDVI. Trees were fitted for each event type: maximum intensity warming events (a), warming events with the maximum temperature drop during the 24 hours following the event (b), maximum duration exposure events (c) and warmest exposure events (d) and were pruned using the complexity parameter associated with minimum error. All trees were fitted using the rpart package (Therneau & Atkinson, 2018) in R (R Core Tean, 2017).

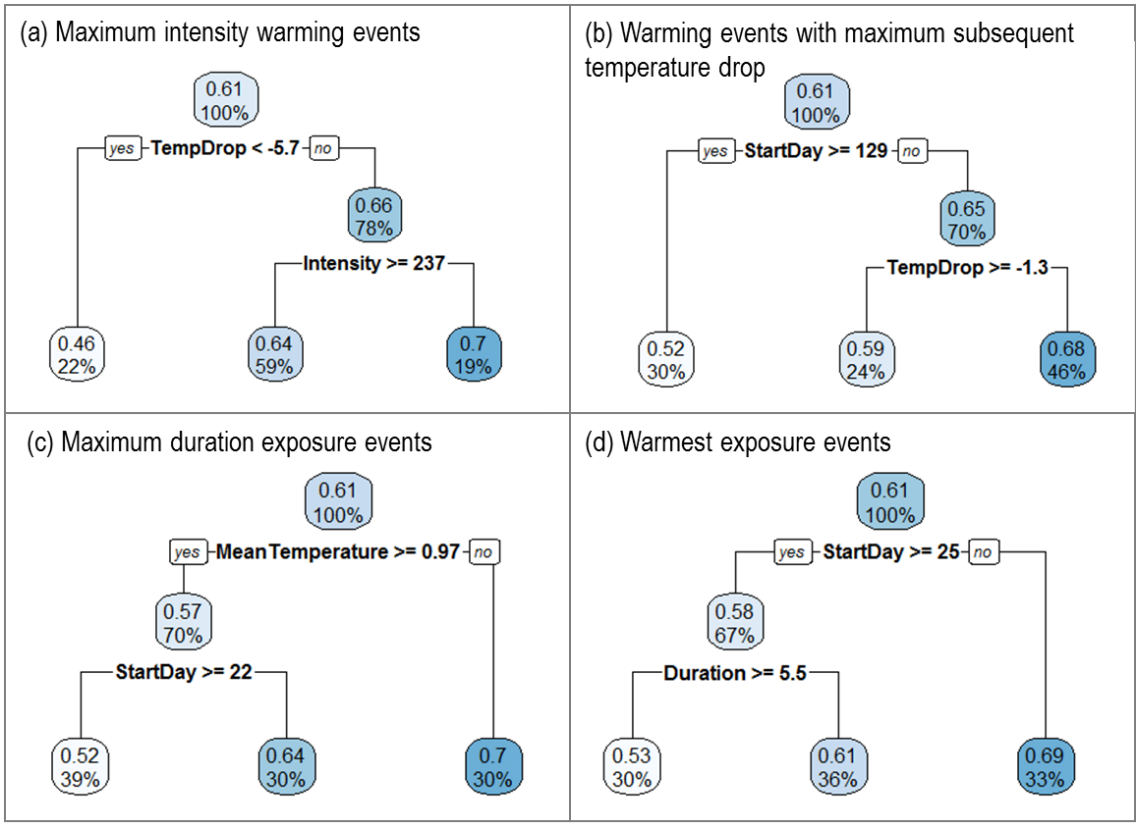

Figure 5.6: Tree-based regression analysis of climatic variables (Table 5.1) calculated for (a) maximum intensity warming events, (b) warming events with the maximum temperature drop during the 24 hours following the event, (c) maximum duration exposure events and (d) warmest exposure events. The variable "TempDrop" shown here refers to the drop in temperature during the 24 hours following the cessation of a warming event. Labels at each tree split show mean NDVI for the labelled grouping and the percentage of the total dataset within the grouping.

5.8 Appendix 2: Linking plot-level NDVI to satellite NDVI

There was a linear correlation between plot-level (measured by hand-held sensors) and MODIS NDVI (Fig. 5.7; F = 243.3, D.F. = 1, 320, p < 0.001, R^2 = 0.43).

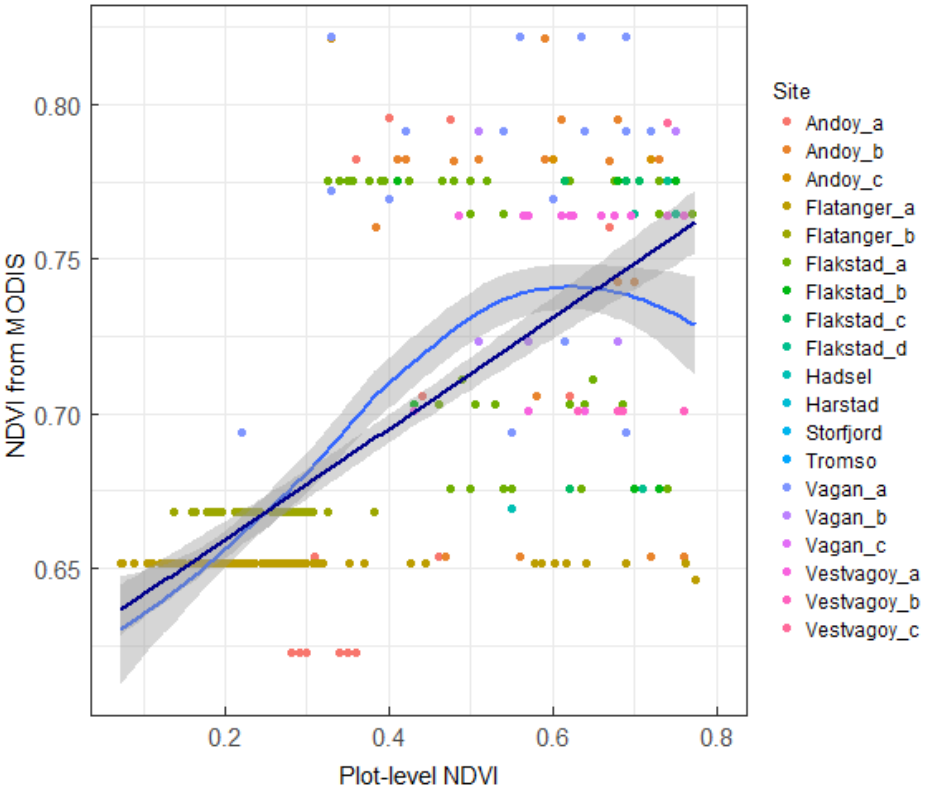

Figure 5.7: Comparison of plot-level NDVI, measured using handheld sensors, and remotely sensed NDVI extracted from MODIS. Points are coloured according to site (within which in many cases plots lie within the same satellite pixel, hence the "rows" of data points). Dark blue line shows linear regression of plot-level and satellite NDVI (R^2 = 0.43, p < 0.001). Light blue line shows a smoothed local regression (RSE = 0.14).

Chapter 6

General Discussion

This thesis has addressed three central themes which are key to understanding extreme event-driven Arctic browning:

i) The impacts of extreme events on net ecosystem CO_2 exchange (NEE), incorporating different types of event, the seasonality of impacts, and both mortality and visible stress responses.

ii) How changes in key CO_2 fluxes (i.e. productivity and respiration of vegetation and respiration from soils), and in related processes such as growth and decomposition rates, can provide mechanistic insight into overall impacts on NEE.

iii) The potential to upscale or assess the extent of browning impacts, either by establishing emergent relationships between browning impacts and remotely sensed vegetation indices, or using remotely sensed or modelled climatic data to quantify extreme event drivers and relate these to browning severity.

These were addressed primarily through field studies, assessing the impacts of browning across boreal, sub-Arctic and High Arctic latitudes, incorporating different event types, different vegetation responses (mortality and visible stress) and different periods of the growing season. Field investigations were extended using spatial analysis to quantify climatic drivers of browning and assess the potential of such an approach to upscale its impacts. The main emerging lessons from this work are discussed here.

6.1 Impacts of extreme event-driven browning on NEE

Carbon cycling in the Arctic plays an important role in the regulation of global climate. As the primary measure of ecosystem CO_2 balance, impacts on net ecosystem exchange (NEE) are central to how extreme event-driven browning will influence sink-source behaviour in Arctic regions, and ultimately how Arctic browning will feedback to climate change. While the scale

of vegetation damage observed following extreme winter events suggested major impacts on NEE were likely, these impacts had not been comprehensively quantified until now.

In Chapter 2, full peak season assessments of the impacts on NEE of extreme event driven Arctic browning were completed at boreal, sub-Arctic and High Arctic latitudes. These assessments covered browning caused by a range of event types (frost drought, extreme winter warming, ice encapsulation and insect outbreak). In Chapter 3, an assessment of the impacts of extreme climatic events at a single sub-Arctic site was carried out at early, peak and late season, and incorporated vegetation stress responses, in addition to the more commonly studied mortality.

It was concluded that browning does consistently drive major reductions in NEE (CO_2 uptake). Peak season reductions ranged from 27-81%, reflecting a marked loss of carbon sequestration capacity at the time when vegetation should be at its most productive. Variation in these site-level reductions depended on the severity of damage at each site and differences in the productivity on unaffected vegetation at different latitudes, rather than on the specific driver of damage. The magnitude of these reductions is in line with considerable negative impacts on NEE indicated by a single measurement set following simulated extreme winter warming (Bokhorst et al., 2011), and found by previous studies of defoliating insect outbreaks (Clark et al., 2009; Heliasz et al., 2011). Furthermore, measurements across the growing season highlighted that in some cases impacts on NEE may be even greater during the shoulder seasons than at the peak of the growing season. This highlights a risk of underestimating browning impacts when relying on peak season measurements alone, and therefore the importance of supporting peak season measurements with full season assessments (Ernakovich et al., 2014; Blume-Werry et al., 2016b). Similarly, major reductions in NEE were identified not just in

vegetation dominated by mortality, but also in vegetation exhibiting signs of stress (visible as deep red anthocyanin pigmentation in evergreen shrubs, Chapter 3). Visible stress responses are a less well understood consequence of extreme event exposure, and their major impacts on NEE suggest that they require further attention to avoid underestimating the effects of extreme events on high latitude vegetation.

The substantial reductions in NEE consistently demonstrated here across a range of latitudes and event drivers suggest that extreme climatic events which drive Arctic browning can have impacts on NEE that are similar to better understood large-scale events such as insect outbreaks and possibly even wildfire (Chapter 2), where these events occur in similar ecosystems. This clearly shows the need to identify emergent relationships across the wide range of events which drive browning, in order to upscale browning impacts on CO_2 uptake across Arctic regions.

6.2 Mechanisms of impacts on NEE

An understanding of the processes underlying the above impacts on NEE is central to predicting how the impacts of browning scale with damage severity, how they may vary according to the characteristics of affected plant communities (e.g. species composition), and how they may affect the longer term responses of Arctic plant communities to climate change. This understanding is needed both at the level of browning impacts, and of its causes. Therefore, key CO_2 fluxes which contribute to NEE (GPP, ecosystem respiration, moss GPP and respiration, and soil respiration) were assessed alongside NEE, and supported with additional measurements of processes such as shoot growth and decomposition (Chapters 2-4). Finally, climate metrics describing extreme event drivers of browning were developed, allowing the climatic processes which result in browning, and subsequent CO_2 flux impacts, to be investigated (Chapter 5).

The contributions of different CO_2 fluxes to overall impacts on NEE are summarised in Figure 6.1. This shows that, across the ecosystem as a whole, reductions in GPP consistently contribute to reductions in NEE, in line with previous attempts to assess the impacts of extreme winter event-driven browning on productivity (Bokhorst et al., 2011; Parmentier et al., 2018). This loss of productivity is likely due both to the loss of live photosynthetic leaf area and reduced photosynthetic capacity in surviving vegetation, as GPP is lowered in plots dominated by vegetation stress, as well as mortality (Steyn et al., 2002). Physiological impacts in surviving vegetation are also indicated by reductions in growth in all affected vegetation, as has previously been reported in vegetation impacted by extreme winter warming, winter exposure and ice encapsulation (Bokhorst et al., 2009; Preece et al., 2012; Blume-Werry et al., 2016). There are differences in the seasonality of the impacts of mortality and stress on GPP, with productivity largely recovering by late season in stressed vegetation, but large reductions remaining in vegetation dominated by mortality. However, the differing impacts of mortality and stress on vegetation respiration are more substantial, with stress driving an unexpected increase in peak season respiration, presumably due to the metabolic cost of breaking down anthocyanin pigmentation, or of increased maintenance and repair needs (Burger & Edwards, 1996; Flexas et al., 2005).

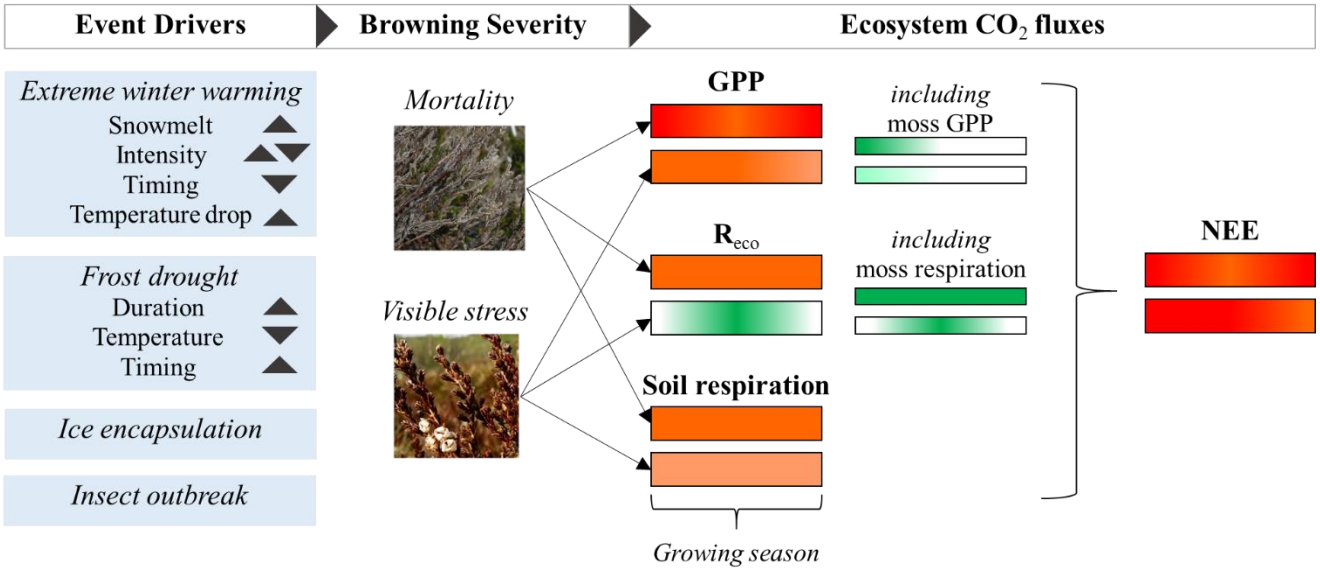

Figure 6.1: Diagram showing extreme winter events which drive browning, their climatic drivers (where assessed here), and their impacts on the ecosystem CO_2 fluxes Gross Primary Productivity (GPP), ecosystem respiration (R_{eco}), soil respiration, GPP and respiration specifically from the moss layer, and Net Ecosystem Exchange (NEE). Arrows next to event drivers show their likely impact on browning severity based on this work. Colour bars for ecosystem CO_2 fluxes are an approximate, qualitative representation of the direction of browning impacts on each flux (light to dark green shows an increase and orange to red shows a decrease in the magnitude of each flux) and the seasonality of impacts (early season to late season shown from left to right). Separate colour bars within each flux are shown for vegetation dominated by mortality and by stress.

Large differences in the contribution of CO_2 fluxes to overall NEE reductions are also seen between vascular vegetation and the moss layer. In contrast to consistent GPP reductions in vascular vegetation, moss GPP increases in plots dominated by mortality during early season. Despite this apparent positive effect of understory browning on moss productivity, consistent increases in moss respiration mean that net CO_2 uptake in the moss layer is reduced, with moss in damaged and stressed plots possibly even converted from a net CO_2 sink to a source for much of the growing season. In addition, negative impacts on moss growth were found following exposure to frost drought, with similar impacts previously reported following

extreme winter warming (Bjerke et al., 2011). This is of interest, as damage in vascular vegetation following frost drought is due to desiccation, of which moss species including that studied here are highly tolerant (Proctor et al., 2007).

In addition to these 'on the ground' assessments of the ecological processes underlying the impacts of browning on NEE, an analysis of the climatic processes driving browning across the region used for field studies was completed (Chapter 5). This analysis supporting existing theory about the mechanisms which are involved in browning driven by extreme climatic events, indicating that periods of exposure and periods of unusual warmth followed by a steep drop in temperature were associated with loss of greenness (Bokhorst et al., 2008; Hancock, 2008; Bjerke et al., 2014, 2017). It also added further depth to this understanding; showing, for example, that while during early winter cold exposure events result in greater NDVI reductions, during late winter the opposite is the case, with warm exposure events resulting in greater loss of greenness, and suggesting that prolonged, warm events (the primary characteristic of extreme winter warming) cause NDVI reductions only in areas accustomed to relatively deep snow cover.

6.3 Upscaling extreme event driven browning

Field assessments of browning impacts on CO_2 fluxes are labour and time intensive and logistically challenging. Methods to upscale these impacts across Arctic landscapes are needed to provide accurate, rapid estimates of the consequences of known events for CO_2 balance, and to improve our understanding of how extreme events influence CO_2 balance at regional scales. In addition to methods for upscaling measured impacts, there is a clear need for a framework to facilitate quantification of the climatic drivers of browning, based on underlying ecological processes. This process-based framework is needed to definitively link browning to specific

climatic conditions, to predict how changes in these conditions will influence the severity of subsequent browning, and, critically, to assess the current and future role of extreme event driven browning in determining the responses of high latitude ecosystems to climate change.

Methods for upscaling browning impacts were investigated by looking for relationships between browning severity and CO_2 flux impacts. There were close linear correlations between the severity of browning and CO_2 uptake at every site, with significant relationships maintained when data from all sites was combined. These clear emergent relationships were present not only between CO_2 uptake and percentage cover of browned vegetation, but also CO_2 uptake and NDVI (at sites where NDVI was measured). This extends studies which have identified strong relationships between LAI, as predicted from NDVI, and CO_2 fluxes in healthy arctic vegetation and shows that relationships between CO_2 uptake and visible greenness are maintained following vegetation damage (Street et al., 2007; Shaver et al., 2007). This was the case even at High Arctic latitudes, where heathland vegetation was sparse, despite previous work which found that such relationships break down where plant growth is weak (Emmerton et al., 2015). These consistent 'NDVI-CO_2 flux' and '% browned-CO_2 flux' relationships suggest that vegetation indices could provide a means of upscaling the impacts of Arctic browning on CO_2 balance. For example, Bokhorst et al., (2009) used remote sensing to estimate the NDVI reduction due to an extreme winter warming event which caused extensive browning, primarily of *Empetrum nigrum* heathland, across an area of more than 1400 km^2. They found a marked NDVI reduction of 26% (from 0.57 to 0.42) across this area. While this drop in NDVI is severe, impacts of a similar scale resulting from a range of extreme event types are not uncommon (Karlsen et al., 2013; Hansen et al., 2014; Bjerke et al., 2014, 2017). According to the relationship identified here between NEE and NDVI in sub-Arctic heathland

(Chapter 2), this decrease in NDVI would be associated with a reduction in NEE of 127%; converting the landscape from a net CO_2 sink to a source.

However, Chapter 3 identified limitations in the use of relationships between CO_2 fluxes and vegetation greenness to upscale browning impacts. Where extreme events result in substantial vegetation stress, it was shown that major impacts on NEE may persist into the peak of the growing season despite the recovery of greenness, due to increased respiration of stressed vegetation. This means that stress in heathland vegetation may cause peak season relationships between NEE and greenness to break down, raising the risk that relying solely on vegetation greenness indices to upscale browning could underestimate its impacts.

6.4 Future directions

6.4.1 Browning impacts and underlying mechanisms

The data presented in Chapters 2-4 represent the most comprehensive study of the impacts of extreme winter events on CO_2 fluxes in high latitude heathlands (the most commonly affected vegetation type) to date. This study demonstrates the scale of these impacts and the differences and commonalities of response between event drivers, across the growing season, and differences between vegetation stress and mortality. This adds to a small but growing body of work describing impacts of winter events on physiological characteristics in affected vegetation, including growth, phenology and reproduction (Bokhorst et al., 2008, 2010, 2011; Preece et al., 2012; Bjerke et al., 2014, 2017).

However a range of unanswered questions remain with regard to the impacts of extreme winter events on vegetation and carbon balance. In particular, Chapter 4 highlights uncertainty around

the impacts of these events on the moss layer. While it is known that extreme winter warming can reduce growth and photosynthesis in dominant moss species (Bjerke et al., 2011), it was expected that such damage would not result from frost drought, due to the high desiccation tolerance of moss. That reductions in moss growth were found one year following a frost drought event demonstrates that further work investigating the responses of this important component of high latitude ecosystems to extreme winter conditions is needed. This work should consider indirect, as well as direct responses, as despite the physiological damage to new shoots suggested by reduced growth rates, moss productivity appears to respond positively to browning during early season. Work considering direct responses should include *ex-situ* shoot-level measurements of photosynthetic capacity and fluorescence. Identifying the changes in environmental conditions which are likely to have promoted productivity in this case would provide a clearer picture of whether indirect impacts of browning on the moss layer might to some extent ameliorate the ecosystem level impacts on CO_2 balance.

A further area requiring further study is the role of vegetation stress in extreme event driven Arctic browning, and its impacts compared to those of mortality. Visible stress responses can affect a high proportion of heathland vegetation following extreme winter events (Bjerke et al., 2017). Chapter 3 shows for the first time that stress following extreme event exposure impacts ecosystem CO_2 fluxes, and that reductions in net CO_2 uptake associated with stress can equal or even exceed those associated with mortality. Future work in relation to this visible stress response should include further studies of shoot-level CO_2 fluxes, to confirm any direct association between visible pigmentation and shoot-level respiration, and should look for evidence of physiological damage, to investigate whether pigmentation signals the presence of damage, or more directly influences CO_2 fluxes. Importantly, the major ecosystem-level impacts of stress observed in Chapter 3 persist even following recovery of greenness,

potentially making their detection more challenging. Further work should include a more detailed assessment of the shoot/leaf level CO_2 fluxes in vegetation exhibiting visible stress. It should consider the mechanisms underlying differences in CO_2 fluxes between stressed and control vegetation; for example, whether these are associated solely with the presence and subsequent break down of anthocyanin pigments, which are known to both reduce light capture for photosynthesis and incur a metabolic cost (Burger & Edwards, 1996; Steyn et al., 2002), or if there is evidence that the unusually high production of these pigments signals physiological damage.

In addition, substantial reductions in soil respiration and decomposition rates reported here indicate large impacts on soil carbon cycling and on the functioning of the soil microbial community. Reduced root growth and changes in the structure of soil organism communities observed following simulated extreme winter warming (Bokhorst et al., 2009; Bokhorst et al., 2012), and reduced soil respiration and hyphal production of mycorrhizal fungi following defoliating insect outbreak (Parker et al., 2017) further point to large below-ground changes following extreme events which drive browning. However, these belowground responses remain little studied. All CO_2 flux impacts of browning, but particularly those on respiration, would also benefit from longer term studies to assess impacts over several years. This could enhance our understanding of the relative consequences of stress and damage over multiple years, and of how autotrophic and heterotrophic respiration are affected by and recover from extreme-event driven browning.

Finally, studies investigating the ecological thresholds beyond which extreme ecological responses are triggered would benefit both our understanding of the mechanisms underlying browning, and our ability to predict the frequency and severity of future extreme event-driven

browning. Relevant ecological thresholds include, for example, the intensity or duration of warmth required for premature dehardening, or for stomatal opening during periods of exposure (Tranquillini, 1982). These studies should both consider mortality and stress responses, particularly as the presence of vegetation stress following an event may be difficult to detect by peak season.

6.4.2 Upscaling browning

Upscaling extreme event driven browning and its impacts poses a number of challenges. NDVI is a well-established indicator of vegetation productivity, and has been used successfully to detect vegetation responses to a range of climatic conditions (Pettorelli et al., 2005). However, it is not currently possible to be certain where remotely sensed NDVI change is due specifically to extreme event-driven browning, as opposed to other browning processes such as changing growing season length or reduced summer warmth. This means that emergent relationships which demonstrate links between NDVI and the CO_2 flux impacts of browning (Chapter 2) are currently only useable where there is prior knowledge of the presence of an extreme-event driven browning event (for example from plot-level observations). In addition, in the absence of any means to identify browning severity over space, and without a framework to quantify and compare climatic drivers in relation to observations of browning severity, it is not yet possible to define 'extreme' thresholds of winter climate conditions beyond which an extreme biological response, such as mortality or a visible stress response, is triggered.

Chapter 5 used ground-level data in areas known to have been affected by extreme event-driven browning to develop a framework of novel metrics which quantify climatic drivers of browning, and showed that these metrics correlate with NDVI change at regional scales. This analysis is a first step towards identifying the conditions and thresholds which trigger extreme

ecological responses. To expand this and move towards the detection and attribution of extreme event driven-browning, a further step would be to analyse NDVI change, in parallel with changes in these climate metrics, over time. For example, using an approach such as that demonstrated by Lloyd-Hughes (2012) and Zscheischler et al., (2013), a three dimensional, structure-based analysis could track change in NDVI, identifying contiguous areas of 'anomalous' NDVI change, and assessing how climate metrics correspond to these spatio-temporal 'events'. This approach could take into account the multivariate/compound nature of extreme climatic events which drive browning, where the 'extreme' condition triggering a response is likely to be the interaction of climate metrics, rather than an anomaly in any single climate variable. However, this approach remains limited by the need to define a threshold beyond which NDVI is anomalous. A better understanding of how reductions in plot-level NDVI following browning scale up to remotely sensed NDVI, of how stress responses influence NDVI at both plot and pixel-level, or possibly the identification of alternative vegetation indices which highlight the particular responses associated with browning (i.e. mortality or deep red pigmentation in evergreen shrubs, Chapter 3) is needed to improve the detection of browning from remotely sensed data and thus avoid the use of arbitrary thresholds for anomalous NDVI which do not adequately represent ecological processes.

6.5 Conclusion

Understanding the responses of high latitude ecosystems to climate change is central to determining feedbacks to global climate. In particular, understanding the consequences of extreme events in winter, including how these may contrast with those of gradual summer warming, remains an important challenge. In this work, the substantial impacts of browning following exposure to extreme winter events on high latitude heathlands have been highlighted. A paucity of knowledge with regard to the implications of these events for ecosystem CO_2

balance has been addressed through detailed assessments of key CO_2 fluxes, incorporating different event drivers, different high latitude regions and different browning responses (mortality and stress). Novel metrics have also been used to quantify the climatic drivers of browning for the first time.

This work has shown that diverse extreme winter events have substantial negative impacts on all key ecosystem CO_2 fluxes (GPP, NEE, R_{eco} and R_{soil}). Net CO_2 uptake across the full growing season was reduced by around half in browned vegetation, while at peak season heavily browned vegetation was converted to a net CO_2 source at some sites. Large-scale impacts on net CO_2 uptake were present both where browning was associated with mortality and with stress. This clearly demonstrates that extreme event driven Arctic browning has major consequences for carbon cycling and source-sink behaviour in Arctic regions experiencing these, and that these considerable negative consequences contrast directly with the more well-understood impacts of summer warming. Further, analysis of the climatic drivers of extreme event driven browning supported previous work in highlighting the importance of factors such as winter exposure, unusual winter warmth, and strong temperature fluctuations in driving browning. This adds to evidence that extreme event driven browning is likely to continue to occur more frequently across Arctic regions with future climate change. These findings therefore have implications for our understanding of both the responses of high latitude vegetation to climate change, and the role of the Arctic in global climate, now and in the future.

References

AMAP (2017). Snow, Water, Ice and Permafrost in the Arctic (SWIPA) 2017. Arctic Monitoring and Assessment Programme (AMAP), Oslo, Norway. PP. xiv + 269

Arctic Council (2016). Arctic Resilience Report. M. Carson and G. Peterson (eds). Stockholm Environment Institute and Stockholm Resilience Centre, Stockholm. http://www. arctic-council.org/arr.

Alatalo JM, Jägerbrand AK & Molau U, (2014). Climate change and climatic events: community, functional and species-level responses of bryophytes and lichens to constant, stepwise, and pulse experimental warming in an alpine tundra. Alpine Botany, **124,** 81–91.

Altwegg R, Visser V, Bailey LD & Erni B, (2017). Learning from single extreme events. Phil. Trans. R. Soc. B, **372**, 20160141.

Anderson HB, Nilsen L, Tømmervik H, Karlsen SR, Nagai S, & Cooper EJ (2016). Using ordinary digital cameras in place of near-infrared sensors to derive vegetation indices for phenology Studies of High Arctic Vegetation. Remote sensing, 8, 847

Arndal MF, Illeris L, Michelsen A., Albert K, Tamstorf M, & Hansen BU, (2009). Seasonal variation in gross ecosystem production, plant biomass, and carbon and nitrogen pools in five High Arctic vegetation types. Arctic, Antarctic, and Alpine Research, **41**, 164–173.

Bailey LD, & van de Pol M, (2016). Tackling extremes: challenges for ecological and evolutionary research on extreme climatic events. Journal of Animal Ecology, **85**, 85–96.

Baranchikov YN, Perevoznikova VD, Vishnyakova ZD, (2001). Carbon emission by soils in forests damaged by the Siberian moth. Russian Journal of Ecology, **33**, 422-425.

Barichivich J, Briffa KR, Myneni R *et al.* (2014). Temperature and snow-mediated moisture controls of summer photosynthetic activity in northern terrestrial ecosystems between 1982 and 2011. Remote Sensing, **6**, 1390–1431.

Benedict JB (1990). Experiments on Lichen Growth. I. Seasonal Patterns and Environmental Controls, Arctic and Alpine Research, **22**, 244-254.

Beniston M, Stephenson DB, Christensen OB *et al.* (2007). Future extreme events in European climate: an exploration of regional climate model projections. Climatic Change, **81**, 71–95.

Bergamini A, Pauli D, Peintinger M, & Schmid B, (2001). Relationships between productivity, number of shoots and number of species in bryophytes and vascular plants. Journal of Ecology, **89**, 920–929.

Bhatt US, Walker DA, Raynolds MK *et al.* (2013). Recent declines in warming and vegetation greening trends over pan-Arctic tundra. Remote Sensing, **5**, 4229–4254.

Bienau MJ, Hattermann D, Kröncke M *et al.* (2014). Snow cover consistently affects growth and reproduction of *Empetrum hermaphroditum* across latitudinal and local climatic gradients. Alpine Botany, **124**, 115–129.

Bieniek PA, Bhatt US, Walker DA *et al.* (2015). Climate drivers linked to changing seasonality of Alaska coastal tundra vegetation productivity. Earth Interactions, **19**, 1–29.

Bintanja R, & Andry O, (2017). Towards a rain-dominated Arctic. Nature Climate Change, **7**, 263.

Bjerke JW, (2009). Ice encapsulation protects rather than disturbs the freezing lichen. Plant Biology, **11**, 227–235.

Bjerke JW, Bokhorst S, Callaghan TV, & Phoenix GK, (2017). Persistent reduction of segment growth and photosynthesis in a widespread and important sub-Arctic moss species after cessation of three years of experimental winter warming. Functional Ecology, **31**, 127–134.

Bjerke JW, Bokhorst S, Callaghan TV, Zielke M, & Phoenix GK, (2013). Rapid photosynthetic recovery of a snow-covered feather moss and *Peltigera* lichen during sub-Arctic midwinter warming. Plant Ecology & Diversity, **6**, 383–392.

Bjerke JW, Bokhorst S, Zielke M, Callaghan TV, Bowles FW, & Phoenix GK, (2011). Contrasting sensitivity to extreme winter warming events of dominant sub-Arctic heathland bryophyte and

lichen species: Bryophyte and lichen sensitivity to winter warming. Journal of Ecology, **99**, 1481–1488.

Bjerke JW, Karlsen SR, Høgda KA *et al.* (2014). Record-low primary productivity and high plant damage in the Nordic Arctic Region in 2012 caused by multiple weather events and pest outbreaks. Environmental Research Letters, **9**, 084006.

Bjerke JW, Treharne R, Vikhamar-Schuler D *et al.* (2017). Understanding the drivers of extensive plant damage in boreal and Arctic ecosystems: Insights from field surveys in the aftermath of damage. Science of The Total Environment, **599–600**, 1965–1976.

Bliss LC, (1971). Arctic and Alpine plant life cycles. Annual Review of Ecology and Systematics, **2**, 405–438.

Blume-Werry G, Kreyling J, Laudon H, & Milbau A, (2016). Short-term climate change manipulation effects do not scale up to long-term legacies: effects of an absent snow cover on boreal forest plants. Journal of Ecology, **104**, 1638–1648.

Blume-Werry G, Wilson SD, Kreyling J, & Milbau A, (2016). The hidden season: growing season is 50% longer below than above ground along an arctic elevation gradient. New Phytologist, **209**, 978–986.

Bokhorst S, Bjerke JW, Bowles FW, Melillo J, Callaghan TV, & Phoenix GK, (2008). Impacts of extreme winter warming in the sub-Arctic: growing season responses of dwarf shrub heathland. Global Change Biology, **14**, 2603–2612.

Bokhorst SF, Bjerke JW, Tømmervik H, Callaghan TV, & Phoenix GK, (2009). Winter warming events damage sub-Arctic vegetation: consistent evidence from an experimental manipulation and a natural event. Journal of Ecology, **97**, 1408–1415.

Bokhorst SF, Bjerke JW, Davey MP *et al.* (2010). Impacts of extreme winter warming events on plant physiology in a sub-Arctic heath community. Physiologia Plantarum, **140**, 128–140.

Bokhorst S, Bjerke JW, Street LE, Callaghan TV, & Phoenix GK, (2011). Impacts of multiple extreme winter warming events on sub-Arctic heathland: phenology, reproduction, growth, and CO_2 flux responses. Global Change Biology, **17**, 2817–2830.

Bokhorst S, Tømmervik H, Callaghan TV, Phoenix GK, & Bjerke JW, (2012). Vegetation recovery following extreme winter warming events in the sub-Arctic estimated using NDVI from remote sensing and handheld passive proximal sensors. Environmental and Experimental Botany, **81**, 18–25.

Bokhorst S, Pedersen SH, Brucker L *et al.* (2016). Changing Arctic snow cover: A review of recent developments and assessment of future needs for observations, modelling, and impacts. Ambio, **45**, 516–537.

Brooks PD, Grogan P, Templer PH, Groffman P, Öquist MG, & Schimel J, (2011). Carbon and nitrogen cycling in snow-covered environments. Geography Compass, **5**, 682–699.

Burger J, & Edwards GE, (1996). Photosynthetic efficiency, and photodamage by UV and visible radiation, in red versus green leaf Coleus varieties. Plant and Cell Physiology, **37**, 395–399.

Callaghan TV, Carlsson BA, Tyler NJC, (1989). Historical records of climate-related growth in Cassiope tetragona from the arctic. Journal of Ecology, **77**, 823–837.

Callaghan TV, Carlsson BA, Sonesson M, & Temesváry A, (1997). Between-year variation in climate-related growth of circumarctic populations of the moss Hylocomium splendens. Functional Ecology, **11**, 157–165.

Callaghan TV, Jonasson C, Thierfelder T *et al.* (2013). Ecosystem change and stability over multiple decades in the Swedish subarctic: complex processes and multiple drivers. Philosophical Transactions of the Royal Society B: Biological Sciences, **368**, 20120488–20120488.

Callaghan TV, Bergholm F, Christensen TR, Jonasson C, Kokfelt U, & Johansson M, (2010). A new climate era in the sub-Arctic: Accelerating climate changes and multiple impacts. Geophysical Research Letters, **37**.

Callaghan TV, Björn LO, Chernov Y *et al.* (2004). Effects on the structure of arctic ecosystems in the short-and long-term perspectives. AMBIO: A Journal of the Human Environment, **33**, 436–447.

Callaghan TV, Johansson M, Brown RD *et al.* (2011). The changing face of Arctic snow cover: a synthesis of observed and projected changes. AMBIO, **40**, 17–31.

Campioli M, Samson R, Michelsen A, Jonasson S, Baxter R, & Lemeur R, (2009). Nonvascular contribution to ecosystem NPP in a subarctic heath during early and late growing season. Plant Ecology, **202**, 41.

Chalker-Scott L, (1999). Environmental significance of anthocyanins in plant stress responses. Photochemistry and Photobiology, **70**, 1–9.

Christensen JHB, Hewitson A, Busuioc A *et al.* 2007: Regional Climate Projections. In: Climate Change 2007: The Physical Science Basis. Contribution of Working Group I to the Fourth Assessment Report of the Intergovernmental Panel on Climate Change [Solomon, S., D. Qin, M. Manning, Z. Chen, M. Marquis, K.B. Averyt, M. Tignor and H.L. Miller (eds.)]. Cambridge University Press, Cambridge, United Kingdom and New York, NY, USA.

Christiansen CT, Svendsen SH, Schmidt NM, & Michelsen A, (2012). High arctic heath soil respiration and biogeochemical dynamics during summer and autumn freeze-in – effects of long-term enhanced water and nutrient supply. Global Change Biology, **18**, 3224–3236.

Clark KL, Skowronski N, & Hom J, (2010). Invasive insects impact forest carbon dynamics. Global Change Biology, **16**, 88–101.

Cornelissen JHC, Van Bodegom PM, Aerts R *et al.* (2007). Global negative vegetation feedback to climate warming responses of leaf litter decomposition rates in cold biomes. Ecology Letters, **10**, 619–627.

Crawford RMM, (2013). Tundra-Taiga Biology. Oxford University Press, Oxford.

Dahl MB, Priemé A, Brejnrod A *et al.* (2017). Warming, shading and a moth outbreak reduce tundra carbon sink strength dramatically by changing plant cover and soil microbial activity. Scientific Reports, **7**, 16035.

DeLuca TH, Zackrisson O, Nilsson M-C, & Sellstedt A, (2002). Quantifying nitrogen-fixation in feather moss carpets of boreal forests. Nature, **419**, 917–920.

Douma JC, van Wijk TM, Lang SI, & Shaver GR, (2007). The contribution of mosses to the carbon and water exchange of arctic ecosystems: quantification and relationships with system properties. Plant, Cell and Environment, **30**, 1205-1215.

Easterling DR, Meehl GA, Parmesan C, Changnon SA, Karl TR, & Mearns LO, (2000). Climate extremes: observations, modeling, and impacts. Science, **289**, 2068–2074.

Elmendorf SC, Henry GHR, Hollister RD *et al.* (2012). Plot-scale evidence of tundra vegetation change and links to recent summer warming. Nature Climate Change, **2**, 453–457.

Elumeeva TG, Soudzilovskaia NA, During HJ, & Cornelissen JHC, (2011). The importance of colony structure versus shoot morphology for the water balance of 22 subarctic bryophyte species. Journal of Vegetation Science, **22**, 152–164.

Emmerton CA, St. Louis VL, Humphreys ER, Gamon JA, Barker, J. D, & Pastorello GZ, (2015). Net ecosystem exchange of CO_2 with rapidly changing high Arctic landscapes. Global Change Biology, **22**, 1185-1200.

Epstein HE, Bhatt US, Raynolds MK *et al.* (2015) Tundra Greenness. In: *Arctic Report Card 2015* http://www.arctic.noaa.gov/Report-Card.

Epstein HE, Bhatt US, Raynolds MK *et al.* (2016) Tundra Greenness. In: *Arctic Report Card 2016* http://www.arctic.noaa.gov/Report-Card.

Epstein HE, Bhatt US, Raynolds MK *et al.* (2017) Tundra Greenness. In: *Arctic Report Card 2017* http://www.arctic.noaa.gov/Report-Card.

Ernakovich JG, Hopping KA, Berdanier AB, Simpson RT, Kachergis EJ, Steltzer H, & Wallenstein MD, (2014). Predicted responses of arctic and alpine ecosystems to altered seasonality under climate change. Global Change Biology, **20**, 3256–3269.

Flexas J, Galmes J, Ribas-Carbo M, & Medrano H, (2005). The effects of water stress on plant respiration. In *Plant Respiration* (eds Lambers H & Ribas-Carbo M), PP. 85–94. Springer, Netherlands.

Flexas J, Bota J, Galmés J, Medrano H, & Ribas-Carbó M, (2006). Keeping a positive carbon balance under adverse conditions: responses of photosynthesis and respiration to water stress. Physiologia Plantarum, **127**, 343–352.

Førland EJ, Benestad RE, Flatøy F *et al.* (2009) Climate development in North Norway and the Svalbard region during 1900–2100. NorACIA. The Norwegian Polar Institute. Report series no. 128, 1–44.

Frank D, Reichstein M, Bahn M, *et al.* (2015) Effects of climate extremes on the terrestrial carbon cycle: concepts, processes and potential future impacts. Global Change Biology, **21**, 2861–2880.

Frost CJ, & Hunter MD, (2004). Insect canopy herbivory and frass deposition affect soil nutrient dynamics and export in oak mesocosms. Ecology, **85**, 3335–3347.

Frost CJ, & Hunter MD, (2008). Insect herbivores and their frass affect *Quercus rubra* leaf quality and initial stages of subsequent litter decomposition. Oikos, **117**, 13–22.

Galloway JN, Dentener FJ, Capone DG *et al.* (2004). Nitrogen cycles: past, present, and future. Biogeochemistry, **70**, 153–226.

Goetz SJ, Bunn AG, Fiske GJ, & Houghton RA, (2005). Satellite-observed photosynthetic trends across boreal North America associated with climate and fire disturbance. Proceedings of the National Academy of Sciences of the United States of America, **102**, 13521–13525.

Gornall JL, Jónsdóttir IS, Woodin SJ, & Van der Wal R, (2007). Arctic mosses govern below-ground environment and ecosystem processes. Oecologia, **153**, 931–941.

Gornall JL, Woodin SJ, Jónsdóttir IS, & van der Wal R, (2011). Balancing positive and negative plant interactions: how mosses structure vascular plant communities. Oecologia, **166**, 769–782.

Gould KS, (2004). Nature's Swiss Army Knife: The Diverse Protective Roles of Anthocyanins in Leaves. BioMed Research International, **2004**, 314–320.

Grace JB, (2006). *Structural Equation Modeling and Natural Systems*. Cambridge University Press, Cambridge.

Grace JB, Anderson TM, Olff H, & Scheiner SM, (2010). On the specification of structural equation models for ecological systems. Ecological Monographs, **80**, 67–87.

Grace JB, Schoolmaster DR, Guntenspergen GR, Little AM, Mitchell BR, Miller KM, & Schweiger EW, (2012). Guidelines for a graph-theoretic implementation of structural equation modeling. Ecosphere, **3**, 73.

Graham MH, (2003). Confronting multicollinearity in ecological multiple regression. Ecology, **84**, 2809–2815.

Graham RM, Cohen L, Petty AA *et al.* (2017). Increasing frequency and duration of Arctic winter warming events. Geophysical Research Letters, **44**, 6974–6983.

Grogan P, & Jonasson S, (2005). Temperature and substrate controls on intra-annual variation in ecosystem respiration in two subarctic vegetation types. Global Change Biology, **11**, 465–475.

Grogan P, & Jonasson S, (2006). Ecosystem CO_2 production during winter in a Swedish subarctic region: the relative importance of climate and vegetation type. Global Change Biology, **12**, 1479–1495.

Grogan P, Michelsen A, Ambus P, & Jonasson S, (2004). Freeze–thaw regime effects on carbon and nitrogen dynamics in sub-arctic heath tundra mesocosms. Soil Biology and Biochemistry, **36**, 641–654.

Guay KC, Beck PSA, Berner LT, Goetz SJ, Baccini A, & Buermann W, (2014). Vegetation productivity patterns at high northern latitudes: a multi-sensor satellite data assessment. Global Change Biology, **20**, 3147–3158.

Gutschick VP, & BassiriRad H, (2003). Extreme events as shaping physiology, ecology, and evolution of plants: toward a unified definition and evaluation of their consequences. New Phytologist, **160**, 21–42.

Hadley JL, & Smith WK, (1986). Wind effects on needles of timberline conifers: seasonal influence on mortality. Ecology, **67**, 12–19.

Hadley JL, & Smith WK, (1989). Wind erosion of leaf surface wax in alpine timberline conifers. Arctic and Alpine Research, **21**, 392–398.

Hancock MH, (2008). An exceptional Calluna vulgaris winter die-back event, Abernethy Forest, Scottish Highlands. Plant Ecology & Diversity, **1**, 89–103.

Hansen BB, Isaksen K, Benestad RE *et al.* (2014). Warmer and wetter winters: characteristics and implications of an extreme weather event in the High Arctic. Environmental Research Letters, **9**, 114021.

He X, He KS, & Hyvönen J, (2016). Will bryophytes survive in a warming world? Perspectives in Plant Ecology, Evolution and Systematics, **19**, 49–60.

Heliasz M, Johansson T, Lindroth A *et al.* (2011). Quantification of C uptake in subarctic birch forest after setback by an extreme insect outbreak. Geophysical Research Letters, **38**.

Hobbie, S. E., & Chapin, F. S. (1998). The Response of Tundra Plant Biomass, Aboveground Production, Nitrogen, and Co2 Flux to Experimental Warming. *Ecology*, *79*(5), 1526–1544. https://doi.org/10.1890/0012-9658(1998)079[1526:TROTPB]2.0.CO;2

Högberg P, Nordgren A, Buchmann N *et al.* (2001). Large-scale forest girdling shows that current photosynthesis drives soil respiration. Nature, **411**, 789–792.

IPCC, 2013: Climate Change 2013: The Physical Science Basis. Contribution of Working Group I to the Fifth Assessment Report of the Intergovernmental Panel on Climate Change [Stocker, T.F., D. Qin, G.-K. Plattner, M. Tignor, S.K. Allen, J. Boschung, A. Nauels, Y. Xia, V. Bex and P.M. Midgley (eds.)]. Cambridge University Press, Cambridge, United Kingdom and New York, NY, USA, 1535 pp

Jentsch A, Kreyling J, & Beierkuhnlein C, (2007). A new generation of climate-change experiments: events, not trends. Frontiers in Ecology and the Environment, **5**, 365–374.

Jepsen JU, Hagen SB, Ims RA, & Yoccoz NG, (2008). Climate change and outbreaks of the geometrids Operophtera brumata and Epirrita autumnata in subarctic birch forest: evidence of a recent outbreak range expansion. Journal of Animal Ecology, **77**, 257–264.

Jepsen JU, Biuw M, Ims RA, Kapari L, Schott T, Vindstad OPL, & Hagen SB, (2013). Ecosystem impacts of a range expanding forest defoliator at the forest-tundra ecotone. Ecosystems, **16**, 561–575.

Jia GJ, Epstein HE, & Walker DA, (2009). Vegetation greening in the Canadian arctic related to decadal warming. Journal of Environmental Monitoring, **11**, 2231.

Johansson C, Pohjola VA, Jonasson C, & Callaghan TV, (2011). Multi-decadal changes in snow characteristics in sub-Arctic Sweden. AMBIO, **40**, 566–574.

Karlsen SR, Jepsen JU, Odland A, Ims RA, & Elvebakk A, (2013). Outbreaks by canopy-feeding geometrid moth cause state-dependent shifts in understorey plant communities. Oecologia, **173**, 859–870.

Kaukonen M, Ruotsalainen AL, Wäli PR *et al.* (2013). Moth herbivory enhances resource turnover in subarctic mountain birch forests, Ecology, **94**, 267–272.

Keuper F, Dorrepaal E, Bodegom PMV, Aerts R, Logtestijn RSPV, Callaghan TV, & Cornelissen JHC, (2011). A Race for Space? How Sphagnum fuscum stabilizes vegetation composition during long-term climate manipulations. Global Change Biology, **17**, 2162–2171.

Keuskamp JA, Dingemans BJJ, Lehtinen T, Sarneel JM, & Hefting MM, (2013). Tea Bag Index: a novel approach to collect uniform decomposition data across ecosystems. Methods in Ecology and Evolution, **4**, 1070–1075.

Kirschbaum MUF, (1988). Recovery of photosynthesis from water stress in Eucalyptus pauciflora—a process in two stages. Plant, Cell & Environment, **11**, 685–694.

Knapp AK, Hoover DL, Wilcox KR *et al.* (2015) Characterizing differences in precipitation regimes of extreme wet and dry years: implications for climate change experiments. Global Change Biology, **21**(7), 2624–2633.

Koller EK, (2011) Controls on the growth of three subarctic dwarf shrubs along the Kårsavagge catchment gradient. Chapter 2 in: Impacts of environmental change on subarctic dwarf shrub communities : landscape gradient and field manipulation approaches. PhD thesis, University of Sheffield.

Körner C, (2016). Plant adaptation to cold climates. F1000Research, **5**.

Kreyling J, (2010). Winter climate change: a critical factor for temperate vegetation performance. Ecology, **91**, 1939–1948.

Kudo G, & Hirao AS, (2006). Habitat-specific responses in the flowering phenology and seed set of alpine plants to climate variation: implications for global-change impacts. Population Ecology, **48**, 49–58.

Kurz WA, Dymond CC, Stinson G *et al.* (2008). Mountain pine beetle and forest carbon feedback to climate change. Nature, **452**, 987–990.

Landi M, Tattini M, & Gould KS, (2015). Multiple functional roles of anthocyanins in plant-environment interactions. Environmental and Experimental Botany, **119**, 4–17.

Larcher W, & Siegwolf R, (1985). Development of acute frost drought in Rhododendron ferrugineum at the alpine timberline. Oecologia, **67**, 298–300.

Larsen KS, Ibrom A, Jonasson S, Michelsen A, & Beier C, (2007). Significance of cold-season respiration and photosynthesis in a subarctic heath ecosystem in Northern Sweden. Global Change Biology, **13**, 1498–1508.

LiCor (1997) *6400-09 Soil CO_2 flux chamber instruction manual*. LiCor, Lincoln, NE, USA.

Litton CM, Raich JW, & Ryan MG, (2007). Carbon allocation in forest ecosystems. Global Change Biology, **13**, 2089–2109.

Lloyd-Hughes B, (2012). A spatio-temporal structure-based approach to drought characterisation. International Journal of Climatology, **32**, 406–418.

Longton RE, (1997) The role of bryophytes and lichens in polar ecosystems. In: Ecology of Arctic Environments (eds S. J. Woodin & M. Marquiss), 69-96. Blackwell Science, Oxford

Mac Arthur A, & Malthus T, (2012). Calluna vulgaris foliar pigments and spectral reflectance modelling. International Journal of Remote Sensing, **33**, 5214-5239.

Macias-Fauria M, Forbes BC, Zetterberg P, & Kumpula T, (2012). Eurasian Arctic greening reveals teleconnections and the potential for structurally novel ecosystems. Nature Climate Change, **2**, 613–618.

Mack MC, Bret-Harte MS, Hollingsworth TN, Jandt RR, Schuur EAG, Shaver GR, & Verbyla DL, (2011). Carbon loss from an unprecedented Arctic tundra wildfire. Nature, **475**, 489–492.

Meisingset EL, Austrheim G, Solberg E, Brekkum Ø and Lande U S (2015). Effekter av klimastress pa hjortens vinterbeiter. Utvikling av blabærlyngen etter tørkevinteren 2014 ˚ Nibio Rapport, **1**, 28.

Miles VV, & Esau I, (2016). Spatial heterogeneity of greening and browning between and within bioclimatic zones in northern West Siberia. Environmental Research Letters, **11**, 115002.

Milner JM, Varpe Ø, van der Wal R, & Hansen BB, (2016). Experimental icing affects growth, mortality, and flowering in a high Arctic dwarf shrub. Ecology and Evolution, **6**, 2139–2148.

Moore DJP, Trahan NA, Wilkes P *et al.* (2013). Persistent reduced ecosystem respiration after insect disturbance in high elevation forests. Ecology Letters, **16**, 731–737.

Myers-Smith IH, Forbes BC, Wilmking M *et al.* (2011). Shrub expansion in tundra ecosystems: dynamics, impacts and research priorities. Environmental Research Letters, **6**, 045509.

Myers-Smith IH, Elmendorf SC, Beck PSA *et al.* (2015). Climate sensitivity of shrub growth across the tundra biome. Nature Climate Change, **5**, 887–891.

Myneni RB, Keeling CD, Tucker CJ, Asrar G, & Nemani RR, (1997). Increased plant growth in the northern high latitudes from 1981 to 1991. Nature, **386**, 698–702.

Oberbaueri SF, & Starr G, (2002). The role of anthocyanins for photosynthesis of Alaskan arctic evergreens during snowmelt. Advances in Botanical Research, **37**, 129–145.

Oechel WC, Vourlitis G, & Hastings SJ, (1997). Cold season CO_2 emission from Arctic soils. Global Biogeochemical Cycles, **11**, 163–172.

Olofsson J, te Beest M, & Ericson L, (2013). Complex biotic interactions drive long-term vegetation dynamics in a subarctic ecosystem. Philosophical Transactions of the Royal Society B: Biological Sciences, **368**, 20120486.

Olsson P-O, Heliasz M, Jin H, & Eklundh L, (2017). Mapping the reduction in gross primary productivity in subarctic birch forests due to insect outbreaks. Biogeosciences, **14**, 1703–1719.

Park T, Ganguly S, Tømmervik H *et al.* (2016). Changes in growing season duration and productivity of northern vegetation inferred from long-term remote sensing data. Environmental Research Letters, **11**, 084001.

Parker TC, Sadowsky J, Dunleavy H, Subke J-A, Frey SD, & Wookey PA, (2017). Slowed biogeochemical cycling in sub-arctic birch forest linked to reduced mycorrhizal growth and community change after a defoliation event. Ecosystems, **20**, 316–330.

Parmentier F-JW, Rasse DP, Lund M *et al.* (2018). Vulnerability and resilience of the carbon exchange of a subarctic peatland to an extreme winter event. Environmental Research Letters, **13**, 065009.

Pearson RG, Phillips SJ, Loranty MM, Beck PSA, Damoulas T, Knight SJ, & Goetz SJ, (2013). Shifts in Arctic vegetation and associated feedbacks under climate change. Nature Climate Change, **3**, 673–677.

Peterson G, & Rocha J, (2016). Arctic regime shifts and resilience. In *Arctic Resilience Report*. Stockholm Environment Institute and Stockholm Resilience Centre, Stockholm. Retrieved from https://www.sei-international.org/mediamanager/documents/Publications/ArcticResilienceReport-2016.pdf

Pettorelli N, Vik JO, Mysterud A, Gaillard J-M., Tucker CJ, & Stenseth NC, (2005). Using the satellite-derived NDVI to assess ecological responses to environmental change. Trends in Ecology & Evolution, **20**, 503–510.

Phoenix GK, & Bjerke JW, (2016). Arctic browning: extreme events and trends reversing arctic greening. Global Change Biology, **22**, 2960–2962.

Phoenix GK, & Lee JA, (2004). Predicting impacts of Arctic climate change: past lessons and future challenges. Ecological Research, **19**, 65–74.

Van de Pol M, Jenouvrier S, Cornelissen JHC, & Visser ME, (2017). Behavioural, ecological and evolutionary responses to extreme climatic events: challenges and directions. Phil. Trans. R. Soc. B, **372**, 20160134.

Post E, & Pedersen C, (2008). Opposing plant community responses to warming with and without herbivores. Proceedings of the National Academy of Sciences, **105**(34), 12353–12358.

Potter JA, Press MC, Callaghan TV, & Lee JA, (1995). Growth responses of Polytrichum commune and Hylocomium splendens to simulated environmental change in the sub-arctic. New Phytologist, **131**, 533–541.

Preece C, Callaghan TV, & Phoenix GK, (2012). Impacts of winter icing events on the growth, phenology and physiology of sub-arctic dwarf shrubs. Physiologia Plantarum, **146**, 460–472.

Preece C & Phoenix GK, (2013). Responses of sub-arctic dwarf shrubs to low oxygen and high carbon dioxide conditions. Environmental and Experimental Botany, **85**, 7–15.

Preece C & Phoenix GK (2014). Impact of early and late winter icing events on sub-arctic dwarf shrubs. Plant Biology, **16**, 125-132.

Price AG, Dunham K, Carleton T, & Band L, (1997). Variability of water fluxes through the black spruce (Picea mariana) canopy and feather moss (Pleurozium schreberi) carpet in the boreal forest of Northern Manitoba. Journal of Hydrology, **196**, 310–323.

Proctor MCF, Oliver MJ, Wood AJ, Alpert P, Stark LR, Cleavitt NL, & Mishler BD, (2007). Desiccation-tolerance in bryophytes: a review. The Bryologist, **110**, 595–621.

R Core Team (2017). R: A language and environment for statistical computing. R Foundation for Statistical Computing, Vienna, Austria. URL https://www.R-project.org/.

Read DJ, Leake JR, & Perez-Moreno J, (2004). Mycorrhizal fungi as drivers of ecosystem processes in heathland and boreal forest biomes. Canadian Journal of Botany, **82**, 1243–1263.

Reichstein M, Bahn M, Ciais P *et al.* (2013). Climate extremes and the carbon cycle. Nature, **500**, 287–295. https://doi.org/10.1038/nature12350

Richter-Menge J, Overland JE, Mathis JT, and Osborne E, (2017) *Arctic Report Card 2017*, http://www.arctic.noaa.gov/Report-Card

Rosseel Y, (2012). lavaan: an R package for structural equation modeling. Journal of Statistical Software, **48**, 1-36.

Ross SE, Callaghan TV, Ennos AR, & Sheffield E, (1998). Mechanics and Growth Form of the Moss Hylocomium splendens. Annals of Botany, **82**, 787–793.

Rustad L, Campbell J, Marion G *et al.* (2001). A meta-analysis of the response of soil respiration, net nitrogen mineralization, and aboveground plant growth to experimental ecosystem warming. Oecologia, **126**, 543–562.

Sakai A, & Larcher W, (1987). *Frost Survival of Plants: Responses and Adaptation to Freezing Stress*. Springer Science & Business Media.

Salemaa M, Mäkipää R, & Oksanen J, (2008). Differences in the growth response of three bryophyte species to nitrogen. Environmental Pollution, **152**, 82–91.

Sarojini BB, Stott PA, & Black E, (2016). Detection and attribution of human influence on regional precipitation. Nature Climate Change, **6**, 669–675.

Schafer KVR, Clark KL, Skowronski N, & Hamerlynck EP, (2010). Impact of insect defoliation on forest carbon balance as assessed with a canopy assimilation model. Global Change Biology, **16**, 546–560.

Schneider CA, Rasband WS & Eliceiri KW, (2012). NIH Image to ImageJ: 25 years of image analysis. Nature methods, **9**, 671-675

Schuur EAG, Vogel JG, Crummer KG, Lee H, Sickman JO, & Osterkamp TE, (2009). The effect of permafrost thaw on old carbon release and net carbon exchange from tundra. Nature, **459**, 556–559.

Shaver GR, Rastetter EB, Salmon V *et al.* (2013). Pan-Arctic modelling of net ecosystem exchange of CO_2. Philosophical Transactions of the Royal Society B: Biological Sciences, **368**, 20120485.

Shaver GR, Street LE, Rastetter EB, Van Wijk MT, & Williams M, (2007). Functional convergence in regulation of net CO_2 flux in heterogeneous tundra landscapes in Alaska and Sweden. Journal of Ecology, **95**, 802–817.

Sippel S, Zscheischler J, & Reichstein M, (2016). Ecosystem impacts of climate extremes crucially depend on the timing. Proceedings of the National Academy of Sciences, **113**, 5768–5770.

Smith MD, (2011). An ecological perspective on extreme climatic events: a synthetic definition and framework to guide future research: Defining extreme climate events. Journal of Ecology, **99**, 656–663.

Solow AR, (2017). On detecting ecological impacts of extreme climate events and why it matters. Phil. Trans. R. Soc. B, **372**, 20160136.

Starr G, & Oberbauer SF, (2003). Photosynthesis of Arctic evergreens under snow: Implications for tundra ecosystem carbon balance. Ecology, **84**, 1415–1420.

Steltzer H, & Welker JM, (2006). Modeling the effect of photosynthetic vegetation properties on the NDVI–LAI relationship. Ecology, **87**, 2765–2772.

Steyn WJ, Wand SJE, Holcroft DM, & Jacobs G, (2002). Anthocyanins in vegetative tissues: a proposed unified function in photoprotection. New Phytologist, **155**, 349–361.

Strauss SY, Rudgers JA, Lau JA, & Irwin RE, (2002). Direct and ecological costs of resistance to herbivory. Trends in Ecology & Evolution, **17**, 278–285.

Street LE, Shaver GR, Williams M, & Wijk MTV, (2007). What is the relationship between changes in canopy leaf area and changes in photosynthetic CO_2 flux in Arctic ecosystems? Journal of Ecology, **95**, 139–150.

Strimbeck GR, DeHayes DH, Shane JB, Hawley GJ, & Schaberg PG, (1995). Midwinter dehardening of montane red spruce during a natural thaw. Canadian Journal of Forest Research, **25**, 2040–2044.

Sturm M, Racine C, & Tape K, (2001). Climate change - Increasing shrub abundance in the Arctic. Nature, **411**, 546–547.

Sturm M, Schimel J, Michaelson G *et al.* (2005). Winter biological processes could help convert arctic tundra to shrubland. Bioscience, **55**, 17–26.

Tape K, Sturm M, & Racine C, (2006). The evidence for shrub expansion in Northern Alaska and the Pan-Arctic. Global Change Biology, **12**, 686–702.

Tenow O, (1972) The outbreaks of Oporinia autumnata Bkh. & Operophthera spp. (Lep., Geometridae) in the Scandinavian mountain chain and northern Finland 1862–1968. Zoologiska Bidrag Från Uppsala, Supplement 2.

Tenow O, & Bylund H, (2000). Recovery of a Betula pubescens forest in northern Sweden after severe defoliation by Epirrita autumnata. Journal of Vegetation Science, **11**, 855–862.

Therneau T & Atkinson B, (2018). rpart: Recursive Partitioning and Regression Trees. R package version 4.1-13. https://CRAN.R-project.org/package=rpart

Tranquillini W, (1982). Frost drought and Its Ecological Significance. In *Physiological Plant Ecology II*. PP. 379–400. Springer, Berlin, Heidelberg.

Tundra Tea project (2018). Protocol available at https://tundratea.wordpress.com. Last accessed May 2018.

Turetsky MR, Bond-Lamberty B, Euskirchen E, Talbot J, Frolking S, McGuire AD, & Tuittila E-S, (2012). The resilience and functional role of moss in boreal and arctic ecosystems. New Phytologist, **196**, 49–67.

Turetsky MR, Mack MC, Hollingsworth TN, & Harden JW, (2010). The role of mosses in ecosystem succession and function in Alaska's boreal forest. Canadian Journal of Forest Research, **40**, 1237–1264.

Uchida M, Kishimoto A, Muraoka H, Nakatsubo T, Kanda H, & Koizumi H, (2010). Seasonal shift in factors controlling net ecosystem production in a high Arctic terrestrial ecosystem. Journal of Plant Research, **123**, 79.

UNEP (2017). The Emissions Gap Report 2017. United Nations Environment Programme (UNEP), Nairobi

Ummenhofer CC, & Meehl GA, (2017). Extreme weather and climate events with ecological relevance: a review. Phil. Trans. R. Soc. B, **372**, 20160135.

Vaganov EA, Hughes MK, Kirdyanov AV, Schweingruber FH, & Silkin PP, (1999). Influence of snowfall and melt timing on tree growth in subarctic Eurasia. Nature, **400**, 149–151.

Vikhamar-Schuler D, Isaksen K, Haugen JE, Tømmervik H, Luks B, Schuler TV, & Bjerke JW (2016). Changes in Winter Warming Events in the Nordic Arctic Region. Journal of Climate, **29**, 6223–6244.

Van der Wal R, Pearce ISK, & Brooker RW, (2005). Mosses and the struggle for light in a nitrogen-polluted world. Oecologia, **142**, 159–168.

Walker DA, Raynolds MK, Daniels FJA *et al.* (2009). The Circumpolar Arctic vegetation map. Journal of Vegetation Science, **16**, 267–282.

Williams M, Street LE, van Wijk MT, & Shaver GR, (2006). Identifying differences in carbon exchange among Arctic ecosystem types. Ecosystems, **9**, 288–304.

Williams CM, Henry HAL, & Sinclair BJ, (2015). Cold truths: how winter drives responses of terrestrial organisms to climate change. Biological Reviews, **90**, 214–235.

Wolf A, Kozlov MV, & Callaghan TV, (2008). Impact of non-outbreak insect damage on vegetation in northern Europe will be greater than expected during a changing climate. Climatic Change, **87**, 91–106.

Wolf S, Keenan TF, Fisher JB *et al*. (2016). Warm spring reduced carbon cycle impact of the 2012 US summer drought. Proceedings of the National Academy of Sciences, **113**, 5880–5885.

Woolgrove CE, & Woodin SJ, (1996). Current and historical relationships between the tissue nitrogen content of a snowbed bryophyte and nitrogenous air pollution. Environmental Pollution, **91**, 283–288.

Xu L, Myneni RB, Chapin III FS *et al*. (2013). Temperature and vegetation seasonality diminishment over northern lands. Nature Climate Change, **3**, 581-586.

Zangerl AR, Arntz AM, & Berenbaum MR, (1997). Physiological price of an induced chemical defense: photosynthesis, respiration, biosynthesis, and growth. Oecologia, **109**, 433–441.

Zhao J, Peichl M, & Nilsson MB, (2017). Long-term enhanced winter soil frost alters growing season CO_2 fluxes through its impact on vegetation development in a boreal peatland. Global Change Biology, **23**, 3139-3153.

Zscheischler J, Mahecha MD, von Buttlar J *et al.* (2014). A few extreme events dominate global interannual variability in gross primary production. Environmental Research Letters, **9**, 035001.

Zscheischler J, Mahecha MD, Harmeling S, & Reichstein M, (2013). Detection and attribution of large spatiotemporal extreme events in Earth observation data. Ecological Informatics, **15**, 66–73.